

**FABRICATION AND MODIFICATION OF COMPRESSION MOLDING  
POLY(HYDROXYBUTYRATE-CO-VALERATE) THIN SHEET**

**By**

**Waree Jaruwattanayon**

**A THESIS**

**Submitted to  
Michigan State University  
in partial fulfillment of the requirements  
for the degree of**

**Packaging -- Master of Science**

**2014**

## ABSTRACT

### FABRICATION AND MODIFICATION OF COMPRESSION MOLDING POLY(HYDROXYBUTYRATE-CO-VALERATE) THIN SHEET

By

Waree Jaruwattanayon

Poly(hydroxybutyrate-co-valerate), PHBV, is a brittle biodegradable polymer. This study focuses on the modification of PHBV for flexible applications. Blending with nanoparticle titanium dioxide ( $\text{TiO}_2$ ) 1% by weight did not result in toughening. Blending with poly(butylene adipate-co-terephthalate) (PBAT or Ecoflex) at various ratios of PHBV/Ecoflex (80/20, 70/30, and 50/50 by weight) for flexibility with and without nanoparticle  $\text{TiO}_2$  also was not promising. Grafting with 2-Hydroxyethyl methacrylate (2HEMA) at ratios of PHBV/2HEMA of 90/10 and 70/30 by weight was also unsuccessful in increasing flexibility. Crosslinking PHBV in the presence of 2,5-Bis(tert-butylperoxy)-2,5-dimethylhexane (L101) resulted in significantly greater elongation at break and slightly higher tensile strength. The crosslinked PHBV had lower crystallinity than PHBV since the crosslinked network impeded crystalline formation, creating voids for favorable paths for gases resulting in higher permeation. The amount of L101 in the crosslinking reaction was investigated at 0.5, 1, 2, 3, and 4 % by weight. The neat PHBV and crosslinked PHBV sheets were not significantly different in tensile strength. The maximum elongation at break was obtained at L101 content of 2 % by weight where it was twice that of neat PHBV. Thermal analysis showed that crystallinity of the crosslinked PHBVs were lower than neat PHBV. Also, the permeability to gases increased with an increase in L101 content.

**To my parents, brother, sisters, and friends**

## **ACKNOWLEDGEMENTS**

This work could not be complete without the financial support from Royal Thai Government, Ministry of Science and Technology.

I would like to express my gratitude to my advisor Prof. Dr. Susan Selke for her understanding, patience, suggestion and encouragement. Her guidance was valuable in my research and writing of this thesis.

I would like to thank s to my committee members Dr. Gary Burgess, Dr. Maria Rubino and Dr. Yan Liu who helped shape this thesis. I also express my sincere thanks to Brian Rook from CMSC for his assistance and training in polymer processing.

I am also thankful to my friends. Dr. Sukeewan, Hayati, Tanatorn, Boo, Pai for their help and friendship.

I would like to thank my parents, brother and sisters for supporting and encouraging me.

## TABLE OF CONTENTS

|  |      |
|--|------|
| <b>LIST OF TABLES</b> .....  | viii |
| <b>LIST OF FIGURES</b> .....   | x    |
| <b>KEY TO SYMBOLS AND ABBREVIATIONS</b> .....  | xiii |
| <b>1. INTRODUCTION</b>   |      |
| <b>1.1 Introduction and motivation</b> .....   | 1    |
| <b>1.2 Goal and objectives</b> .....   | 2    |
| <b>1.3 Research plan</b> .....   | 3    |
| 1.3.1 Selection of modification methods for improving<br>poly(hydroxybutyrate-co-valerate) properties..... | 3    |
| 1.3.2 Selection of the optimum amount of an initiator in order to gain<br>maximum elongation at break..... | 3    |
| <b>2. LITERATURE REVIEW</b>  |      |
| <b>2.1 Introduction</b> .....  | 4    |
| <b>2.2 Biodegradable polymers</b> .....  | 6    |
| 2.2.1 Petroleum based biodegradable polymers.....  | 7    |
| 2.2.1.1 Aliphatic polyesters.....  | 7    |
| 2.2.1.2 Aliphatic-aromatic copolymers.....   | 9    |
| 2.2.2 Bio-based polymers.....  | 10   |
| 2.2.2.1 Starch.....  | 10   |
| 2.2.2.2 Cellulose.....   | 12   |
| 2.2.2.3 Soy based bioplastic.....  | 12   |
| 2.2.2.4 Zein bioplastic.....   | 13   |
| 2.2.2.5 Polylactic acid.....   | 14   |
| 2.2.2.6 Polyhydroxyalkanoates.....   | 16   |
| <b>2.3 Biodegradable polymer modification for flexibility</b> .....  | 17   |
| 2.3.1 Polymer blends.....  | 17   |
| 2.3.1.1 Characterization of polymer blends.....  | 20   |
| 2.3.2 Polymer grafting.....  | 21   |
| 2.3.3 Crosslinking polymers.....   | 23   |
| <b>2.4 Poly(hydroxybutyrate-co-valerate)</b> .....   | 25   |
| 2.4.1 Poly(hydroxybutyrate-co-valerate) structure and properties.....                                      | 27   |
| 2.4.2 Enhancement of poly(hydroxybutyrate-co-valerate) properties.....                                     | 28   |
| 2.4.2.1 Poly(hydroxybutyrate-co-valerate) blends.....  | 28   |
| 2.4.2.2 Poly(hydroxybutyrate-co-valerate) grafting and crosslinking.....                                   | 30   |
| <b>2.5 Biodegradation of poly(hydroxybutyrate-co-valerate)</b> .....                                       | 31   |
| 2.5.1 Biodegradation mechanism.....  | 32   |
| 2.5.2 Biodegradation evaluation.....   | 34   |
| 2.5.3 Biodegradation of poly(hydroxybutyrate-co-valerate).....   | 35   |

|            |   |    |
|------------|---|----|
| <b>3.</b>  | <b>MATERIALS AND METHODS</b>  |    |
| <b>3.1</b> | <b>Materials</b>  | 37 |
| 3.1.1      | Polyhydroxybutyrate-co-valerate   | 37 |
| 3.1.2      | Poly(butylene adipate-co-terephthalate)   | 37 |
| 3.1.3      | Triethyl citrate  | 37 |
| 3.1.4      | Titanium dioxide  | 38 |
| 3.1.5      | 2-Hydroxyethyl methacrylate   | 38 |
| 3.1.6      | 2,5-Bis(tert-butylperoxy)-2,5-dimethylhexane  | 38 |
| <b>3.2</b> | <b>Equipment</b>  | 39 |
| 3.2.1      | Processing equipment  | 39 |
| 3.2.2      | Compression molding   | 40 |
| 3.2.3      | Mechanical properties   | 41 |
| 3.2.4      | Thermal properties  | 41 |
| 3.2.5      | Permeability test equipment   | 42 |
| 3.2.6      | Statistical analysis  | 42 |
| <b>3.3</b> | <b>Poly(hydroxybutyrate-co-valerate) and modified poly(hydroxybutyrate-co-valerate) sheet fabrication</b>                           | 42 |
| <b>3.4</b> | <b>Investigation of the properties of poly(hydroxybutyrate-co-valerate) and modified poly(hydroxybutyrate-co-valerate) sheet</b>    | 44 |
| <b>4.</b>  | <b>SELECTION OF MODIFICATION METHOD FOR IMPROVING POLYHYDROXYBUTYRATE-CO-VALERATE PROPERTIES FOR COMPRESSION MOLDING THIN SHEET</b> |    |
| <b>4.1</b> | <b>Introduction</b>   | 45 |
| <b>4.2</b> | <b>Fabrication of modified polyhydroxybutyrate-co-valerate</b>  | 45 |
| 4.2.1      | Fabrication of poly(hydroxybutyrate-co-valerate) blend with titanium dioxide  | 45 |
| 4.2.2      | Fabrication of poly(hydroxybutyrate-co-valerate)/poly(butylene adipate-co-terephthalate) blend                                      | 47 |
| 4.2.3      | Fabrication of poly(hydroxybutyrate-co-valerate)/poly(butylene adipate-co-terephthalate)/titanium dioxide blend                     | 48 |
| 4.2.4      | Fabrication of poly(hydroxybutyrate-co-valerate)/triethyl citrate blend   | 48 |
| 4.2.5      | Fabrication of poly(hydroxybutyrate-co-valerate) grafted with 2-hydroxyethyl methacrylate   | 49 |
| 4.2.6      | Fabrication of crosslinked poly(hydroxybutyrate-co-valerate)  | 50 |
| <b>4.3</b> | <b>Results and discussion</b>   | 51 |
| 4.3.1      | Visual characteristics of poly(hydroxybutyrate-co-valerate) and modified poly(hydroxybutyrate-co-valerate)                          | 51 |
| 4.3.2      | Mechanical properties of poly(hydroxybutyrate-co-valerate) and modified poly(hydroxybutyrate-co-valerate)                           | 56 |
| 4.3.3      | Thermal properties of poly(hydroxybutyrate-co-valerate) and modified poly(hydroxybutyrate-co-valerate)                              | 64 |
| 4.3.4      | Permeation properties of poly(hydroxybutyrate-co-valerate) and modified poly(hydroxybutyrate-co-valerate)                           | 85 |
| 4.3.4.1    | Water vapor permeability  | 88 |
| 4.3.4.2    | Oxygen and carbon dioxide permeability  | 98 |

|   |            |
|---|------------|
| 4.4 Conclusion.....   | 101        |
| <b>5. INFLUENCE OF THE AMOUNT OF INITIATOR ON THE DEGREE OF PHBV<br/>CROSSLINKING AND ITS PROPERTIES</b>                                    |            |
| 5.1 Introduction.....   | 102        |
| 5.2 Fabrication of crosslinked polyhydroxybutyrate-co-valerate with<br>different amounts of initiator.....                                  | 103        |
| 5.3 Results and discussion.....   | 106        |
| 5.3.1 Visual characteristics of the crosslinked poly(hydroxybutyrate-co-<br>valerate)s.....   | 106        |
| 5.3.2 Mechanical properties of crosslinked poly(hydroxybutyrate-co-<br>valerate)s.....  | 108        |
| 5.3.3 Thermal properties of crosslinked poly(hydroxybutyrate-co-<br>valerate).....  | 113        |
| 5.3.4 Permeation properties of crosslinked poly(hydroxybutyrate-co-<br>valerate).....   | 119        |
| 5.4 Conclusion.....   | 124        |
| <b>6. CONCLUSIONS AND RECOMMENDATIONS FOR FUTURE WORK</b>   |            |
| 6.1 Summary and conclusions .....   | 125        |
| 6.1.1 Selection of modification method for improving polyhydroxybutyrate-<br>co-valerate properties for compression molding thin sheet..... | 125        |
| 6.1.2 Influence of the amount of initiator on the degree of polyhydroxybutyrate-<br>co-valerate crosslinking and its properties.....        | 127        |
| 6.2 Problems and recommendations for future work.....   | 128        |
| <b>APPENDICES.....</b>  | <b>129</b> |
| Appendix A- Mechanical properties of neat PHBV and modified PHBV<br>material sheets.....  | 130        |
| Appendix B- Thermal properties of neat PHBV and modified PHBV<br>material sheets.....   | 132        |
| Appendix C- Permeation properties of neat PHBV and modified PHBV<br>material sheets.....  | 136        |
| <b>REFERENCES.....</b>  | <b>138</b> |

## LIST OF TABLES

|                  |   |     |
|------------------|---|-----|
| <b>Table 4.1</b> | Visual characteristics of poly(hydroxybutyrate-co-valerate) and modified poly(hydroxybutyrate-co-valerate) in different forms in the experiment.....        | 55  |
| <b>Table 4.2</b> | Mechanical properties of all compositions of modified poly(hydroxybutyrate-co-valerate) material sheets.....  | 60  |
| <b>Table 4.3</b> | Thermal properties of all compositions of modified poly(hydroxybutyrate-co-valerate).....   | 67  |
| <b>Table 4.4</b> | Permeation properties of all compositions of modified poly(hydroxybutyrate-co-valerate).....  | 90  |
| <b>Table 5.1</b> | Visual characteristics of PHBV and crosslinked poly(hydroxybutyrate-co-valerate) with L101 of 0.5, 1, 2, 3, and 4 %wt.....                                  | 107 |
| <b>Table 5.2</b> | Mechanical properties of crosslinked poly(hydroxybutyrate-co-valerate) at various initiator contents compared to neat poly(hydroxybutyrate-co-valerate)..   | 110 |
| <b>Table 5.3</b> | Thermal properties of crosslinked poly(hydroxybutyrate-co-valerate) at various initiator contents compared to neat poly(hydroxybutyrate-co-valerate)..      | 116 |
| <b>Table 5.4</b> | Permeability properties of crosslinked poly(hydroxybutyrate-co-valerate) at various initiator contents compared to neat poly(hydroxybutyrate-co-valerate).. | 120 |
| <b>Table A-1</b> | Tensile strength of all compositions of modified PHBV material sheets.....  | 130 |
| <b>Table A-2</b> | Elongation at break of all compositions of modified PHBV material sheets.....   | 130 |
| <b>Table A-3</b> | Tensile strength of crosslinked PHBV at various initiator contents compared to neat PHBV.....   | 131 |
| <b>Table A-4</b> | Elongation at break of crosslinked PHBV at various initiator contents compared to neat PHBV.....  | 131 |
| <b>Table B-1</b> | Crystallization temperature of all compositions of modified PHBV material Sheets.....   | 132 |
| <b>Table B-2</b> | The first melting temperature of all compositions of modified PHBV material Sheets.....   | 132 |
| <b>Table B-3</b> | The second melting temperature of all compositions of modified PHBV material sheets.....  | 133 |



|                  |   |     |
|------------------|---|-----|
| <b>Table B-4</b> | Heat of fusion of all compositions of modified PHBV material sheets.....                                    | 133 |
| <b>Table B-5</b> | Crystallization temperature of crosslinked PHBV at various initiator contents compared to neat PHBV.....    | 134 |
| <b>Table B-6</b> | The first melting temperature of crosslinked PHBV at various initiator contents compared to neat PHBV.....  | 134 |
| <b>Table B-7</b> | The second melting temperature of crosslinked PHBV at various initiator contents compared to neat PHBV..... | 135 |
| <b>Table B-8</b> | Heat of fusion of crosslinked PHBV at various initiator contents compared to neat PHBV.....                 | 135 |
| <b>Table C-1</b> | Water vapor permeation of all compositions of modified PHBV material sheets.....                            | 136 |
| <b>Table C-2</b> | Oxygen permeation of all compositions of modified PHBV material sheets.....                                 | 136 |
| <b>Table C-3</b> | Carbon dioxide permeation of all compositions of modified PHBV material sheets.....                         | 137 |
| <b>Table C-4</b> | Water vapor permeation of crosslinked PHBV at various initiator contents compared to neat PHBV.....         | 137 |
| <b>Table C-5</b> | Carbon dioxide permeation of crosslinked PHBV at various initiator contents compared to neat PHBV.....      | 137 |

## LIST OF FIGURES

|                    |  |    |
|--------------------|--|----|
| <b>Figure 2.1</b>  | Number of landfills in the United States from 1988 to 2009.....            | 5  |
| <b>Figure 2.2</b>  | Poly(butylene succinate) molecular structure.....                          | 7  |
| <b>Figure 2.3</b>  | Polycaprolactone molecular structure.....                                  | 8  |
| <b>Figure 2.4</b>  | Polyglycolide molecular structure.....                                     | 8  |
| <b>Figure 2.5</b>  | Poly(butylene adipate-co-terephthalate) molecular structure.....           | 9  |
| <b>Figure 2.6</b>  | Amylose molecular structure.....   | 11 |
| <b>Figure 2.7</b>  | Amylopectin molecular structure.....                                       | 11 |
| <b>Figure 2.8</b>  | Cellulose molecular structure.....   | 12 |
| <b>Figure 2.9</b>  | Molecular structure of D-lactide, L-lactide, and Meso-lactide.....         | 14 |
| <b>Figure 2.10</b> | Molecular structure of poly(lactic acid).....                              | 15 |
| <b>Figure 2.11</b> | Molecular structure of PHAs.....   | 16 |
| <b>Figure 2.12</b> | Polymer blend phase diagram.....   | 19 |
| <b>Figure 2.13</b> | Graft copolymer diagram.....   | 21 |
| <b>Figure 2.14</b> | Molecular crosslinking.....  | 24 |
| <b>Figure 2.15</b> | Molecular structure of PHBV.....   | 26 |
| <b>Figure 2.16</b> | Biodegradation mechanism of polymers.....                                  | 33 |
| <b>Figure 3.1</b>  | Co-rotating mini twin screw extruder.....                                  | 39 |
| <b>Figure 3.2</b>  | Compression molding machine.....   | 40 |
| <b>Figure 4.1</b>  | Poly(hydroxybutyrate-co-valerate) neat resins.....                         | 52 |
| <b>Figure 4.2</b>  | Brittleness of PHBV/TiO <sub>2</sub> sheet and crosslinked PHBV sheet..... | 54 |
| <b>Figure 4.3</b>  | Tensile strength of PHBV material sheets.....                              | 62 |

|                    |  |     |
|--------------------|--|-----|
| <b>Figure 4.4</b>  | Elongation at break of PHBV material sheets.....   | 63  |
| <b>Figure 4.5</b>  | Two melting temperatures ( $T_m$ ) of neat PHBV.....   | 65  |
| <b>Figure 4.6</b>  | Crystallization temperature ( $T_c$ ) of neat PHBV.....  | 66  |
| <b>Figure 4.7</b>  | Thermal decomposition profile of neat PHBV.....  | 68  |
| <b>Figure 4.8</b>  | Endothermic and exothermic profiles of neat PHBV and PHBV/ $TiO_2$ 1%wt.....   | 70  |
| <b>Figure 4.9</b>  | Thermal decomposition profiles of PHBV and PHBV/ $TiO_2$ 1%wt.....   | 71  |
| <b>Figure 4.10</b> | Endothermic and exothermic profiles of neat PHBV<br>and PHBV/Ecoflex blends.....   | 73  |
| <b>Figure 4.11</b> | Thermal decomposition profiles of neat PHBV and PHBV/Ecoflex blends.....   | 74  |
| <b>Figure 4.12</b> | Endothermic and exothermic profiles of neat PHBV<br>and PHBV/Ecoflex/ $TiO_2$ blends.....  | 75  |
| <b>Figure 4.13</b> | Thermal decomposition profiles of neat PHBV<br>and PHBV/Ecoflex/ $TiO_2$ blends.....   | 76  |
| <b>Figure 4.14</b> | Endothermic and exothermic profiles of neat PHBV and PHBV/TEC blends.....  | 78  |
| <b>Figure 4.15</b> | Thermal decomposition profiles of neat PHBV and PHBV/TEC blends.....   | 79  |
| <b>Figure 4.16</b> | Endothermic and exothermic profiles of neat PHBV and PHBV-g-2HEMAs....   | 81  |
| <b>Figure 4.17</b> | Thermal decomposition profiles of neat PHBV and PHBV-g-2HEMAs.....   | 82  |
| <b>Figure 4.18</b> | Endothermic and exothermic profiles of neat PHBV and crosslinked PHBV.....   | 83  |
| <b>Figure 4.19</b> | Thermal decomposition profiles of neat PHBV and crosslinked PHBV.....  | 84  |
| <b>Figure 4.20</b> | Water vapor permeation of PHBV material sheets.....  | 92  |
| <b>Figure 4.21</b> | Oxygen permeation of PHBV material sheets.....   | 93  |
| <b>Figure 4.22</b> | Carbon dioxide permeation of PHBV material sheets.....   | 94  |
| <b>Figure 5.1</b>  | Shearing force profile of the molten PHBV crosslinked with a presence of<br>L101 vs. time in the mini twin screw extruder indicating the maximum<br>force of molten polymer reached the highest at reaction time of 1 min..... | 104 |
| <b>Figure 5.2</b>  | PHBV neat resin and crosslinked PHBV with L101 of 0.5, 1, 2, 3, and 4 %wt..  | 105 |

|                   |  |     |
|-------------------|--|-----|
| <b>Figure 5.3</b> | Tensile strength of neat PHBV and crosslinked PHBV sheets.....   | 111 |
| <b>Figure 5.4</b> | Elongation at break of neat PHBV and crosslinked PHBV sheets.....  | 112 |
| <b>Figure 5.5</b> | Endothermic and exothermic profiles of neat PHBV and crosslinked PHBVs<br>with L101 at 0.5, 1, 2, 3 and 4 %wt..... | 117 |
| <b>Figure 5.6</b> | Thermal decomposition profiles of neat PHBV and crosslinked PHBVs<br>with L101 at 0.5, 1, 2, 3 and 4 %wt.....      | 118 |
| <b>Figure 5.7</b> | Water vapor permeation of neat PHBV and crosslinked PHBV sheets.....   | 121 |
| <b>Figure 5.8</b> | Carbon dioxide permeation of neat PHBV and crosslinked PHBV sheets.....  | 122 |

## KEY TO SYMBOLS AND ABBREVIATIONS

|                    |   |   |
|--------------------|---|---|
| $\Phi_1, \Phi_2$   | = | Volume fraction of polymer 1 and 2, respectively                            |
| $\chi_{12}$        | = | Flory-Huggins interaction parameter between polymer 1 and 2                 |
| A                  | = | Cross-sectional area  |
| ATRP               | = | Atom transfer radical polymerization  |
| CO <sub>2</sub> TR | = | Carbon dioxide transmission rate  |
| D                  | = | Diffusion coefficient   |
| DSC                | = | Differential scanning calorimetry   |
| E <sub>p</sub>     | = | Activation energy   |
| EPA                | = | Environmental Protection Agency   |
| F                  | = | Flow rate   |
| HB                 | = | Hydroxybutyrate   |
| 2HEMA              | = | 2-Hydroxyethyl methacrylate   |
| $\Delta H_m$       | = | Melting enthalpy or heat of fusion  |
| $\Delta H_m^0$     | = | Melting enthalpy or heat of fusion of 100% crystalline polymer              |
| HV                 | = | Hydroxyvalerate   |
| L101               | = | Luperox 101, Lupersol 101, or 2,5-bis(tert-butylperoxy) -2,5-dimethylhexane |
| MSW                | = | Municipal solid waste   |
| O <sub>2</sub> TR  | = | Oxygen transmission rate  |
| P3/4HB             | = | Poly(3-hydroxybutyrate-co-4-hydroxybutyrate)                                |
| PBAT               | = | Poly(butylene adipate-co-terephthalate)                                     |
| PHA                | = | Polyhydroxyalkanoate  |

|                                 |   |   |
|---------------------------------|---|---|
| PHB                             | = | Polyhydroxybutyrate                                     |
| PHBV                            | = | Poly(hydroxybutyrate-co-valerate)                       |
| PHV                             | = | Polyhydroxyvalerate                                     |
| PLA                             | = | Poly(lactic acid)                                       |
| psi                             | = | Pounds per square inch                                  |
| q                               | = | Quantity of permeant passing through a polymer          |
| R                               | = | Gas constant  |
| t                               | = | Travelling time of a permeant passing through a polymer |
| T                               | = | Temperature in Kelvin                                   |
| T <sub>c</sub>                  | = | Crystallization temperature                             |
| TEC                             | = | Triethyl citrate  |
| T <sub>g</sub>                  | = | Glass transition temperature                            |
| TGA                             | = | Thermogravimetric analysis                              |
| TiO <sub>2</sub>                | = | Titanium dioxide  |
| T <sub>m</sub>                  | = | Melting temperature                                     |
| w <sub>1</sub> , w <sub>2</sub> | = | Weight fraction of polymer 1 and 2, respectively        |
| wt                              | = | Weight  |
| WVP                             | = | Water vapor permeability                                |
| WVTR                            | = | Water vapor transmission rate                           |

# 1. INTRODUCTION

## 1.1 Introduction and motivation

Polymers have been used increasingly these days since they have many superior properties over other materials. Plastics of today are mostly products from the petrochemical industry. Over the past century, natural resources including petroleum, oil and natural gas have been enormously used in every activity. Awareness has been raised concerning the depletion of natural resources. Petroleum is one of the greatest concerns. In addition, petrochemical processes for polymer production, especially refinery processes, involve combustion reactions and releases of combustion by-products, which are toxic substances, and other greenhouse gases. These substances have been released to the atmosphere contributing to pollution problems in our ecosystem [1]. Moreover, plastics from everyday life have been accumulating leading to massive waste, which needs waste management measures. All of these burdens have led to research and development of innovative materials.

Biodegradable polymers are alternative materials for this solution, which have been developed and implemented in many areas, especially in packaging applications. Poly(hydroxybutyrate-*co*-valerate), PHBV, is a biodegradable polymer which is formed in bacterial cells as an energy reservoir. With an absence of amino acid producing substances in the media substrate, PHBV is created in the cells. However, PHBV possesses high brittleness, tackiness and lack of elongation [2, 3]. To overcome these drawbacks, there are various plausible modification methods that have been used. These include adding plasticizers to the polymer for improving

flexibility [4, 5]. Nanoparticle inclusions such as titanium dioxide can be applied in order to toughen polymeric materials [6, 7]. Blending with other polymers can improve ductility of the material [8]. Grafting a polymer can enhance mechanical properties [9] and crosslinking can improve ductility and elongation of polymers [10, 11].

## **1.2 Goal and objectives**

The goal of this study focuses on the improvement of PHBV properties so it can be effectively used for flexible applications as well as maintaining its biodegradability. To achieve this goal, crosslinking with the help of an initiator was used to enhance PHBV's mechanical properties.

The objectives of the study were to:

1. Select modification methods for improving PHBV properties
2. Select the optimum amount of an initiator in order to gain maximum elongation at break.



### 1.3 Research plan

#### *1.3.1 Selection of modification methods for improving poly(hydroxybutyrate-co-valerate) properties*

A number of modification methods were selected in efforts to improve PHBV properties. First, PHBV was fabricated by adding TiO<sub>2</sub> to toughen PHBV. Second, PHBV was blended with Ecoflex in order to gain flexibility. Third, PHBV was blended with Ecoflex and added TiO<sub>2</sub> in order to impart both toughening and flexibility to PHBV. Fourth, PHBV was blended with triethyl citrate (TEC) as a plasticizer to improve flexibility. Fifth, 2-hydroxyethyl methacrylate (2HEMA) was grafted onto PHBV in order to diminish PHBV brittleness. Finally, PHBV was crosslinked in the presence of an initiator (2,5-Bis(tert-butylperoxy)-2,5-dimethylhexane, L101). Visual observation, mechanical properties, thermal properties, and permeability were examined.

#### *1.3.2 Selection of the optimum amount of an initiator in order to gain maximum elongation at break*

From the results of the experiments discussed above, crosslinking was chosen as the preferred modification method for improving PHBV properties. In this section, investigation of the optimum amount of L101 was performed in order to obtain maximum elongation at break. L101 was evaluated at 0.5, 1, 2, 3, and 4 %wt. Visual observation, and evaluation of mechanical, thermal and permeability properties were used.

## **2. LITERATURE REVIEW**

### **2.1 Introduction**

Plastics, as we know, have a tremendous impact on today's life. They are constituents of many household products around us since they were first commercially introduced in the 1930's. Since then they have become increasingly used. However, plastics are obtained from petroleum resources which may become short in the near future. In addition, a lot of concerns about environmental issues have been cited regarding plastics, especially plastic packaging, after it has been used and becomes trash needing to be disposed. A significant increase in oil prices is another impetus to the change of using biobased polymers instead of their conventional counterparts. According to the US Environmental Protection Agency (US EPA or EPA for short), municipal solid waste (MSW) increased from 88.1 million tons in 1960 to 253.7 million tons in 2005 but dropped a little to 250.4 million tons in 2010 and increased to 250.9 million tons in 2012 [12]. MSW has been handled by processes such as recycling, landfilling, and incineration. The recycling rate has continuously increased from 6.4% in 1960 to 34.5 % in 2012 [12]. Landfilling is also one of the ways to manage the increasing garbage, especially plastics packaging. According to the 2009 EPA report, the number of landfills decreased from 7,924 in 1988 to 1,908 in 2009 as indicated in Figure 2.1 but the landfill sizes increased [13].

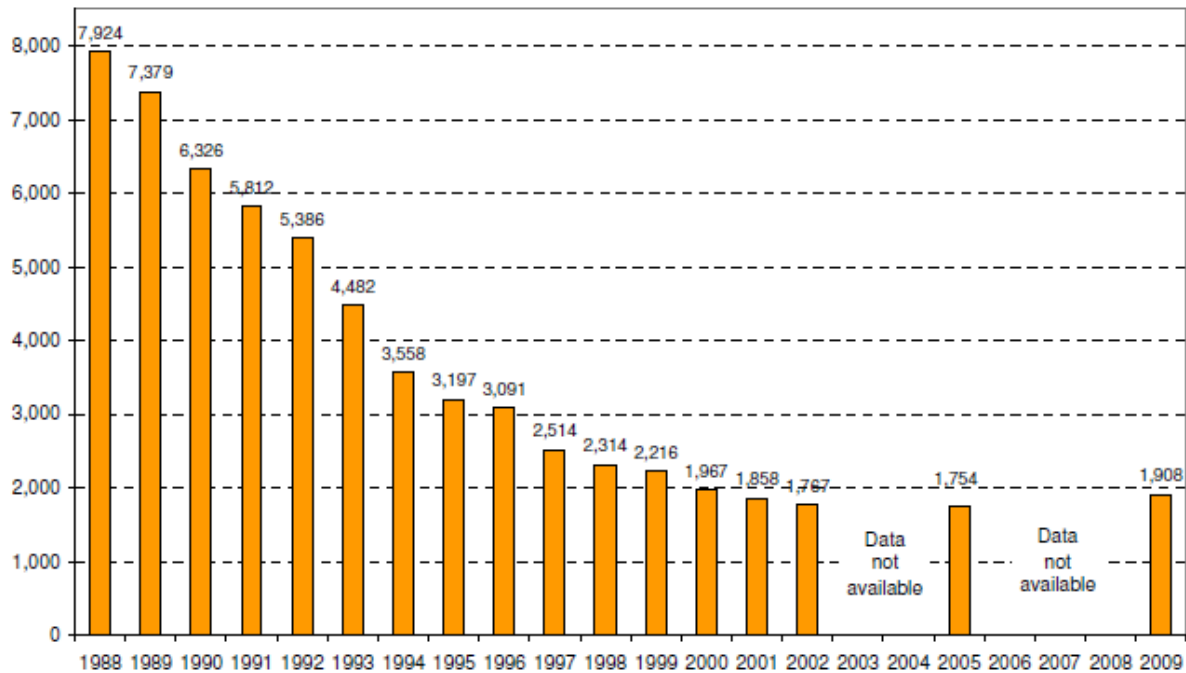


*Figure 2.1 Number of Landfills in the United States from 1988 to 2009 [13]*

The quantity of MSW discarded to landfill has increased from 82.5 million tons in 1960 to 131.9 million tons in 2009. However, there are many problems in recycling and landfill. In recycling, energy is used (but generally less than in production of new products) during the process which can release greenhouse gases, resulting in environmental problems such as global warming, extreme climate changes and so on [14, 15]. In landfilling, in addition, some of the degradable wastes remain in place, as there is not enough moisture and oxygen for microorganisms to totally degrade such massive waste. This leads to a slow degradation process. Moreover, leachate, a liquid produced by waste, is another problem in landfills. It can contaminate the water reservoirs nearby. Methane gas, a greenhouse gas, from the waste is also a problem and it needs to be monitored and carefully collected out of the sites; otherwise it will release to the atmosphere and cause global warming [16]. In addition to those processes

mentioned above, petroleum based polymers used in household products cannot be easily degraded. Therefore, a potential solution to these problems is to find a new plastic material which can naturally degrade and leave no residue in the environment. The material in the question is biodegradable plastic.

## **2.2 Biodegradable polymers**

Biodegradable plastics are defined as “a degradable plastic in which the degradation results from the action of naturally-occurring micro-organisms such as bacteria, fungi, and algae and results finally in production of carbon dioxide and water” according to ASTM D6400-04 [17]. Biodegradable polymers can be classified into two categories depending on their original sources – petroleum based polymers obtained from petroleum products; and bio-based polymers obtained from natural resources. Examples of biodegradable petroleum based polymers are polycaprolactone, polybutylene succinate terephthalate, and polyvinyl alcohol. For bio-based polymers, polysaccharides, proteins, lipids, polyesters obtained from microorganisms such as polyhydroxyalkanoates (PHAs) and polyesters from polymerization of natural monomers such as polylactic acid (PLA) are examples [18].

### 2.2.1 Petroleum based biodegradable polymers

Several petroleum based biodegradable polymers can be found in today's products. Despite being synthetic polymers, they can be naturally degraded in certain environments.

#### 2.2.1.1 Aliphatic polyesters

Most petroleum-based biodegradable polymers are aliphatic polyesters. Many different monomers can be used to produce these polyesters. They are obtained mostly from ring opening polymerization processes [19, 20].

Poly(butylene succinate), PBS, a crystalline thermoplastic, is produced by condensation polymerization of glycols like ethylene with aliphatic dicarboxylic acids like succinic acid or adipic acid [21]. PBS is produced under the trade name Bionolle® by Showa HighPolymer, Japan and the name Enpol® by Ire Chemical, Korea [22]. The properties are similar to polyethylene and polypropylene in elongation and tensile strength. Moreover, PBS has better processability than PLA. This results in suitability for packaging applications [23].

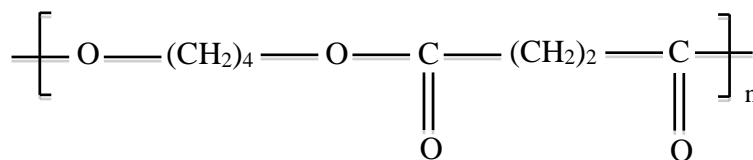
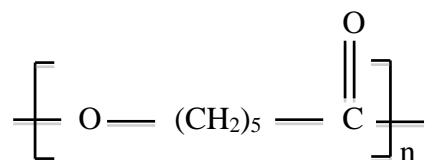


Figure 2.2 Poly(butylene succinate) molecular structure

Polycaprolactone, PCL, a semi-crystalline polymer, is produced by ring opening polymerization of  $\epsilon$ -caprolactone with the help of tin acetate as a catalyst [24]. It is sold under the trade name CAPA® from Solvay, Belgium; Celgreen® from Daicel, Japan; and Tone® from Union Carbide, USA [9].



*Figure 2.3 Polycaprolactone molecular structure*

Polyglycolide, PGA, a crystalline linear polyester, is obtained by ring opening polymerization of cyclic lactone. It has high mechanical properties. However, it has some drawbacks in instability in solvents and high degradation rate [25, 26].

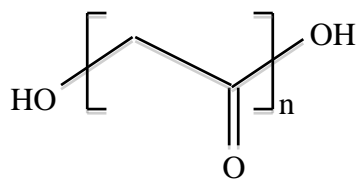


*Figure 2.4 Polyglycolide molecular structure*

Poly(trimethylene carbonate), PTMC, a flexible polymer, is produced by ring opening polymerization of trimethylene carbonate using diethylzinc as a catalyst. The resulting polymer has poor mechanical properties [27].

#### 2.2.1.2 Aliphatic-aromatic copolymers

Many aliphatic petroleum based biodegradable polymers have been used in several applications. However, there are some drawbacks. These aliphatic polymers tend to have low mechanical properties but high degradation rates, whereas aromatic biodegradable polymers have low degradation rates. In order to trade off the properties of both, aliphatic-aromatic copolyesters have been prepared by copolymerization of aliphatic and aromatic monomers.

Poly(butylene adipate-co-terephthalate), PBAT, is prepared by polycondensation of 1,4-butanediol, and an adipic acid and terephthalic acid mixture. Ecoflex® is its trade name from BASF, Germany; Origo-Bi® from Novamont, Italy; and Easter Bio® from Eastman Chemical, USA. It has high mechanical properties when it contains more than 35 mol % terephthalic acid; however, with more than 55 mol % terephthalic acid, its biodegradability is decreased dramatically [28, 29].

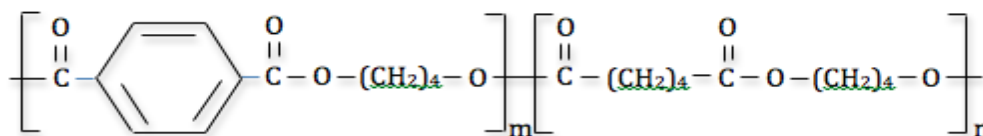


Figure 2.5 Poly(butylene adipate-co-terephthalate) molecular structure

Biomax®, DuPont, USA, has produced this polymer by modification of poly(ethylene terephthalate) with diethylene glycol and dimethylglutarate monomers. By adding the monomers, it leads to weak bonds in the Biomax structure, which are vulnerable to hydrolysis. The degradation process of Biomax is that it first degrades by hydrolysis and then biodegrades by action of microorganisms [30].

### *2.2.2 Bio-based polymers*

Bio-based polymers derive from renewable resources such as starch, corn and microorganisms. They are mostly used as disposable goods especially catering items such as food trays, bowls and kitchen utensils, etc.

#### *2.2.2.1 Starch*

Starch, a renewable resource material, is obtained from plants. It is a cheap and available material consisting of chains of two types of starch, amylose and amylopectin, in different ratios from 18-33 % amylose and 72-81 % amylopectin. This results in different types and properties of starch. Amylose is a linear chain of D-glucose joined by  $\alpha$ -1, 4 linkages in the main chains with molecular weight of 2,000 – 150,000. Amylopectin is a branched chain of D-glucose with the branches joined by  $\alpha$ -1, 6 linkages and  $\alpha$ -1, 4 linked backbone. Amylopectin has molecular weight of 65 – 500 million [31, 32, 33]. Amylose in starch ranges from 17% in cassava to 27% in maize. Figure 2.6 and 2.7 show the molecular structures of amylose and amylopectin.



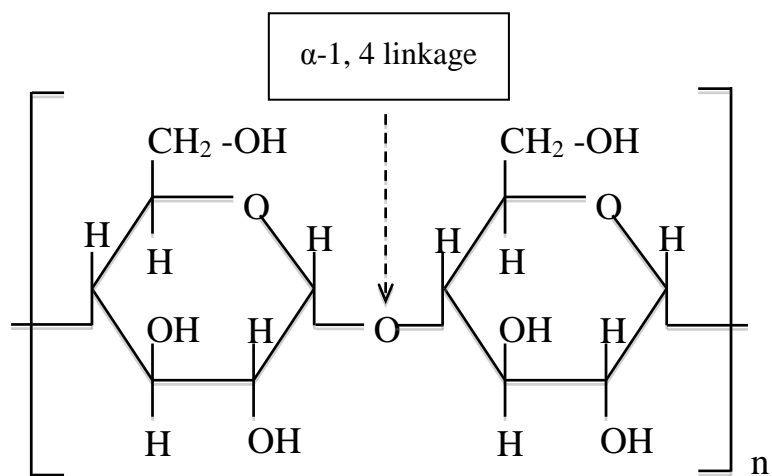


Figure 2.6 Amylose molecular structure

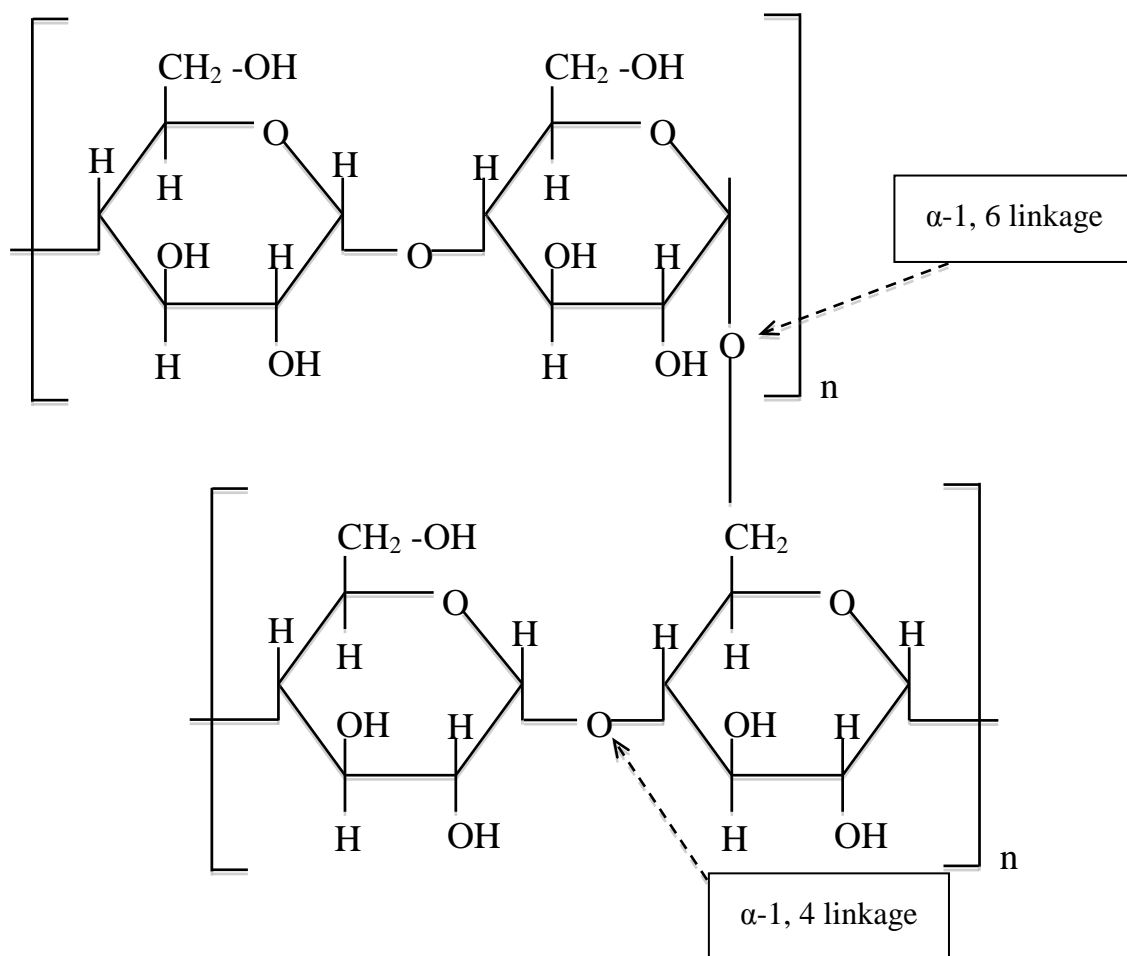


Figure 2.7 Amylopectin molecular structure

### 2.2.2.2 Cellulose

Cellulose is a renewable resource that consists of long linear chain molecules of  $\beta$ -1,4 linked D-glucose as shown in Fig. 2.8. It is obtained from plant and microorganism cell walls. Unlike starch, it cannot be dissolved in water. Generally, it is used as a reinforcement material in polymer applications [34, 35]. Moreover, cellulose is a main constituent in the paper industry.

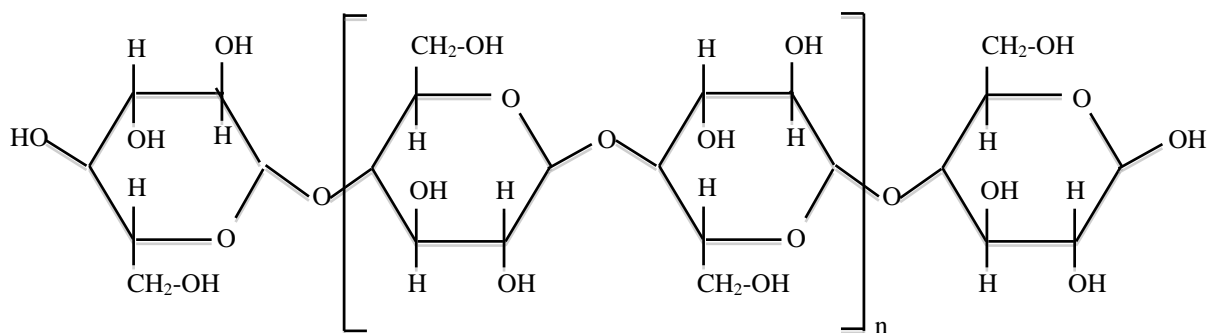


Figure 2.8 Cellulose molecular structure

### 2.2.2.3 Soy based bioplastic

Soybean is an inexpensive and versatile resource for fabrication of plastics. It consists of 18-20% oil, 40-45% protein, 25-30% carbohydrate and 3% other constituents. Soybean has mostly been used for production of soybean oil, and the remaining material after oil production is used as livestock feed. For polymers, soybean, with amino acids and other side chains as its structure, is fabricated as edible and nonedible film by adding plasticizers for flexibility and crosslinking agents such as glutaraldehyde, formaldehyde, gossypol and lactic acid for water resistance and mechanical strength [36, 37]. Felix et al. blended soy protein and albumin in

several different ratios in the presence of 40% wt. glycerol. They found that, at 50/50% wt., the soy protein and albumin blend reached the highest stress when compared to other ratios of the blends [37]. Zhou et al. studied a blend of guanidine hydrochloride modified plasticized soy meal (mPSM) with polybutylene adipate-co-terephthalate (PBAT) compared to a blend of plasticized soy meal (PSM) with PBAT at the same ratio of 60% wt. PBAT. The PSM/PBAT blend had lower tensile strength and elongation at break than the mPSM/PBAT blend [38].

#### *2.2.2.4 Zein bioplastic*

Zein is a protein from corn (maize). It is soluble in alcohol solution and used in the production of coatings, binders, adhesives and biomaterials including food packages [39, 40]. Du et al. reported on blends of zein and polyurethane at different ratios. With an increase of polyurethane weight in the blends, tensile strength decreased whereas elongation increased [40]. Zein is also used for fabrication of composite materials. Zein/montmorillonite (MMT) nanocomposite films were produced by two different approaches, solvent casting and blown extrusion at 0, 1, 3, 5, and 10% wt MMT. The resulting tensile strength of the blends increased with an increase of MMT and reached maximum values at 5% wt MMT for the solvent casting method and 1% wt MMT for the blown extrusion method. Adding MMT in the blends beyond those values decreased tensile strength. Water vapor permeability of the blends was decreased with an increase of MMT [41].

#### 2.2.2.5 Polylactic acid

Poly(lactic acid), PLA, is a biodegradable aliphatic polyester. It is mostly derived by catalytic ring-opening polymerization of lactide monomers. The molecular structure of PLA is composed of L-lactide, D-lactide, and Meso or L,D-lactide as shown in Figure [42].

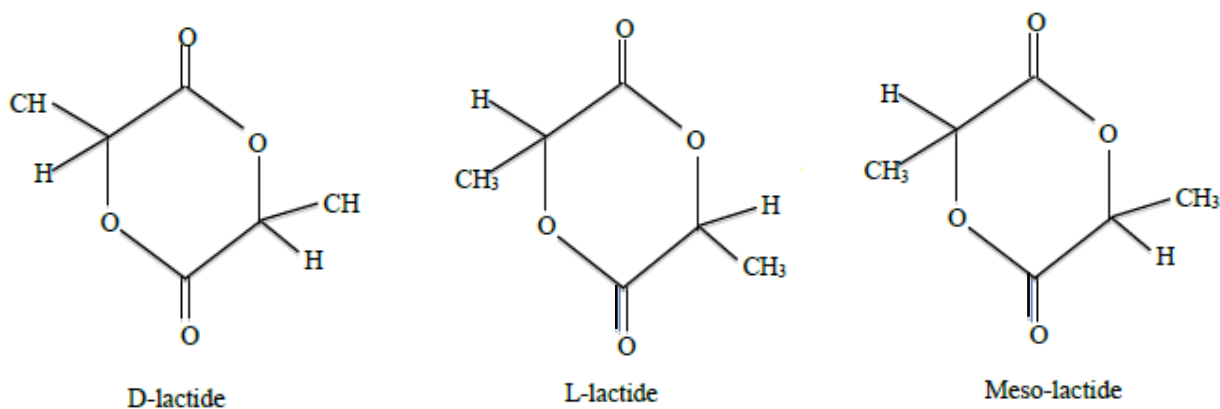
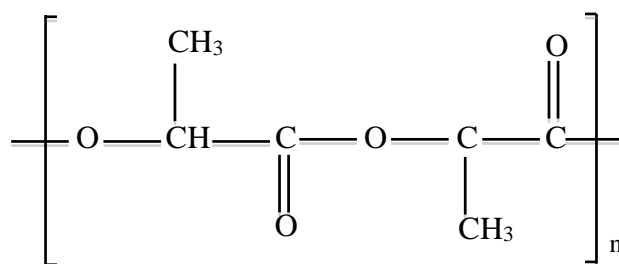


Figure 2.9 Molecular structure of D-lactide, L-lactide, and Meso-lactide

The production of PLA is done by first depolymerization of low molecular weight PLA under low pressure in order to obtain three different lactides. Then all lactides undergo catalytic ring-opening polymerization to produce high molecular weight PLA. With various contents of L-lactide and D-lactide, special types of PLA for different applications are obtained. PLLA, poly-L-lactide, contains a high amount of L-lactide. PDLA, poly-D-lactide, on the other hand, has a high amount of D-lactides. Both are considered to be semicrystalline homopolymers. PDLA, poly-DL-lactide, is a copolymer of D-lactide and L-lactide. At low D-lactide content in predominantly PLLA, it is semicrystalline; as D-lactide content increases, it becomes amorphous [42, 43].

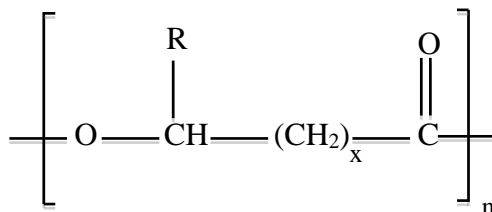


*Figure 2.10 Molecular structure of poly(lactic acid)*

PLA has glass transition temperature ( $T_g$ ) and melting temperature ( $T_m$ ) ranging from 50-80 °C and 130-180 °C, respectively [44]. It has both high tensile strength and Young's modulus whereas its elongation is low. PLA has better barrier for water vapor, oxygen, and carbon dioxide than polystyrene (PS) and starch based polymers [45, 46]. PLA is mostly used in packaging applications, especially in food packages, but its usage is limited in flexible applications due to its lack of flexibility. Many efforts have been made to improve the properties of PLA for suitable applications. PLA was blended with poly(trimethylene carbonate) and talc; the resulting elongation was increased compared to neat PLA even if tensile strength was lower [47]. PLA/PCL (polycaprolactone)/EPO (epoxidized palm oil) blends were studied by Jaffar et al. who found that PLA/PCL (80/20 %wt) with an increase of EPO content increased elongation and reached maximum elongation at EPO 10% wt [48].

#### 2.2.2.6 Polyhydroxyalkanoates

Polyhydroxyalkanoates, PHAs, are linear biodegradable polyesters which are found in bacterial cells. The production of PHAs is based on a fermentation process with control of the carbon substrate and then isolation of PHA from bacteria cells. The most common type of PHA is polyhydroxybutyrate, PHB. Another type of PHA often seen is polyhydroxyvalerate, PHV. The molecular structures of PHB and PHV are shown in Fig. 2.11 [49].



R = CH<sub>3</sub> is PHB

R = CH<sub>2</sub>CH<sub>3</sub> is PHV

*Figure 2.11 Molecular structure of PHAs*

PHAs have a high potential to be used as renewable polymers due to their biodegradability and stiffness for rigid packaging applications. However, brittleness is a serious drawback, so the use of PHAs in flexible applications is limited. Alternatively, the copolymer of PHB and PHV, poly(hydroxybutyrate-*co*-valerate), PHBV, was fabricated in order to improve flexibility but its properties have not yet been accepted by the flexibles industry [18, 49].

## **2.3 Biodegradable polymer modification for flexibility**

### *2.3.1 Polymer blends*

Polymer materials in use today have some limits to their potential use in certain applications. Instead of development of brand new materials, blending is one of the ways to gain some desired properties. It is an inexpensive and easy process. Blending is also useful for optimizing some properties between two or more polymers for specific uses.

Moreover, polymer blends are basically developed for solving polymer application issues, especially for biodegradable polymers, which have many drawbacks largely in polymer processing and application. PHBV has low melt strength, high stiffness, and a low crystallization rate that needs some time to solidify. This, in turn, results in tackiness which is not desirable for processing. A polymer blend is a physical mixture of more than one type of polymer and the resultant polymer is called a polymer alloy. It can be either miscible, immiscible, or partially immiscible. The majority of blends are immiscible due to a weak interface between the two components. The thermodynamic equation of polymer miscibility between two compositions is shown in the following formula [50, 51].

$$\Delta G_{\text{mix}} = \Delta H_{\text{mix}} - T\Delta S_{\text{mix}}$$

where  $\Delta G_{\text{mix}}$  = the free energy of mixing (Gibbs free energy)

$\Delta H_{\text{mix}}$  = the enthalpy of mixing

$\Delta S_{\text{mix}}$  = the entropy of mixing

Miscibility occurs when  $\Delta G_{\text{mix}}$  is less than zero. Otherwise, immiscibility will be observed.

Moreover, the polymer mixing also needs to follow the equation below in order to avoid phase separation [50].

$$\left( \frac{\partial^2 DG_{\text{mix}}}{\partial \phi_i^2} \right)_{T,P} > 0$$

where  $\phi$  = volume fraction of polymer i in the polymer mixture

The critical point of the spinodal (the boundary of single phase and separated phases) appears as shown in Figure 2.12. The lower critical solution temperature (LCST) is the temperature below which all compositions of a polymer mixture are miscible. The upper critical solution temperature (UCST) is the temperature above which all compositions of a polymer mixture are miscible.



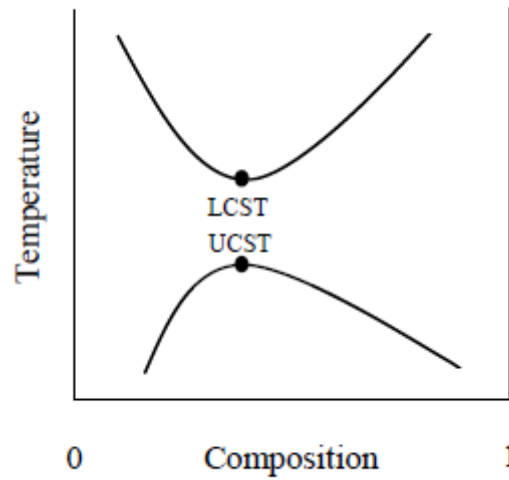


Figure 2.12 Polymer blend phase diagram, adapted from [50]

For binary polymer blends, the free energy can be calculated using the Flory-Huggins model [50].

$$\Delta G_{mix} = kTV \left[ \frac{j_1}{V_1} \ln j_1 + \frac{j_2}{V_2} \ln j_2 \right] + j_1 j_2 \chi_{12} kTV / v_r$$

where  $\Delta G_{mix}$  = the free energy of mixing (Gibbs free energy)

$V$  = total volume

$R$  = gas constant

$\phi_1, \phi_2$  = volume fraction of component 1 and 2

$V_1, V_2$  = molecular volume of component 1 and 2

$v_r$  = molecular volume of a specific segment

$k$  = Boltzmann's constant

$\chi_{12}$  = Flory-Huggins interaction parameter

### 2.3.1.1 Characterization of polymer blends

A miscible blend appears to be a single phase, which basically exhibits a single glass transition temperature ( $T_g$ ). The  $T_g$  of the blend has a value between that of each polymer. For partially miscible and immiscible blends, there will be two  $T_g$ s which belong to each of the polymers. In miscible blends,  $T_g$  can be estimated from the weight fraction of the components in the blend [52].

$$T_g = w_1 T_{g1} + w_2 T_{g2}$$

where  $w_1$  = weight fraction of component 1

$w_2$  = weight fraction of component 2

Blending can be done in mixers and extruders. With shearing force in the equipment, polymer structures break into droplets and mix together, leading to a dispersed phase of one polymer into the continuous phase of another [53]. This behavior of the blend is immiscible. Miscibility of the blends is dependent upon molecular structure, interfacial interaction including polarity, solubility and rheological behaviors of the polymer constituents. Poor blending gives unstable immiscible blends, in which the interfacial force between the two polymers is compromised, resulting in poor mechanical properties. Strong interface interaction between the two polymers gives small droplets dispersed evenly into the continuous phase leading to enhanced properties. This blend is considered as a compatible blend [54, 55, 56]. However, most polymer blends are incompatible, and have weak interfaces in the blend structure resulting in poor properties. Adding of compatibilizer is an answer to this situation. It is added to the blends during the blending process in order to reduce interfacial tension, improve dispersion

and enhance stabilization of the blends [57]. A typical compatibilizer structure is a block copolymer which is miscible in both polymers, or one side of its structure is miscible in one polymer and the other side is miscible in another polymer [57]. The resulting blend is compatible and results in property enhancement. Another method to create a compatible blend is reactive compatibilization. This process involves adding functional groups into the blends during blending in the presence of a catalyst. It creates end group reactions, chain cleavage, bond formation and crosslinking, resulting in interfacial interactions in the blends [55, 57, 58].

### 2.3.2 Polymer grafting

Polymer grafting is a polymer modification method involving adding monomers onto other polymer chains (backbone) at different spots of the main chain in order to enhance characteristic properties of the backbone and obtain desired properties for suitable applications such as thermal and mechanical resistance. The backbone polymer can be a homopolymer or a copolymer and the monomers as a side chain can be one or more different types. The monomers are bonded covalently onto the polymer main chains and the resulting polymers (copolymers) are branched polymer chains as shown in Figure 2.13 [59, 60, 61, 62].

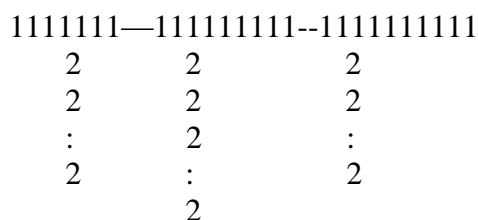


*Figure 2.13 Graft copolymer diagram, adapted from [59]*

Functional groups in the main chain are essential in the grafting process. They are effective sites for monomer side chains to be covalently bonded onto the backbone. There are two different types of grafting process, grafting from and grafting to. Grafting from is a process in which active sites at functional groups are initiated and then they are polymerized onto the backbone which is previously not initiated. Grafting to is a process in which active spots of both the backbone and monomers are initiated and then polymerization occurs on the reactive sites [60, 63].

Grafting processes can be carried out by different methods. The principle of grafting is to create active sites at functional groups or free radicals on the backbone chain initiating the grafting reaction. There are several grafting processes. Chemical grafting is the process of adding chemicals as initiators to create active spots in the backbone. In radiation grafting, active sites are initiated and controlled by radiation. Enzymatic grafting is another technique with mild environment requirements. Enzymes are used to initiate active sites. In the plasma initiated grafting process, surface grafting is initiated by plasma exposure. The reaction steps of all grafting methods are electron-induced excitation, ionization and dissociation [63].

Polymer grafting normally has an advantage over polymer blending. In the grafting process, two components are covalently bonded, while in blending, two polymers are mixed physically creating a weak interface between them [59, 60].

In a grafted polymer, the  $T_g$  is found as the  $T_g$  of each polymer constituent in the blend or graft polymer, corresponding to the  $T_g$  of each homopolymer. Crystallinity of the grafted polymer

normally consists of crystallinity of each homopolymer in the polymer. If each homopolymer is crystalline, the resulting grafted polymer will have two melting temperatures ( $T_{ms}$ ) [64].

Suchao-in et al. reported compatibility of starch grafted poly(butylene succinate) was improved and mechanical properties increased when compared to neat poly(butylene succinate) [65]. Vlcek et al. stated grafting methyl methacrylate onto cellulose diacetate using the atom transfer radical polymerization (ATRP) method, is a modern process to create free radicals. Grafted materials with several lengths and densities can be obtained [66]. Grafting of epoxy onto grapheme oxide in various ratios was reported to significantly increase tensile strength compared to neat epoxy with inherent brittle behavior [67].

### *2.3.3 Crosslinking polymers*

Crosslinking is another polymer modification method in which polymer chains are covalently bonded within molecular chains (intramolecular crosslinking) or between chains (intermolecular crosslinking) in multiple dimensions, as shown in Fig. 2.14. It is an irreversible reaction and resulting polymer properties are dependent upon the degree of crosslinking. At a low degree of crosslinking, crystalline polymers have lower crystallinity because the crosslinked portions in the structure interfere with chain orientation. This results in a polymer with lower melting temperature, soft and elastic characteristics. Crosslinking reduces the free volume due to the change in molecular alignment, resulting in a higher  $T_g$  [60].



*Figure 2.14 Molecular crosslinking, adapted from [60]*

*(a) Intramolecular crosslinking (b) Intermolecular crosslinking*

In crosslinked polymers, polymer chains are restricted and cannot easily move with respect to one another. However, crosslinking gives elasticity to amorphous structures. The properties of crosslinked polymer are enhanced depending on the degree of crosslinking. The crosslinked material has good resistance to light, heat, and chemicals and good mechanical strength [60].

Crosslinking processes are similar to those of grafting. In chemical processes, a conventional method is redox reactions. Free radicals are created and reaction occurs. This method is simple and it can be performed at room temperature and in aqueous solution. Another chemical method is living radical formation. Chain growth occurs in the presence of monomers and the chain can continue to grow as long as the monomers are supplied. The constantly growing chains are not hindered by chain termination since the process is controlled by allowing a higher initiation rate than the propagation rate or by eliminating chain termination. In the enzymatic method, enzymes are used to initiate the reaction sites and the crosslinking reaction occurs. This method is mostly used in the grafting process. A polycondensation reaction is a

crosslinking process with an elimination of two reaction sites (functional groups). When two functional groups are eliminated the reaction occurs, simultaneously producing byproducts [60, 63].

Moreover, the use of interpenetrating polymer networks (IPN) is another way for crosslinking. IPN performs by combining two polymer networks and crosslinking one polymer in the presence of another. It differs from chemical crosslinking in that no induced covalent bonds are involved between the two polymers. Elastomer crosslinking is the crosslinking process that is used in elastomers. Elastomers inherently deform under load, resulting in limitations on their use in many applications. The best known elastomer crosslinking is vulcanization. It is a chemical process in which long chain molecules are crosslinked into a 3-dimensional network. The polymer first appears to be thermoplastic and then becomes elastic or hard, depending on the degree of crosslinking. The resulting polymer has mechanical strength, elasticity, rigidity, and durability in deformation under different conditions [60]. The radiation technique is a crosslinking process that uses radiation to induce free radicals in the polymer chain. The reaction occurs at free radical sites [60, 63].

## **2.4 Poly(hydroxybutyrate-*co*-valerate)**

Poly(hydroxybutyrate-*co*-valerate), PHBV for short, is a copolymer in the family of polyhydroxyalkanoates (PHAs). It is a biodegradable aliphatic copolyester produced and stored in bacterial cells as an energy source [2, 18, 68]. Its structure is shown in Fig. 2.15.

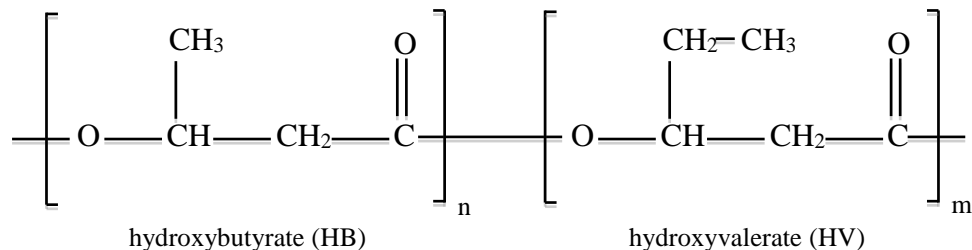


*Figure 2.15 Molecular structure of PHBV*

The properties are dependent upon the ratio of the length of PHB and PHV chains. The most common form of PHA is poly(3-hydroxybutyrate) (PHB) which has a methyl group as a side group and x as 1 (see Fig 2.11). Another form of PHA is polyhydroxyvalerate (PHV) with an ethyl group as a side group and x as 1. PHB has high crystallinity and excellent mechanical properties, similar to polypropylene (PP) [3, 69]. However it has disadvantages of high brittleness and low elongation. An alternative to overcome the drawbacks is its copolymer, PHBV. PHBV has higher toughness and lower melting point than PHB [3].

PHBV is a copolymer of polyhydroxybutyrate (PHB) and polyhydroxyvalerate (PHV) and is a thermoplastic hydrophilic aliphatic biodegradable polymer in the family of polyhydroxyalkanoates (PHAs). PHBV is produced in order to improve the properties of PHB which is the most common form of PHAs [2, 18]

PHBV is produced by fermentation of bacteria in the presence of a carbon source with a lack of one of the elements that is essential to amino acid production along with adding propionic acid. This results in production of PHBV in the bacteria cells. With the control of ratios of



ingredients in the media, PHBV with various ratios of PHB and PHV can be obtained (see Fig. 2.15) [2].

PHBV's price is high due to the costly production when compared to petroleum-based resins. Biopol, the PHBV trade name, was approximately US\$ 4-8 per kg as reported in 1998 compared to petroleum resins such as polypropylene at US\$ 0.6-0.9 per kg [70]. Therefore, its price was a barrier to its application. However, there have been efforts to develop bacteria strains and improve the production process to be able to reduce the cost of PHBV, for example, *Alcaligenes eutrophus* produced by ZENECA Bio Product, UK, *Alcaligenes latus* manufactured by Biotechnologische Forschungs Gesellschaft, Austria and so on [71].

#### 2.4.1 Poly(hydroxybutyrate-co-valerate) structure and properties

The properties of PHBV vary depending on the quantity of hydroxyvalerate (HV) in the structure. HV makes PHBV more flexible than PHB, which is more stiff and brittle and inappropriate for many applications, even if its properties are similar to polypropylene [3, 72]. In addition to the flexibility derived by copolymerization, PHBV possesses a lower  $T_g$ ,  $T_m$ , percent crystallinity, tensile strength and flexural modulus, but greater elongation and impact strength than PHB. The lower  $T_m$  is beneficial for thermal processing. This is because the low processing temperature reduces thermal degradation of the plastic [2, 18]. Luzier reported that PHBV with 20 % HV which was produced by ICI had significantly reduced percent crystallinity, from 80 % (with 0 % HV) to 35 %, resulting in a reduction of  $T_m$  from 177 °C to 130 °C, and of tensile strength from 40 MPa to 20 MPa [2]. Chen and Wu stated similarly that

$T_m$  and tensile strength were reduced with an increase in the quantity of HV [73]. However, PHBV, even though its properties are a little better than PHB, still possesses brittleness, low elongation at break, high crystallinity, and tackiness for several minutes until it solidifies [74, 75, 76, 77]. These characteristics of PHBV mean it is still not suitable to be used in flexible applications.

#### *2.4.2 Enhancement of poly(hydroxybutyrate-co-valerate) properties*

##### *2.4.2.1 Poly(hydroxybutyrate-co-valerate) blends*

PHBV blending is one of the practical ways to overcome its drawbacks for commercial applications. Wang et al. studied a blend film of PHBV and poly(3-hydroxybutyrate-co-4-hydroxybutyrate (P3/4HB) prepared by a solvent-casting method. The blend was miscible as evidenced by the single  $T_g$  observed. It has a helical structure like neat PHBV as measured by FTIR. The elongation at break increased when P3/4HB increased. This means the more P3/4HB in the blend, the greater the amount of ductility observed [78]. A PHBV/PHB blend was studied by Sombatmankhong et al. It was useful for bone scaffolds at 50/50 w/w which indicated maximum alkaline phosphatase (ALP) activity [79]. There was also a study of PHBV/poly(3-hydroxybutyrate-co-3-hydroxypropionate (PHBP). The blend at 1/1 was produced by a solvent-casting method in chloroform and crystallization was analyzed by FTIR. Yoshie et al. found that, at lower spherulite growth rates, both components can have more phase separation. HV units of PHBV were included in the PHB lattice of PHBP, while HP units hardly penetrated the PHBV lattice [80].

Park et al. also investigated PHBV blends with poly(butadiene-co-acrylonitrile) (NBR). A single  $T_g$  was observed and shifted with composition of the blend. This means the blend was miscible, corresponding to the fact that NBR suppressed PHBV crystallization. In addition, tensile strength was lower while elongation at break was greater with a higher amount of NBR [81]. Crystallization of PHBV blends with poly(dicyclohexylitaconate) was also studied. The blend was immiscible as shown by FTIR [82]. Another study by Li et al. examined melt blending of PHBV and poly(propylene carbonate) (PPC) at 30:70 w/w. FTIR and SEM study showed that the blend was immiscible with PPC as the continuous phase and PHBV as the dispersed phase [83]. Differential scanning calorimetry (DSC) was applied in analysis of blends of PHBV/poly(ethylene succinate) (PES) prepared by chloroform. The blends were immiscible as observed by having two  $T_g$ s. The crystallization process was not changed in the blend and tensile strengths of the specimens decreased while elongation increased with higher amounts of PES [84]. In a degradation study of PHBV blends, Imam et al. observed PHBV/cornstarch blends in natural compost for more than 125 days. They found that weight loss of 50% wt of the cornstarch blend was highest followed by 30% wt of cornstarch and then neat PHBV. Starch in the blend expedited PHBV degradation [85]. Furthermore, degradation of a PHBV and polypropylene (PP) blend film at 4:1 prepared by pressing in a hot plate was investigated by Goncalves et al. The film was buried in soil for 120 days. The degradation occurred at the polymer interfaces of the blend and amorphous portion of PP by microbial activity. This resulted in a change in the morphology of the blend structure. For neat PHBV, it was totally degraded through the action of microorganisms within 30 days [86].

#### 2.4.2.2 *Poly(hydroxybutyrate-co-valerate) grafting and crosslinking*

Lao et al. reported 2-hydroxyethyl methacrylate, 2HEMA, was grafted onto the surface of PHBV film in the presence of an initiator, benzophenone (BP) or H<sub>2</sub>O<sub>2</sub>. Fourier transform infrared spectroscopy (FTIR) showed the resulting PHBV was successfully grafted. The grafting process was easy and fast [87]. In addition, PHBV grafted with 2HEMA also was investigated by Wang et al. HEMA was grafted on PHBV in the presence of Lupersol 101 as an initiator in an extruder, in a reactive extrusion process. The existence of grafting was confirmed by nuclear magnetic resonance spectroscopy (NMR). The resulting material was still rigid, brittle and tacky and took a long time to solidify [88]. Wang et al. stated that PHBV grafted with poly(N-vinylpyrrolidone) (PVP) had a higher Young's modulus while its elongation was decreased. Hydrophilicity of the grafted PHBV was increased as measured by water contact angle [89]. Another study of PHBV grafting involved photografting of polyacrylamide. The grafted material was found to have a lower degree of crystallinity than PHBV since grafting hindered the crystallization process. This could be observed by a decrease in endothermic enthalpy or heat of fusion [90]. Gamma irradiation was also used for grafting acrylic acid onto a PHBV surface. The degree of grafting obtained was dependent upon the acrylic acid concentration and radiation dose. The functionalized material was suitable for biomolecules to be attached for tissue engineering [91].

Crosslinking is another modification method for improving serious drawbacks of PHBV properties, especially a lack of flexibility and low elongation. Fei et al. studied blending of 4,4-dihydroxydiphenylpropane (BPA) in PHBV and *p-tert*-butylphenol (TBP) in PHBV. FTIR

revealed that there was a strong H-bond between the blend components, and DSC showed that crystallization of PHBV was decreased by BPA and TBP [92]. Furthermore, PHBV itself was crosslinked with the help of dicumyl peroxide as an initiator. NMR, which was used for indication of the reaction location of the crosslinking, indicated that the reaction position was tertiary carbons in PHBV. Crystallinity and crystallization temperature ( $T_c$ ) and  $T_m$  decreased with a greater amount of initiator. Additionally, compression molded films from the modified PHBV had greater elongation when compared to neat PHBV [93].

## **2.5 Biodegradation of poly(hydroxybutyrate-co-valerate)**

Plastic, as we know, is durable and persistent and does not easily degrade in normal environments. This problem is recognized and waste disposal is becoming a concern in many countries. Plastic is one of the major solid wastes, which are created every year and must be managed properly. As mentioned earlier in this chapter, recycling, landfilling and incineration are used to manage solid wastes [12, 94]. However, one of the alternative ways to manage this problem is to use biodegradable polymers. This is becoming attractive to many researchers. Biodegradable plastics are vulnerable to microbial degradation resulting in reducing waste volume for landfilling. They are considered as environmental friendly materials. They have a potential use in agricultural areas. For example, biodegradable mulch film has been used to control sunlight and insects for perishable products. It can degrade and leave no residue [94].

Biodegradation is the process of microbial attack in order to break down plastic materials (see biodegradable plastic definition in section 2.2). The process occurs in a damp environment.

This means, without the presence of water, microorganisms are unable to consume polymer molecules. The biodegradation steps are that microorganisms release enzymes to depolymerize plastic materials until the material becomes water-soluble intermediates. The molecules in the intermediates need to be sufficiently tiny so they can be transported into the microorganism cells and leave water and carbon dioxide as by products. This process only occurs on the polymer surface since enzymes cannot penetrate deep into the polymer matrix. There are many processes before biodegradation takes place. These processes are able to facilitate biodegradation: chemical hydrolysis, thermal degradation and chain scission and oxidation processes. These reduce the size of the polymer chains so that enzymatic degradation is expedited [94, 95].

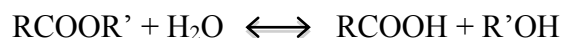
Furthermore, the biodegradation process not only depends upon the processes as mentioned earlier, but also on other parameters such as temperature, humidity, pH, salinity, oxygen and nutrient supply. This means these parameters can affect a number of microorganisms and activity of different types of microorganisms resulting in different biodegradation rates. The difference in plastic type and structure also influences biodegradation. Homopolymers and copolymers biodegrade differently. In the same polymer, biodegradation results differ in the crystalline and amorphous portions [94, 95].

#### *2.5.1 Biodegradation mechanism*

Polymer biodegradation consists of two main steps, the primary step and the biodegradation step. The primary step (depolymerization) is considered as a pretreatment. The goal is to

reduce the size of molecular chains of plastics in order for microorganisms to bring them into their cells. Either photodegradation, thermal degradation, chemical hydrolysis or oxidative chain scission is involved. The second step is biodegradation (mineralization) [94, 95]. Biodegradation can occur in two different atmospheres, aerobic and anaerobic. Aerobic conditions require oxygen for microorganisms to consume to undergo reaction. An anaerobic environment, on the other hand, is biodegradation without oxygen. This step involves transportation of tiny polymer fragments into cells, assimilation by the microorganisms and mineralization. The process produces many byproducts such as water, minerals, carbon dioxide, methane (from anaerobic environments), hydrogen, nitrogen, and new biomass [95].

Chemical hydrolysis and oxidation mostly occur in the depolymerization step. The following reaction shows hydrolysis of polyester in the presence of acid as a catalyst [94, 95].



The reaction produces acid (RCOOH), which can expedite the reaction. Enzymes, additionally, can be used as catalysts in biological hydrolysis [94, 95, 96].

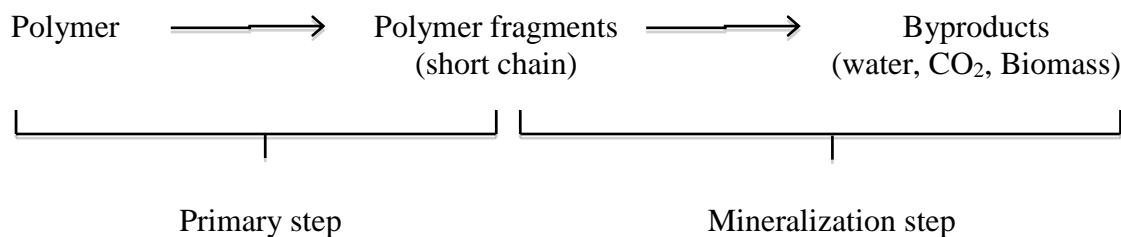
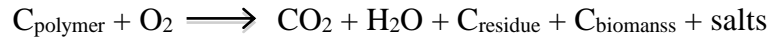


*Figure 2.16 Biodegradation mechanism of polymers*

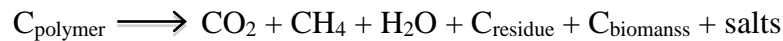
### 2.5.2 Biodegradation evaluation

Biodegradation assessment can be performed in many ways: weight loss, consumed oxygen (BOD), dissolved organic carbon (DOC) and released carbon dioxide. Moreover, infrared (IR), ultraviolet (UV), nuclear magnetic resonance (NMR), electron microscope and mechanical resistance can be used in determining the biodegradation [95].

In aerobic environments, microorganisms use oxygen to oxidize polymers (carbon source) and create end products of biomass, carbon dioxide and water. The following is the respiratory reaction in microorganism cells [95].



In an anaerobic environment, with an absence of oxygen, the reaction evolves methane as shown below [95].



Carbon dioxide evolution in the mineralization step is evaluated for biodegradation. It is used in the percent biodegradation calculation as shown in the following equation [96].



$$\% \text{ Biodegradability} = \frac{(CO_2)_T - (CO_2)_B}{ThCO_2} \cdot 100$$

where  $(CO_2)_T$  = cumulative amount of carbon dioxide evolved in reactor containing polymer, g

$(CO_2)_B$  = cumulative amount of carbon dioxide evolved in blank reactor, g

$ThCO_2$  = theoretical amount of carbon dioxide created by the polymer, which can be calculated in the equation below

$$ThCO_2 = M_{TOT} \times C_{TOT} \times \frac{44}{12}$$

where  $M_{TOT}$  = total dry solids in grams

$C_{TOT}$  = the proportion of total organic carbon in total dry solids in the plastic sample in grams

44 = molecular mass of  $CO_2$

12 = atom mass of C

### 2.5.3 Biodegradation of poly(hydroxybutyrate-co-valerate)

PHBV is a biodegradable polymer and is susceptible to microbial degradation. There is much research focusing on PHBV biodegradability. Sang et al. conducted a biodegradability test of PHBV in soil. The result showed that fungal biomass increased with respect to time of exposure indicating degradation of PHBV. Scanning electron microscopy (SEM) also showed

the increase of fungal cells [97]. Similarly, SEM proved that PHBV cracked and degraded on its surface [98]. Biodegradation of PHBV also was determined in pilot scale compared to lab scale. PHBV completely degraded in a pilot scale facility. Both biodegradability test results were not different and the percent of biodegradability was 81% [99]. Additionally, PHBV can be completely biodegraded in soil in 30 days [86, 100].

Also, anaerobic conditions were evaluated for PHBV biodegradability. Abou-Zeid et al. studied biodegradability of PHBV and PHB in two anaerobic sludges at 37 °C and the evolution of methane was detected along with weight loss. PHBV gave lower biodegradation than PHB which is in contrast to the result in aerobic conditions [101].

### 3. MATERIALS AND METHODS

#### 3.1 Materials

##### *3.1.1 Polyhydroxybutyrate-co-valerate*

Polyhydroxybutyrate-co-valerate, PHBV, in pelletized form, was manufactured by Monsanto, UK. It was donated to Michigan State University.

##### *3.1.2 Poly(butylene adipate-co-terephthalate)*

Poly(butylene adipate-co-terephthalate), PBAT, was supplied in pelletized form by BASF (Florham Park, N.J., USA) under the trade name Ecoflex® F (BX7011).

##### *3.1.3 Triethyl citrate*

Triethyl citrate, 99% was supplied by Sigma-Aldrich. It is a transparent liquid. It has been used as a plasticizer in plastic fabrication.

#### *3.1.4 Titanium dioxide*

Titanium dioxide,  $\text{TiO}_2$ , was purchased from Nanostructured & Amorphous Materials Inc., NM, USA. It is in the form of nano-particles in powder rutile form with a size of  $10 \times 40$  nanometers and 98% purity.

#### *3.1.5 2-Hydroxyethyl methacrylate*

2-Hydroxyethyl methacrylate, 2HEMA, was supplied by Sigma-Aldrich. It is in liquid form with 97% purity and the boiling point of  $67^\circ\text{C}$ . It was used for grafting onto PHBV.

#### *3.1.6 2,5-Bis(tert-butylperoxy)-2,5-dimethylhexane*

2,5-Bis(tert-butylperoxy)-2,5-dimethylhexane, L101, is an initiator for polymer reactions. It is a clear liquid product of Arkema Inc., under the trade name of Luperox 101 and was purchased from Sigma-Aldrich. It has a density of  $0.877\text{ g/cm}^3$  at  $25^\circ\text{C}$ , boiling point of  $55\text{--}57^\circ\text{C}$  at 7 mmHg and flash point of  $65^\circ\text{C}$ .

## 3.2 Equipment

### 3.2.1 Processing equipment

Melt modified extrudates were produced using a co-rotating mini twin screw extruder, DSM Micro 15 compounder, The Netherlands, with 150 mm screw length, 18:1 length to diameter (L/D) ratio, and 15 cc. capacity. The extrudates were introduced to an injection molding machine in order to shape them into disks except for the crosslinked PHBV materials, which were immediately collected from the DSM and cut into pellets, since the reaction time was important to the degree of crosslinking. Figure 3.1 shows the twin screw extruder.

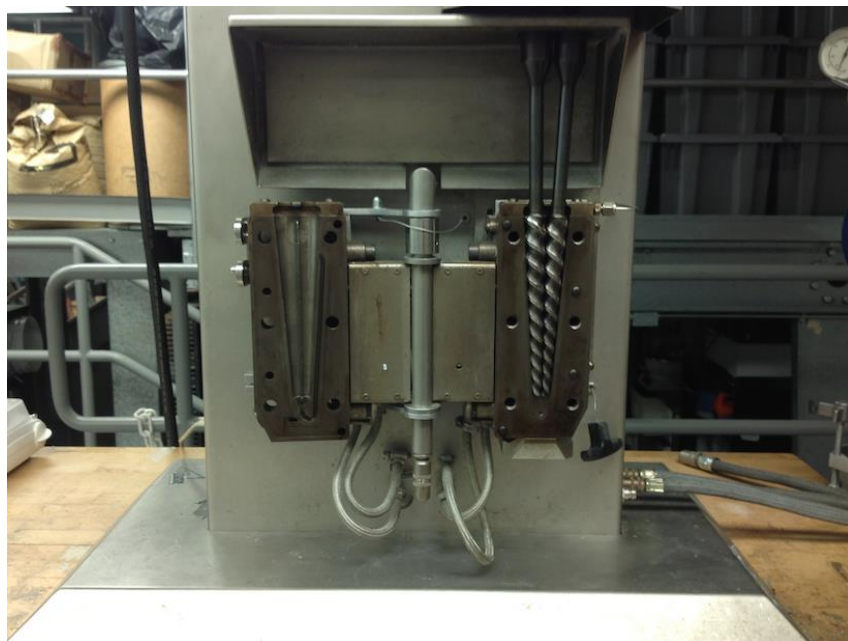


*Figure 3.1 Co-rotating mini twin screw extruder*

### *3.2.2 Compression molding*

A compression molding machine (M CARVER, Carver Laboratory Press, Menomonee Falls, Wisconsin, USA) was used to transform disk and pellet extrudates into thin sheet. All compositions of modified PHBV and neat PHBV were put in a thin aluminum frame with inner size of  $180 \times 180 \text{ mm}^2$  and thickness of 0.25 mm. and compressed at  $165^\circ\text{C}$  and 20,000 psi for 5 minutes. All the materials were cooled with a cooling unit, attached to the compression molding machine for 15 min. The cooling unit used tap water to cool the compression molded material. The compression molding machine is shown in Figure 3.2



*Figure 3.2 Compression molding machine*

### *3.2.3 Mechanical properties*

Mechanical properties of all PHBV sheets were measured using an Instron Tensile Tester 5565 (Instron, Inc., Norwood, MA, USA), according to ASTM D882-12 [102]. The sheets were conditioned at 23°C, 50% RH for more than 48 hours in accordance with ASTM D618-13 [103]. Then, the sheets were cut into 1 in. wide by 7 in. long samples. The tests were carried out with a grip separation rate of 0.5 in./min, and initial grip separation of 5 in.

### *3.2.4 Thermal properties*

Thermogravimetric analysis (TGA) and derivative thermogravimetry (DTG) of all PHBV materials were obtained using a TGA 2950 (TA Instruments, New Castle, DE, USA) in order to measure weight change as a function of temperature. 10 to 30 mg of the material was heated from 30 °C to 700 °C, at a heating rate of 10 °C/min., under a nitrogen atmosphere.

Differential scanning calorimetry (DSC) of all PHBV materials was performed using a model Q-100 DSC (TA Instruments, New Castle, DE), in accordance with ASTM D3418-03 [104]. DSC indicates the crystallization temperature ( $T_c$ ), enthalpy of cold crystallization ( $\Delta H_c$ ), melting temperature ( $T_m$ ), and melting enthalpy or heat of fusion ( $\Delta H_m$ ). The materials weighing between 5 and 10 mg were put in a non-hermetic aluminum pan. The temperature interval was between -50 and 180 °C, at a heating rate of 10 °C/min.

### *3.2.5 Permeability test equipment*

Mocon Permatran-W 3/33, Mocon Oxtran 2/21, and Permatran-C 4/41 are water vapor, oxygen, and carbon dioxide permeability test equipment for polymer films. In this study, the permeability test conditions were 23°C, 50% relative humidity (RH) for oxygen and carbon dioxide permeability, following ASTM D3985-05, and 23°C, 100% RH for water vapor permeability, following ASTM F1249-05 [105, 106].

### *3.2.6 Statistical analysis*

Analysis of variance (ANOVA) and Tukey tests were performed in order to determine significant differences at the 95% confidence level ( $p \leq 0.05$ ).

## **3.3 Poly(hydroxybutyrate-co-valerate) and modified poly(hydroxybutyrate-co-valerate) sheet fabrication**

PHBV neat resins were compression molded into sheets as described in section 3.2.2.

All modified PHBV sheets were produced in a co-rotating mini twin-screw extruder, DSM Micro 15 compounder, Netherlands. The raw materials were placed in the extruder. The production proceeded until the maximum shearing force was reached. The maximum shearing force indicated mixing at which the force from the extruder overcame the viscosity of the melt polymer and designated the residence time in this study. The residence time (reaction time)



was important since PHBV has inherent thermal degradation when exposed to high temperature. The resulting extrudates were transferred through a preheated cylinder at 155 °C to an injection molding machine set at 155 °C, to form into disks. The disks were compression molded as described in section 3.2.2. The extrusion conditions for each type of modified PHBV were as follows:

- For PHBV/TiO<sub>2</sub> blends: PHBV resins and TiO<sub>2</sub> 1% by weight were mixed in the extruder at 165 °C for 1 min.
- For PHBV/Ecoflex blends: PHBV and Ecoflex resins were mixed in the extruder at 165 °C for 2 min.
- For PHBV/Ecoflex blend/TiO<sub>2</sub> blends: PHBV, Ecoflex and TiO<sub>2</sub> were mixed in the extruder at 165 °C for 2 min.
- For PHBV/Triethyl citrate: PHBV and triethyl citrate were mixed in the extruder at 165 °C for 30 seconds.
- For PHBV grafted with 2HEMA materials: PHBV, 2HEMA and L101, as an initiator for the grafting reaction, were mixed in the extruder at 165 °C for 1 min.
- For crosslinked PHBV: PHBV and L101 were mixed in the extruder at 165 °C for 1 min.

### **3.4 Investigation of the properties of poly(hydroxybutyrate-co-valerate) and modified poly(hydroxybutyrate-co-valerate) sheet**

The properties of PHBV and modified PHBV sheets were determined as follows.

Visual appearance: PHBV and all modified PHBV were examined for visual characteristics of color and texture.

Mechanical properties: tensile strength and elongation at break were investigated by the Tensile Tester in order to obtain the material resistance under load.

Thermal properties: TGA and DSC were performed in order to determine the thermal behavior of the materials. The obtained TGA profile indicates thermal degradation characteristics (weight change) of the materials from 23 °C – 600 °C. DSC showed thermal profiles, both endothermic and exothermic behaviors, from which transition properties,  $T_c$ ,  $T_m$ ,  $\Delta H_c$ , and  $\Delta H_m$  can be determined. The tests were performed in the temperature range of -30 °C to 180 °C.

Permeability properties: WVTR, O<sub>2</sub>TR, and CO<sub>2</sub>TR indicate the ability of the polymer materials to allow water vapor, oxygen and carbon dioxide, respectively, to penetrate through the materials. All the samples were masked with aluminum foil in order to reduce the area to 3.14 in<sup>2</sup> since each of the modified PHBV sheets was produced in small quantity by the mini screw extruder.

## **4. SELECTION OF MODIFICATION METHOD FOR IMPROVING POLYHYDROXYBUTYRATE-CO-VALERATE PROPERTIES FOR COMPRESSION MOLDING THIN SHEET**

### **4.1 Introduction**

In this study, PHBV was modified and fabricated in order to improve its drawbacks of high crystallinity resulting in brittleness and low elongation. This prevents it from being used in packaging applications where flexibility is important. To overcome this problem, PHBV was modified in different ways.

### **4.2 Fabrication of modified polyhydroxybutyrate-co-valerate**

#### *4.2.1 Fabrication of polyhydroxybutyrate-co-valerate blend with titanium dioxide*

Titanium dioxide,  $\text{TiO}_2$ , in nanoparticle form was chosen in order to gain more toughening of PHBV.  $\text{TiO}_2$  has been known as a filler for polymers that contributes to reinforcement of the polymers. The size of the particles has an important effect on mechanical properties. Large particles give mechanical strength to polymers but toughness decreases. Nanoparticles enhance modulus and toughness. Additionally, the particles have high surface area leading to more interfacial force between the particles and the polymers. However, they tend to agglomerate, so the shearing force during processing has to be high enough to overcome this behavior [107].

Neat PHBV resin was dried in a vacuum oven at 80 °C for 4 hours and cooled down in a desiccator at room temperature. PHBV resins and TiO<sub>2</sub> were introduced to a co-rotating mini twin screw extruder (DSM Micro 15 compounder, Netherlands). The extruder was set at 165 °C for all three temperature zones and a screw speed of 150 rpm. At the beginning of the blending process, PHBV was soft like rubber and tacky. The force increased steeply and reached a maximum, at which point the blend was well mixed. Further processing beyond the maximum shearing force degraded the PHBV since it is susceptible to thermal degradation so the point of maximum shear force was chosen as the processing time (a residence time of 1 min.). The PHBV/TiO<sub>2</sub> was transferred by a pre-heated cylinder set at 155 °C into the injection molding machine where the disk mold was attached and set at 40 °C. The PHBV/TiO<sub>2</sub> disk obtained was cooled at room temperature. Afterward, the PHBV/TiO<sub>2</sub> disk was placed in an aluminum frame of 180×180 mm<sup>2</sup> and thickness of 0.25 mm. Then it was compressed into a sheet in a compression molding machine at 165 °C and 20,000 psi for 5 min. The sheet was cooled by a cooling unit attached to the compression molding machine (M CARVER, Carver Laboratory Press, Menomonee Falls, Wisconsin, USA) for 15 min. The cooling unit used cold tap water.

#### *4.2.2 Fabrication of polyhydroxybutyrate-co-valerate/poly(butylene adipate-co-terephthalate) blend*

Ecoflex is a trade name for poly(butylene adipate-co-terephthalate), PBAT, which is a petroleum-based biodegradable polymer, first commercialized by BASF, Germany [8, 108]. It is an aliphatic-aromatic copolyester consisting of 1,4-butanediol acid, adipic acid, and terephthalic acid monomers [108, 109, 110]. The molecular structure of PBAT is shown in Figure 2.5

It is a soft material, which has low tensile strength, high elasticity, fracture durability, water and oil resistance and full biodegradability within a few weeks with the aid of enzymes [108, 110, 111]. In addition, it possesses high hydrophilicity and high gas permeability [108, 111]. PBAT is suitable for film extrusion and has been used in polymer blends for flexibility [8, 112, 113]. It has a low  $T_g$  which makes it suitable to be a toughening agent in polymer blends [113, 114, 115].

Ecoflex neat resin and PHBV neat resin were dried at 80 °C for 4 hours in a vacuum oven and cooled at room temperature in a desiccator. Both Ecoflex and PHBV neat resins in different ratios were simultaneously placed into the co-rotating mini twin screw extruder. The extruder was set at 165 °C for all three temperature zones and a screw speed of 150 rpm. The residence time was 2 min., at which time the maximum shearing force was reached. Thereafter, the process of transforming from the extrudate into the blended sheet was identical to that of the PHBV/TiO<sub>2</sub> blend.

#### *4.2.3 Fabrication of polyhydroxybutyrate-co-valerate/poly(butylene adipate-co-terephthalate) /titanium dioxide blend*

Both Ecoflex and TiO<sub>2</sub> can be effective in toughening polymer materials. In this experiment, blends of PHBV/Ecoflex/TiO<sub>2</sub> were developed for evaluation of the effect of both simultaneously.

PHBV and Ecoflex resins were vacuum dried at 80 °C for 4 hours and cooled in a desiccator at room temperature. All materials including TiO<sub>2</sub> were placed in the mini screw extruder which was set at 165 °C for all three temperature zones with a screw speed of 150 rpm. The residence time for the process was 2 min. at which time the maximum shearing force was reached. Thereafter, the process of transforming from the extrudate into the blended sheet was identical to that of the PHBV/TiO<sub>2</sub> blend.

#### *4.2.4 Fabrication of polyhydroxybutyrate-co-valerate/triethyl citrate blend*

Triethyl citrate (TEC) is used as a plasticizer. Plasticizers are lubricating materials that facilitate processability and give flexibility and elongation to polymers. Triethyl citrate has been used in many industries such as polymers and personal care and cosmetics [116, 117].

PHBV resin was vacuum dried at 80 °C for 4 hours and cooled at room temperature in a desiccator. PHBV was introduced to the extruder together with triethyl citrate. The extruder temperature in the three temperature zones was 165 °C and the screw speed was 150 rpm. The

reaction proceeded for 30 seconds at which time the maximum shearing force was reached. The transformation process from the extrudate to sheet was identical to the PHBV/TiO<sub>2</sub> blend.

#### *4.2.5 Fabrication of polyhydroxybutyrate-co-valerate grafted with 2-hydroxyethyl methacrylate*

2-Hydroxyethyl methacrylate (2HEMA) is a monomer used in many studies as a grafting monomer [118, 119, 120]. Grafting is a process that attaches monomers onto the polymer backbone, creating a branched structure in the polymer. Grafting improves elongation of the polymers [59, 60].

In this experiment, neat PHBV resin was dried in a vacuum oven at 80 °C for 4 hours and cooled in a desiccator at room temperature. 2HEMA and PHBV were placed into the mini twin screw extruder together with 2,5-bis(tert-butylperoxy)-2,5-dimethylhexane (L101) as an initiator. L101 is a peroxide used as a crosslinking agent with a molecular formula of C<sub>16</sub>H<sub>34</sub>O<sub>4</sub> and molecular weight of 290.44 g/mol. It is a colorless liquid with a boiling point of 55-57 °C at 7 mmHg and flash point of 65 °C [121]. The extruder was set at 165 °C for all three temperature zones with a screw speed of 150 rpm. The reaction time for the grafting process was 1 min. at which time the maximum shearing force was reached. The subsequent process, which transformed the extrudate to the grafted PHBV sheet, was similar to the PHBV/TiO<sub>2</sub> blend.

#### *4.2.6 Fabrication of crosslinked polyhydroxybutyrate-co-valerate*

Neat PHBV resin was dried at 80 °C for 4 hours in a vacuum oven and then cooled at room temperature in a desiccator. PHBV was introduced into the mini twin screw extruder together with L101 as an initiator (crosslinker). The extruder was set at 165 °C for all three temperature zones. The residence time (reaction time) was 1 min., selected on the basis of the maximum shearing force. The resulting extrudate was removed from the extruder in a strand form with low viscosity and tackiness. The extrudate was placed on aluminum trays at room temperature in order to cool and solidify. Afterwards, the extrudate was cut into pellets. The resulting crosslinked pellets were placed in a 180×180 mm<sup>2</sup> aluminum frame with a thickness of 0.25 mm. and then compressed between aluminum plates at 165 °C, 20000 psi for 5 min. to form compression molded sheet, as described previously.



### 4.3 Results and discussion

#### 4.3.1 *Visual characteristics of PHBV and modified PHBV*

PHBV resin is yellow, rigid and soft under compression [122]. It possesses high crystallinity and poor thermal stability, which is a serious concern during processing [123]. Its slow crystallization rate and low melt strength are crucial properties that hinder the ability to process PHBV in cast and blown film applications. When PHBV is exposed to high temperature in the extrusion process, the melt is sticky, similar to a heated starch solution. It can stick to any surface to which it is exposed. PHBV melt possesses elastomeric behavior so its strands can be stretched. It also exhibits slow solidification, as was observed by Wang and Schertz [77]. After cooling down, it becomes rigid and does not adhere to surfaces. In order to obtain a desirable film, a super cooling system needs to be promptly connected to the die [124]. However, PHBV and all modified PHBVs in this study were sticky and could not be directly formed into sheet due to the unavailability of a super cooling unit. The PHBV sheet was flexible but brittle when folded. The PHBV resin is shown in Figure 4.1. Table 4.1 indicates visual characteristics of PHBV and modified PHBVs in different forms.



*Figure 4.1 Poly(hydroxybutyrate-co-valerate) neat resins*

The PHBV/TiO<sub>2</sub> 1%wt. extrudate had low melt strength, elastomeric behavior and stuck to surfaces such as the die. This led to an inability to instantly form polymer sheets. It was necessary to form a disk-like shape in the injection mold before compression into film. After cooling down, the material became rigid but soft, similar to a hard rubber as indicated in Table 4.1. The PHBV/TiO<sub>2</sub> 1%wt. sheet was yellow in color and showed brittleness (cracks) all over the sheet when it was bent slightly as shown in Figure 4.2 (a).

The PHBV/Ecoflex blends (PHBV/Ecoflex: 80/20, 70/30, and 50/50 %wt) possessed low melt strength, stickiness and were elastomeric. However, with an increase in Ecoflex content, the extrudates appeared to have a bit more melt strength. All PHBV/Ecoflex blends could not be formed into sheets directly from the extrudate since they stuck to the die surface. They needed to be previously formed into a disk-like shape in the injection mold. When cooled, the

PHBV/Ecoflex blends were yellow, rigid but soft, similar to a hard rubber. The PHBV/Ecoflex blend sheets were flexible but brittle if folded as shown in Table 4.1.

The PHBV/Ecoflex/TiO<sub>2</sub> blends (PHBV/Ecoflex/TiO<sub>2</sub>: 79/20/1, 69/30/1, and 49.5/49.5/1 %wt.) had low melt strength, elastomeric texture, and stickiness. When the Ecoflex content increased, the blended extrudates showed higher melt strength. Yet, the extrudates of the blends could not be formed directly into sheets due to stickiness in the die. A disk-like shape was necessary to be formed in the injection molder. The blends were rigid but soft like a hard rubber. The compressed PHBV/Ecoflex/TiO<sub>2</sub> sheets, when cooled, were yellow, flexible but brittle when bent for PHBV/Ecoflex/TiO<sub>2</sub> 79/20/1 and 69/30/1 wt., and brittle when folded for PHBV/Ecoflex/TiO<sub>2</sub> 49.5/49.5/1 wt.

The PHBV/TEC (80/20 %wt.) blend had low melt strength, elastomeric characteristics and stickiness. This led to an inability to immediately form a PHBV/TEC sheet. Therefore, a disk-like shaped PHBV/TEC was produced in the injection molding machine. The blend was yellow in color, rigid but soft, similar to hard rubber when cooled. However, an oily liquid was observed on the surface of the PHBV/TEC blend due to the migration of the plasticizer. Next, it was compressed into sheet. The PHBV/TEC blend sheet was brittle when folded.

Grafted PHBVs with 2HEMA (PHBV/2HEMA: 90/10 and 70/30 %wt.) had low melt strength, stickiness and elastomeric behavior. Like other modified PHBV as stated previously, they could not be formed as sheet directly from the extrudates because the blended extrudates were sticky to surfaces like the die. It was necessary to form a disk-like shape in the injection

molder. The grafted PHBVs with 2HEMA were yellow, rigid but soft like hard rubber, when cooled. The grafted sheets were brittle when folded.

Crosslinked PHBV formed using L101 2%wt. possessed low melt strength, elastomeric behavior and stickiness. The extrudate was discharged from the extruder so rapidly that the preheated cylinder could not immediately collect the extrudate for injection molding. Instead, the extrudate was collected as strands. When cooled, it was cut into pellets. The material was yellow, rigid but soft like a hard rubber. The crosslinked PHBV sheet, as shown in Figure 4.2 (b), was more flexible than PHBV but still was brittle when it was folded.



a



b

*Figure 4.2 Brittleness of PHBV/TiO<sub>2</sub> sheet (a) and crosslinked PHBV sheet (b)*

Table 4.1 Visual characteristics of PHBV and modified PHBVs in different forms in the experiment.

| Material   | Extrudate  | Disk form   | Sheet form                                      |
|--|--|---|---|
| Neat PHBV  | -  | -   | Yellow, flexible but brittle when folded        |
| Blend of PHBV/TiO <sub>2</sub> nanoparticle 1% wt.       | Low melt strength,<br>Sticky when heated,<br>Rigid when cooled | Rigid but soft like hard rubber   | Yellow, brittle on the sheet when slightly bent |
| Blend of PHBV/Ecoflex : 80/20 %wt                        |  |   | Yellow, flexible but brittle when folded        |
| Blend of PHBV/Ecoflex : 70/30 %wt                        |  |   | Yellow, flexible but brittle when folded        |
| Blend of PHBV/Ecoflex : 50/50 %wt                        |  |   | Yellow, flexible but brittle when folded        |
| Blend of PHBV/Ecoflex/TiO <sub>2</sub> : 79/20/1 %wt     |  |   | Yellow, flexible but brittle when bent          |
| Blend of PHBV/Ecoflex/TiO <sub>2</sub> : 69/30/1 %wt     |  |   | Yellow, flexible but brittle when bent          |
| Blend of PHBV/Ecoflex/TiO <sub>2</sub> : 49.5/49.5/1 %wt |  |   | Yellow, flexible but brittle when folded        |
| Blend of PHBV/Triethyl citrate : 80/20 %wt               |  | Rigid but soft like hard rubber,<br>Oily liquid migration to the material surface | Yellow, flexible but brittle when folded        |
| Grafted PHBV with 2HEMA : 90/10 %wt (L101 0.1%wt)        |  | Rigid but soft like hard rubber   | Yellow, flexible but brittle when folded        |
| Grafted PHBV with 2HEMA : 70/30 %wt (L101 0.1%wt)        |  |   | Yellow, flexible but brittle when folded        |
| Crosslinked PHBV (L101 2%wt) rxn time 1 min              |  |   | Yellow, flexible but brittle when folded        |

#### *4.3.2 Mechanical properties of PHBV and modified of PHBV*

The most important property for polymer sheet and film is flexibility, which can be indicated by elongation. The selection of modification methods for the research was based on improving elongation. Basically, neat PHBV is brittle (low elongation); tacky, which is a problem in film processing for both cast and blown film; and has low melt strength. PHBV has mechanical properties similar to those of polypropylene [123]. As a first attempt, TiO<sub>2</sub> nanoparticles were chosen as a toughening agent for neat PHBV. According to Carballeira et al., TiO<sub>2</sub> contributed to toughness of epoxy resin [107]. Also TiO<sub>2</sub> increased the modulus of elasticity [125]. In this study, the PHBV/TiO<sub>2</sub> sheet had cracks all over the sheet. The tensile strength of the modified PHBV was less than of neat PHBV, as was elongation. However, the difference in tensile strength was not statistically significant as opposed to the elongation. The lower elongation at break in PHBV/TiO<sub>2</sub> occurred since TiO<sub>2</sub> probably aggregated and interfered with the PHBV structure. According to Zhu et al., PLA with the incorporation of TiO<sub>2</sub> had lower elongation at break due to aggregation of TiO<sub>2</sub> in the PLA matrix [126]. This material is not suitable for sheet/film applications. Mechanical properties, tensile strength and elongation at break for all modified PHBVs are shown in Table 4.2, Figure 4.3 and Figure 4.4.

In the second attempt, poly(butylene adipate-co-terephthalate), PBAT or Ecoflex, was used as a blend with PHBV. PBAT has been used in blending with other polymers for flexibility [113]. Eslami et al. reported that ductility of PLA/PBAT blends increased with the presence of PBAT, which consequently contributed to higher strain at break [127]. The resulting PHBV/Ecoflex blends in all compositions appeared to have significantly lower elongation at break than neat

PHBV, as indicated in Table 4.2 and Figure 4.4. According to Shahlari et al., elongation of PLA/PBAT blends improves when the content of PBAT is more than that of PLA. In that case PLA/PBAT 20/80 resulted in high elongation and PLA was present as the dispersed phase and PBAT was the continuous phase in the blend [113]. In this experiment, then, lower elongation of the blends than neat PHBV was attributed to less PBAT in the blend than PHBV. In this research, the main focus is PHBV. Therefore, PBAT content that was more than half of the material was not of interest.

In the third attempt, PBAT and TiO<sub>2</sub> were blended with PHBV. In this experiment, it was expected that both PBAT and TiO<sub>2</sub> might contribute to flexibility of the blends. However, the polymer blends in all ratios of PHBV and PBAT at TiO<sub>2</sub> 1%wt. possessed significantly lower tensile strength and elongation than neat PHBV. This is because the PBAT ratio in the blends was less than PHBV and TiO<sub>2</sub> may aggregate in the blends as stated in the discussion of the PHBV/TiO<sub>2</sub> blend and PHBV/PBAT blends. Tensile strength and elongation are shown in Table 4.2, Figure 4.3 and Figure 4.4.

In the fourth attempt, triethyl citrate (TEC) was added to PHBV in order to increase flexibility and elongation of PHBV and also promote processability. Zhang and Sun proved that acetyl triethyl citrate, a plasticizer, improved elongation of a PLA/starch/maleic anhydride blend [128]. However, the PHBV/TEC blends showed lower elongation and tensile strength than PHBV, in accordance with the result that was reported by Yang et al. [129]. Epoxidized soybean oil (ESO) and TEC were used as plasticizer of ethyl cellulose (EC) film. It was found that as the content of TEC and ESO increased, elongation at break of the films decreased when

compared to EC without plasticizer [129]. Table 4.2, Figure 4.3 and Figure 4.4 show the tensile strength and elongation at break of the TEC-plasticized PHBV. TEC did not provide flexibility of the PHBV/TEC blend.

In the fifth attempt, 2HEMA and PHBV were introduced into the reactor along with L101 as an initiator for grafting. A grafting process can be used to improving elongation through creation of a graft polymer. According to Wang et al., elongation of the graft copolymer of poly(caprolactone monoacrylate) and cellulose diacetate was found to be higher with an increase of degree of grafting [130]. Additionally, elongation of ethyl methacrylate grafted onto acacia gum improved when compared to that of acacia gum [131]. In contrast, in this experiment, the elongation of 2HEMA grafted onto PHBV in two different ratios, PHBV/2HEMA 70/30 and 90/10, were significantly less than PHBV itself, as were the tensile strengths. Similarly, Wang and Schertz reported that PHBV-g-2HEMA they obtained was brittle and rigid [77]. Table 4.2, Figure 4.3 and Figure 4.4 show the mechanical properties of PHBV-g-2HEMA. This experiment did not produce grafted PHBV that was suitable for use in applications that require flexibility.

The final attempt was based on observation of the melting behavior of PHBV. The flow behavior of neat PHBV in the liquid state was similar to that of uncured natural rubber. In order to cure the rubber from a liquid to an elastic material, vulcanization is used. Vulcanization is a crosslinking process and has been widely used in the rubber industry. Crosslinking is a process in which the molecular chains of a polymer are covalently bonded within and/or between other polymer molecular chains, resulting in a network matrix in multiple directions. The crosslinked



polymer possesses greater elongation than the un-crosslinked. In this experiment, neat PHBV and L101 2%wt. as an initiator for the reaction were introduced into the mini twin screw extruder. The crosslinking reaction (chemical reaction) took place for 1 min. The resulting crosslinked PHBV exhibited twice the elongation at break as the neat PHBV and the tensile strength was also a little higher. However, the apparent increase in tensile strength of the crosslinked PHBV was not statistically significant. Table 4.2 and Figures 4.3 and 4.4 illustrate the mechanical properties of the crosslinked PHBV. The results of this experiment agreed with the findings about crosslinked PHBV reported by Fei et al. [93], who found that PHBV crosslinked with dicumyl peroxide as initiator had higher elongation than neat PHBV. Therefore, the crosslinked PHBV with L101 as initiator obtained in this study was selected to potentially use in flexible applications.

Table 4.2 Mechanical properties of all compositions of modified PHBV material sheets

| Material   | Tensile strength (MPa)    | Elongation at break (%)      |
|--|---------------------------|------------------------------|
| Neat PHBV  | 19.84±0.54 <sup>a</sup>   | 15.04±0.59 <sup>b</sup>      |
| Blend of PHBV/TiO <sub>2</sub> nanoparticle 1%wt         | 18.64±0.55 <sup>a</sup>   | 10.60±0.50 <sup>c,d</sup>    |
| Blend of PHBV/Ecoflex : 80/20 %wt                        | 9.64±1.34 <sup>c,d</sup>  | 5.43±1.27 <sup>e,f,g,h</sup> |
| Blend of PHBV/Ecoflex : 70/30 %wt                        | 8.58±0.89 <sup>d,e</sup>  | 8.37±1.74 <sup>c,d,e</sup>   |
| Blend of PHBV/Ecoflex : 50/50 %wt                        | 4.16±0.45 <sup>f</sup>    | 4.47±0.12 <sup>f,g,h</sup>   |
| Blend of PHBV/Ecoflex/TiO <sub>2</sub> : 79/20/1 %wt     | 12.54±1.02 <sup>b</sup>   | 3.57±0.65 <sup>g,h</sup>     |
| Blend of PHBV/Ecoflex/TiO <sub>2</sub> : 69/30/1 %wt     | 11.30±1.20 <sup>b,c</sup> | 3.83±1.29 <sup>g,h</sup>     |
| Blend of PHBV/Ecoflex/TiO <sub>2</sub> : 49.5/49.5/1 %wt | 6.31±0.56 <sup>e,f</sup>  | 6.47±1.07 <sup>e,f,g</sup>   |

All measurements were performed in triplicate.

Values are reported as mean ± standard deviation.

Different letter designations for values in the same column indicate significant differences ( $p \leq 0.05$ ).

Table 4.2 (Cont'd)

| <b>Material</b>                                     | <b>Tensile strength (MPa)</b> | <b>Elongation at break (%)</b> |
|---|-------------------------------|--------------------------------|
| Blend of PHBV/Triethyl citrate : 80/20 % wt         | 4.82±1.19 <sup>f</sup>        | 2.57±0.31 <sup>h</sup>         |
| Grafted PHBV with 2HEMA : 90/10 % wt (L101 0.1% wt) | 10.91±0.16 <sup>b,c,d</sup>   | 7.51±0.02 <sup>d,e,f</sup>     |
| Grafted PHBV with 2HEMA : 70/30 % wt (L101 0.1% wt) | 12.54±0.21 <sup>b</sup>       | 11.40±1.51 <sup>c</sup>        |
| Crosslinked PHBV (L101 2% wt) rxn time 1 min        | 20.45±0.66 <sup>a</sup>       | 37.20±2.25 <sup>a</sup>        |

All measurements were performed in triplicate.

Values are reported as mean ± standard deviation.

Different letter designations for values in the same column indicate significant differences ( $p \leq 0.05$ ).

The residence time in the extruder of crosslinked PHBV was 1 min.

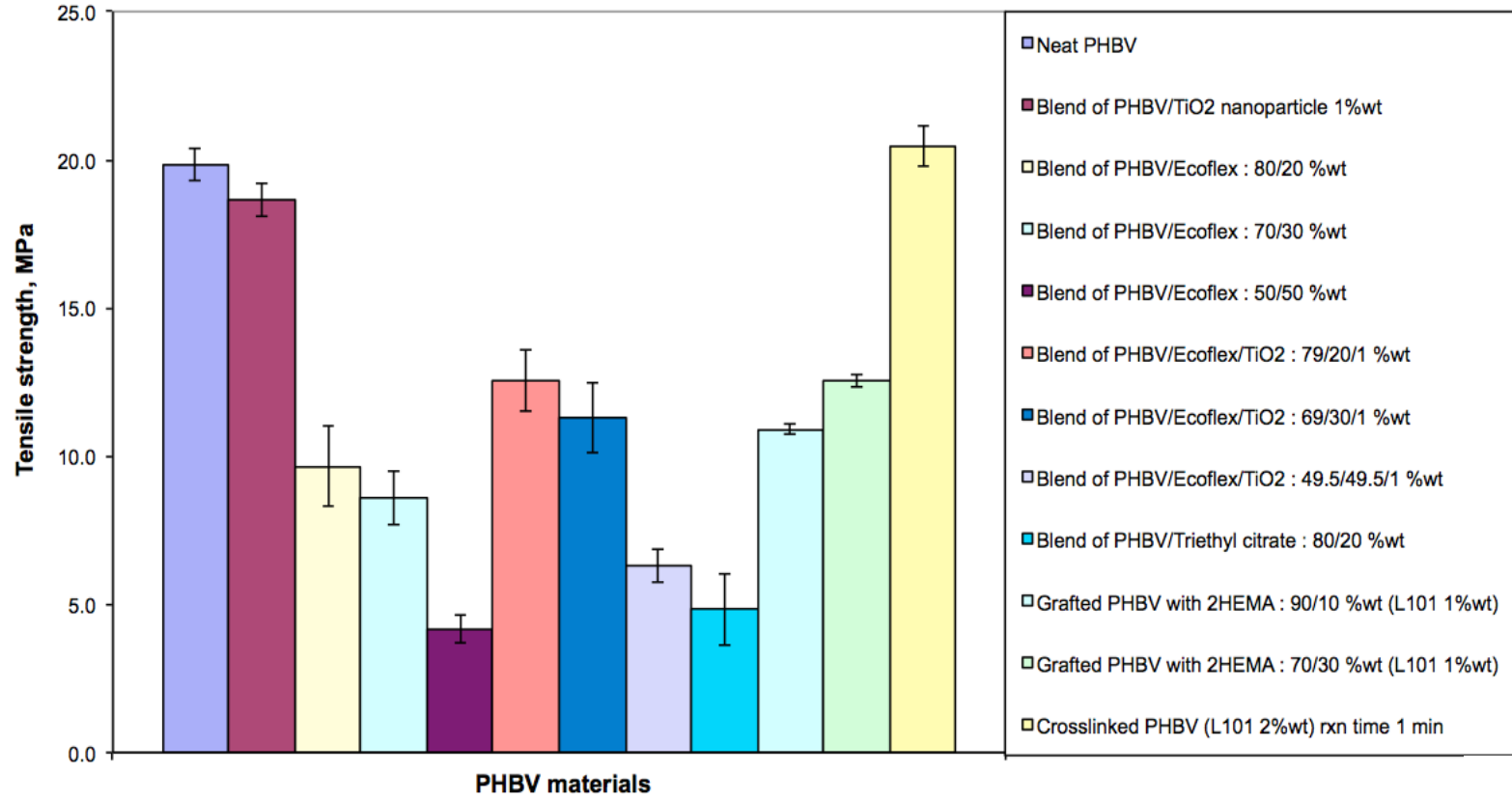


*Figure 4.3 Tensile strength of PHBV material sheets*

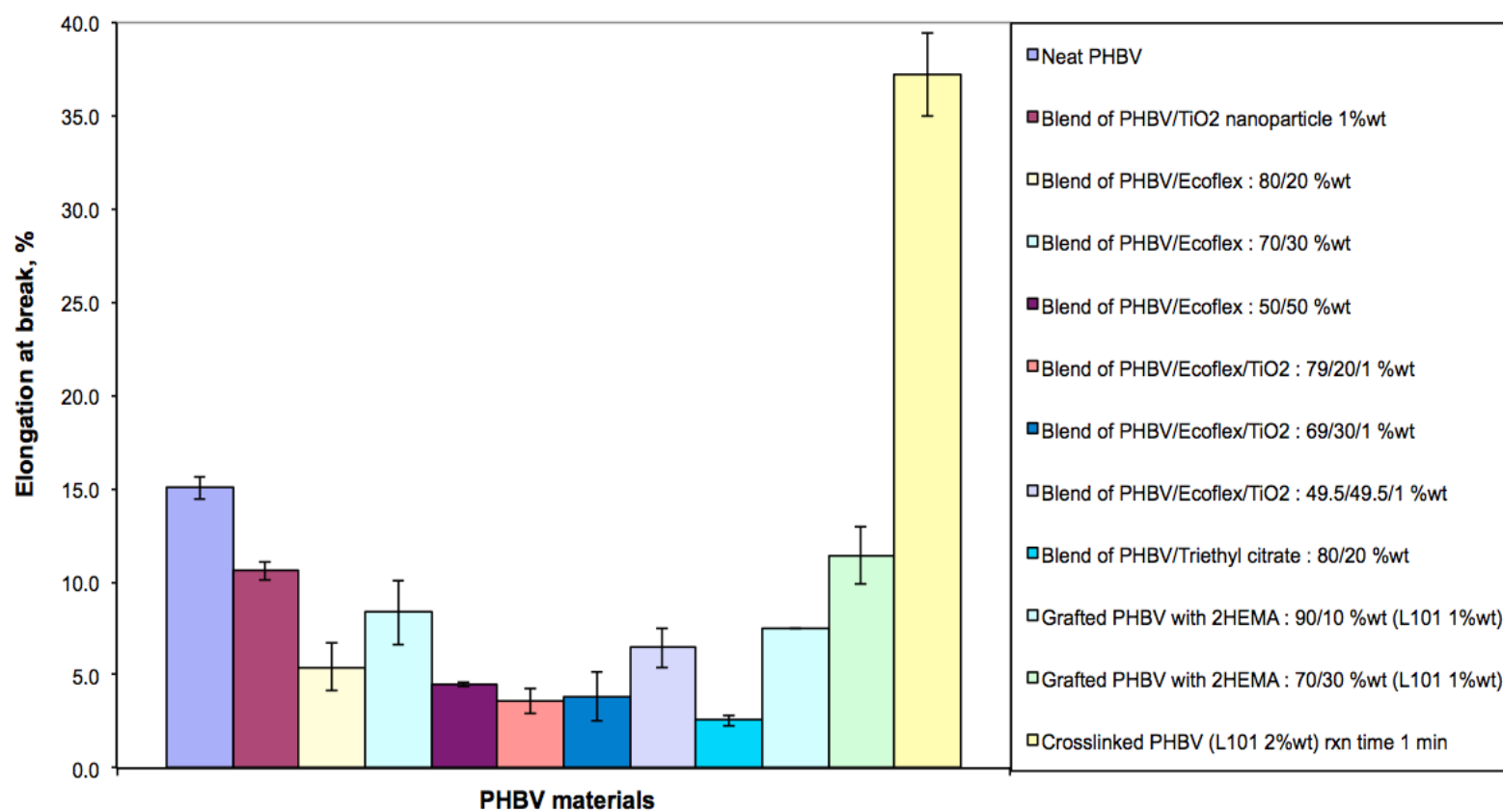


Figure 4.4 Elongation at break of PHBV material sheets

#### 4.3.3 Thermal properties of PHBV and modified PHBV

Differential scanning calorimetry (DSC) was used in the study of thermal properties of PHBV and the modified PHBV materials. Neat PHBV shows two relatively high melting temperatures ( $T_m$ ). The lower melting temperature corresponds to less perfect crystals which melt at a lower temperature. Then, PHBV recrystallizes with a more perfect structure and subsequently melts at a higher temperature [132, 133, 134, 135]. Moreover, the amount of hydroxyvalerate in PHBV influences the  $T_m$  of PHBV. With a higher HV portion in PHBV molecular chains, the  $T_m$  of PHBV decreases [136]. In Figure 4.5, the DSC indicates two  $T_m$ s at  $149.31 \pm 0.67$  and  $156.82 \pm 0.56$  °C. The glass transition temperature ( $T_g$ ) of PHBV was not observed in this research. However, Ferreira et al. reported that the  $T_g$  of neat PHBV was around 0 °C and could not easily be noticed. This is due to the fact that PHBV crystallizes rapidly and there is little amorphous matrix present. These characteristics result in less mobility of the polymer for characterization of  $T_g$  [137]. The peak crystallization temperature ( $T_c$ ) of PHBV was  $107.71 \pm 0.40$  °C as indicated in Figure 4.6.  $T_c$  is the temperature at which maximum crystal formation occurs. The heat of fusion ( $\Delta H_m$ ) indicates the heat required for melting crystallites of polymer.  $\Delta H_m$  of PHBV was  $65.31 \pm 0.33$  J/g. The crystallinity of PHBV can be obtained by using equation 4.1 [138]. The thermal properties of PHBV are indicated in Table 4.3

$$\%Crystallinity = \frac{\Delta H_m}{\Delta H_m^0} \times \frac{100}{w} \quad (4.1)$$

where  $\Delta H_m$  is the enthalpy of melting of PHBV (J/g)

$\Delta H_m^0$  is the enthalpy of melting of 100% crystallinity PHBV (perfect crystalline PHBV) that is 109 J/g [139]

$w$  is the weight fraction of PHBV in the material.

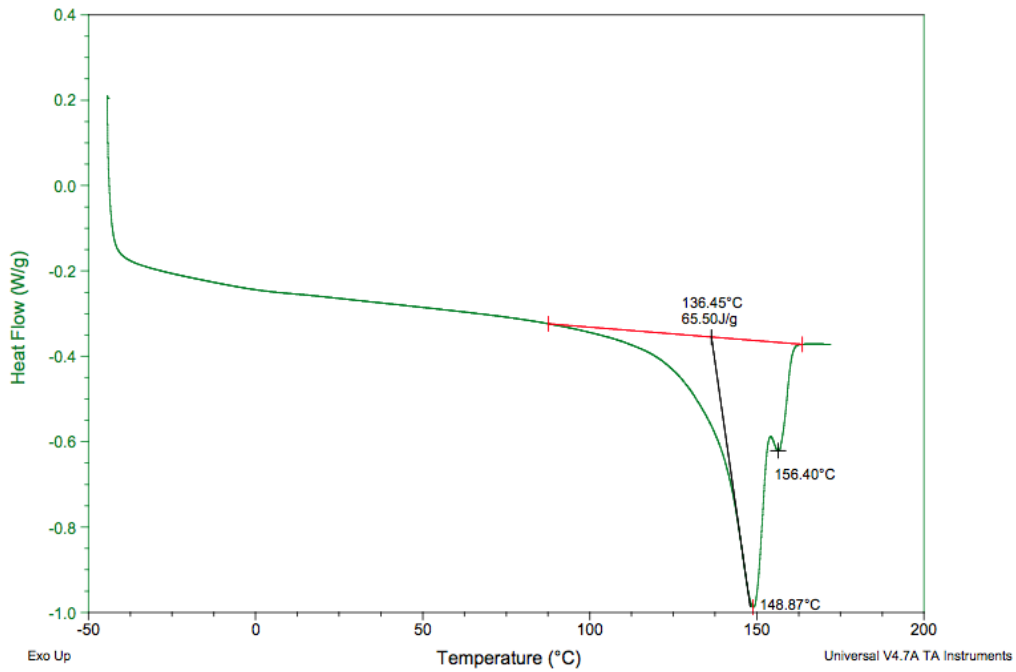


Figure 4.5 Two melting temperatures ( $T_m$ ) of neat PHBV

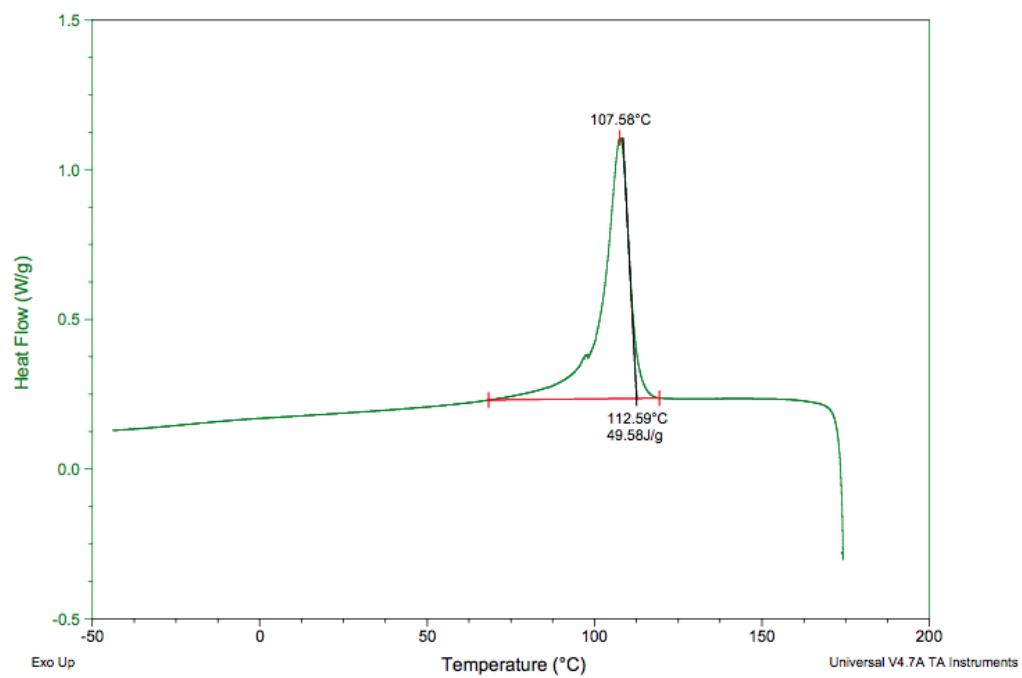


Figure 4.6 Crystallization temperature ( $T_c$ ) of neat PHBV



Table 4.3 Thermal properties of all compositions of modified PHBV

| Material  | T <sub>c</sub> (°C)        | T <sub>m</sub> (°C)        |                            | Heat of fusion,<br>ΔH <sub>m</sub> (J/g) | PHBV<br>Crystallinity (%)   |
|---|----------------------------|----------------------------|----------------------------|--|-----------------------------|
| Neat PHBV   | 107.71±0.40 <sup>a</sup>   | 149.31±0.67 <sup>b</sup>   | 156.82±0.56 <sup>b,c</sup> | 65.31±0.33 <sup>a</sup>                  | 59.92±0.30 <sup>a</sup>     |
| Blend of PHBV/TiO <sub>2</sub> nanoparticle 1% wt         | 109.88±0.27 <sup>a</sup>   | 153.20±0.27 <sup>a</sup>   | 159.77±0.22 <sup>a</sup>   | 59.49±0.22 <sup>b</sup>                  | 55.13±0.20 <sup>b,c</sup>   |
| Blend of PHBV/Ecoflex : 80/20 % wt                        | 70.24±1.05 <sup>e</sup>    | 142.96±0.53 <sup>e</sup>   | 156.64±0.58 <sup>c</sup>   | 50.77±0.17 <sup>c,d</sup>                | 58.22±0.19 <sup>a,b</sup>   |
| Blend of PHBV/Ecoflex : 70/30 % wt                        | 68.77±1.14 <sup>e</sup>    | 143.70±1.23 <sup>d,e</sup> | 156.81±0.66 <sup>b,c</sup> | 46.12±0.85 <sup>e,f</sup>                | 60.44±1.11 <sup>a</sup>     |
| Blend of PHBV/Ecoflex : 50/50 % wt                        | 75.83±0.20 <sup>d</sup>    | 143.34±0.36 <sup>e</sup>   | 156.45±0.29 <sup>c</sup>   | 31.73±0.18 <sup>i</sup>                  | 58.23±0.33 <sup>a,b</sup>   |
| Blend of PHBV/Ecoflex/TiO <sub>2</sub> : 79/20/1 % wt     | 84.68±0.49 <sup>c</sup>    | 145.83±0.20 <sup>c,d</sup> | 157.73±0.12 <sup>b,c</sup> | 49.02±0.24 <sup>d,e</sup>                | 56.93±0.28 <sup>a,b,c</sup> |
| Blend of PHBV/Ecoflex/TiO <sub>2</sub> : 69/30/1 % wt     | 81.57±0.49 <sup>c</sup>    | 146.01±0.14 <sup>c,d</sup> | 157.88±0.20 <sup>b,c</sup> | 43.95±0.38 <sup>f,g</sup>                | 58.43±0.51 <sup>a,b</sup>   |
| Blend of PHBV/Ecoflex/TiO <sub>2</sub> : 49.5/49.5/1 % wt | 82.46±1.17 <sup>c</sup>    | 146.59±0.33 <sup>c</sup>   | 158.39±0.28 <sup>a,b</sup> | 31.85±0.14 <sup>i</sup>                  | 59.03±0.26 <sup>a</sup>     |
| Blend of PHBV/Triethyl citrate : 80/20 % wt               | 70.39±5.37 <sup>e</sup>    | 130.98±0.88 <sup>g</sup>   | 146.51±0.38 <sup>e</sup>   | 40.54±2.92 <sup>h</sup>                  | 46.49±3.35 <sup>d</sup>     |
| Grafted PHBV with 2HEMA : 90/10 % wt (L101 0.1% wt)       | 105.00±0.18 <sup>a,b</sup> | 149.62±0.23 <sup>b</sup>   | 158.01±0.44 <sup>b,c</sup> | 53.07±1.35 <sup>c</sup>                  | 54.10±1.37 <sup>c</sup>     |
| Grafted PHBV with 2HEMA : 70/30 % wt (L101 0.1% wt)       | 101.04±2.10 <sup>b</sup>   | 146.46±1.84 <sup>c</sup>   | 156.33±1.22 <sup>c</sup>   | 40.88±1.31 <sup>g,h</sup>                | 53.58±1.71 <sup>c</sup>     |
| Crosslinked PHBV (L101 2% wt)                             | 100.00±1.24 <sup>b</sup>   | 140.16±0.81 <sup>f</sup>   | 148.89±0.98 <sup>d</sup>   | 51.42±0.32 <sup>c,d</sup>                | 47.17±0.29 <sup>d</sup>     |

All measurements were performed in triplicate.

Values are reported as mean ± standard deviation.

Different letter designations for values in the same column indicate significant differences ( $p \leq 0.05$ ).

The residence time in the extruder of crosslinked PHBV was 1 min.

Thermal decomposition of PHBV can be investigated using thermogravimetric analysis (TGA). As can be seen in Figure 4.7, the TGA thermogram of PHBV is steep which indicates a narrow decomposition temperature range. PHBV exhibited onset and maximum temperatures (at which the decomposition rate was maximum), of around 300 °C and 330 °C, respectively. The ending of decomposition was around 340 °C.

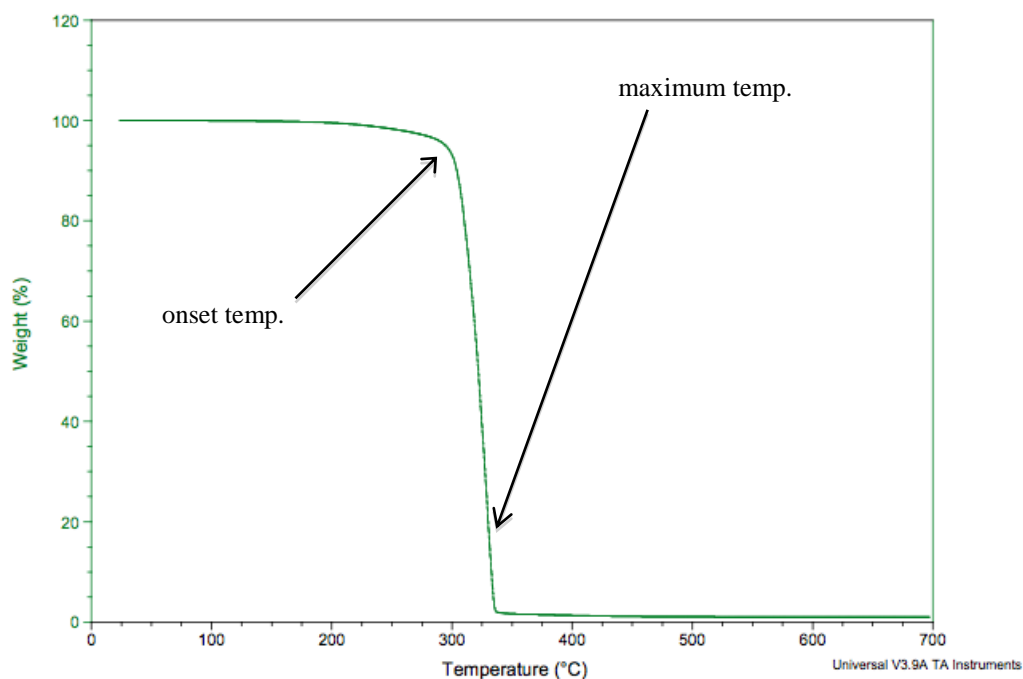
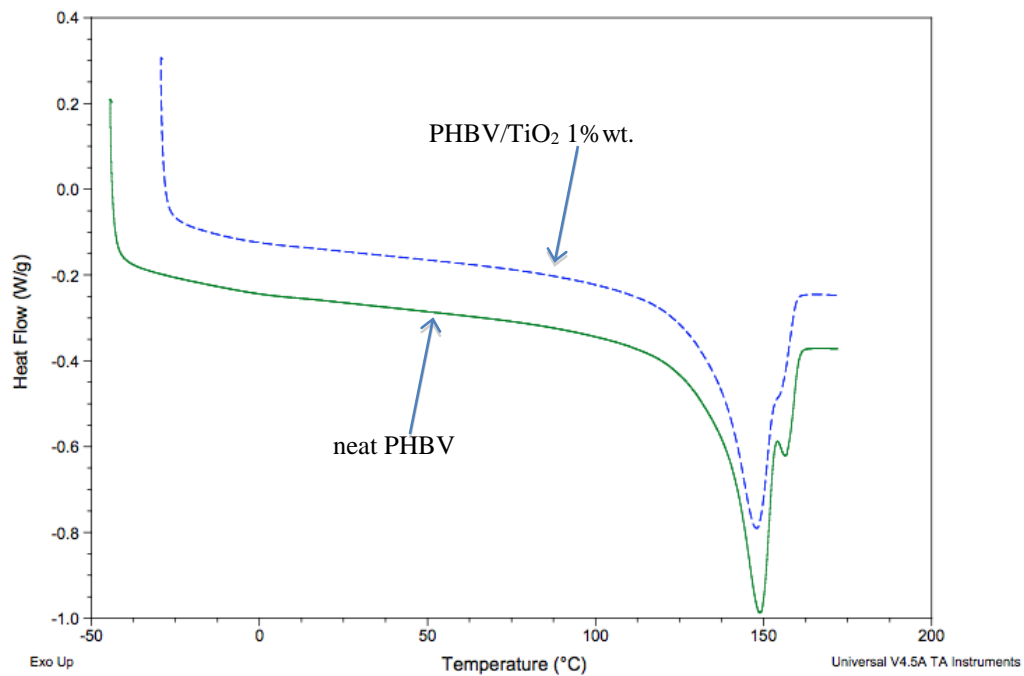


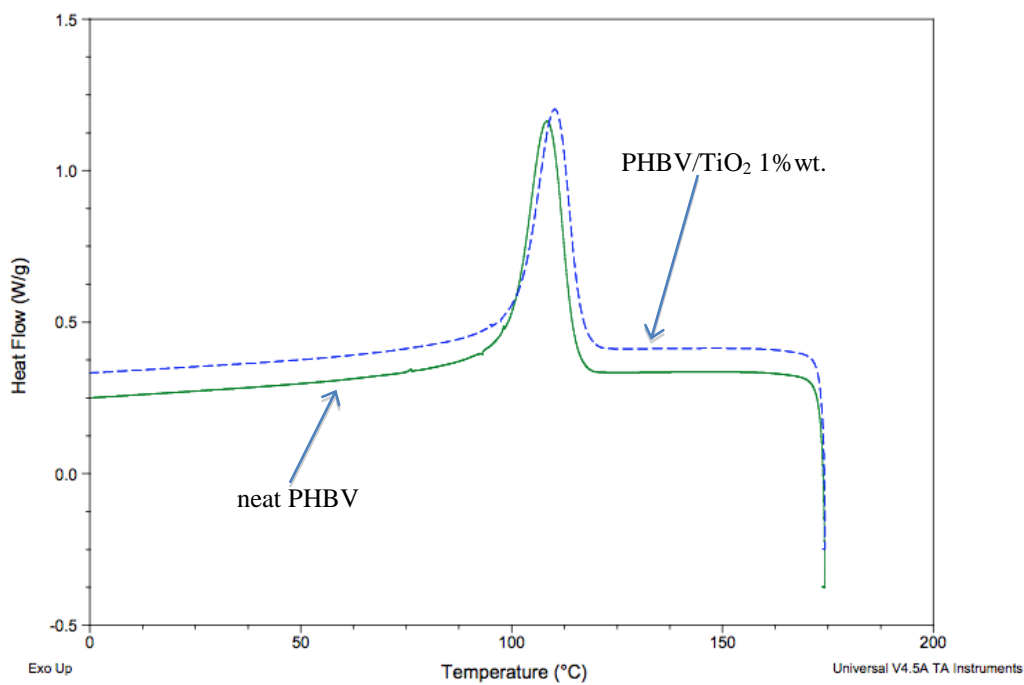
*Figure 4.7 Thermal decomposition profile of neat PHBV*

The presence of other substances in the PHBV matrix is crucial to thermal properties of the materials. In the first trial, the PHBV/TiO<sub>2</sub> material had two melting temperature peaks ( $153.20 \pm 0.27$  °C and  $159.77 \pm 0.22$  °C) similar to those in the heating profile of neat PHBV as shown in Table 4.3. and Figure 4.8 (a). Since TiO<sub>2</sub> is an inorganic compound which has a much higher melting temperature, around 1855 °C [140], the melting points in the thermal cycle involved PHBV. As stated previously, PHBV has two melting points which involved

primary formed crystallites melting at the lower temperature and the recrystallized matrix formed during heat exposure in the DSC melting at the higher temperature [132, 133, 134, 135]. However, in this study, the two melting temperatures of PHBV/TiO<sub>2</sub> shifted slightly to higher temperatures when compared to those of PHBV. This result corresponded to the result from Buzarovka et al., which reported the  $T_{ms}$  of PHBV/TiO<sub>2</sub> blends slightly shifted to higher temperatures, although the  $T_{ms}$  were not dependent upon the TiO<sub>2</sub> quantity [135]. The crystallization temperature ( $T_c$ ) of the PHBV/TiO<sub>2</sub> blend ( $109.88 \pm 0.27$  °C) in this study was not statistically different when compared to PHBV and its cooling cycle behavior in DSC was similar to that of neat PHBV as can be seen in Figure 4.8 (b). According to Buzarovka et al., although the PHBV/TiO<sub>2</sub> blend had slightly higher  $T_c$  with an increase in TiO<sub>2</sub> content, there was no robust evidence that TiO<sub>2</sub> showed a nucleating effect on the polymer [135]. Thus, in this study, PHBV/TiO<sub>2</sub> with no significant difference in  $T_c$  indicated that TiO<sub>2</sub> probably did not have a significant nucleating effect to facilitate the crystallinity of the PHBV/TiO<sub>2</sub> blend [135]. The heat of fusion of the PHBV/TiO<sub>2</sub> ( $59.49 \pm 0.22$  J/g) was slightly lower than that of PHBV. This indicated a slightly lower percent crystallinity in the blend than in PHBV. For thermal decomposition of PHBV/TiO<sub>2</sub>, Buzarovka et al. stated that with an increase of TiO<sub>2</sub> in the blend, the decomposition temperature slightly shifted to a higher value [135]. In this study, in contrast, thermal decomposition of PHBV/TiO<sub>2</sub> and PHBV was essentially identical, as can be seen in Figure 4.9. This might be because the TiO<sub>2</sub> content in the PHBV/TiO<sub>2</sub> was so small that it did not influence the thermal behavior of the PHBV.



(a)



(b)

Figure 4.8 Endothermic (a) and exothermic (b) profiles of neat PHBV and PHBV/TiO<sub>2</sub> 1%wt.

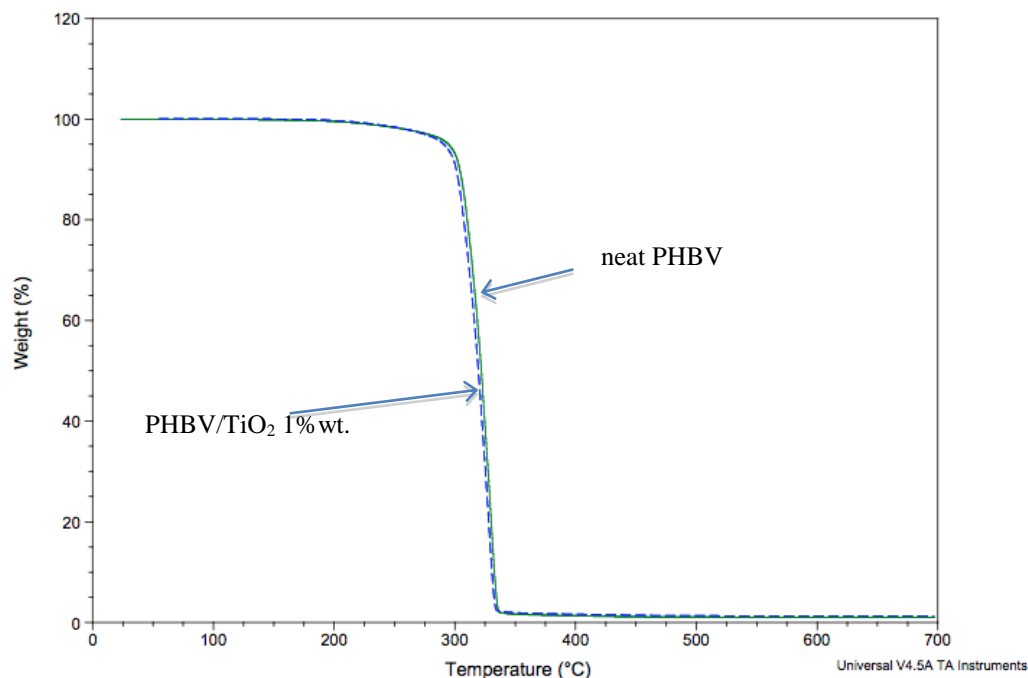


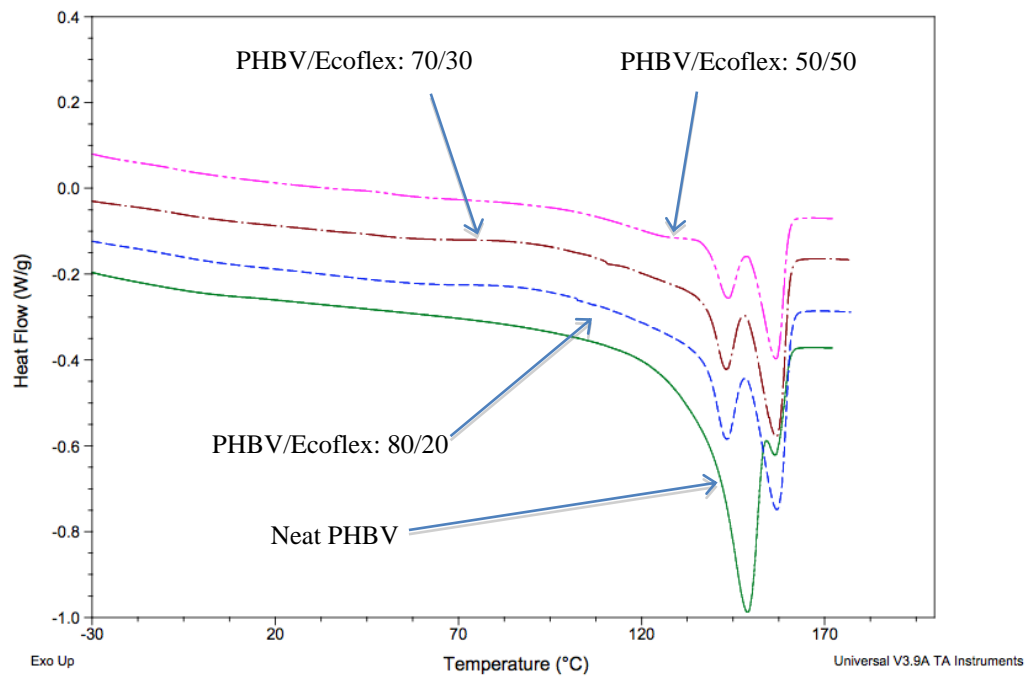
*Figure 4.9 Thermal decomposition profiles of PHBV and PHBV/TiO<sub>2</sub> 1%wt.*

Ecoflex blended with PHBV changed the thermal transition characteristics of the blend. Figure 4.10 shows the heating cycle (a) and cooling cycle (b) profiles of PHBV and PHBV/Ecoflex blends. Table 4.3 shows the thermal properties of PHBV/Ecoflex at different ratios of Ecoflex. The  $T_m$ s of the PHBV/Ecoflex blends were  $142.96 \pm 0.53$  °C and  $156.64 \pm 0.58$  °C for 80/20 %wt.,  $143.70 \pm 1.23$  °C and  $156.81 \pm 0.66$  °C for 70/30 %wt., and  $143.34 \pm 0.36$  °C and  $156.45 \pm 0.29$  °C for 50/50 %wt. The  $T_m$ s of the three compositions of PHBV/Ecoflex blends were not significantly different from each other. However, they were lower than those of the neat PHBV sheet. These results corresponded to the behavior of PHBV/Joncryl blends reported by Duangphet et al [141]. The crystallization rate can be indirectly indicated by the  $T_m$ ; the lower  $T_m$  indicates reduced crystallization [141]. In this study, the heat of fusion values of the blends ( $50.77 \pm 0.17$  J/g for 80/20,  $46.12 \pm 0.85$  J/g for 70/30, and  $31.73 \pm 0.18$  J/g for

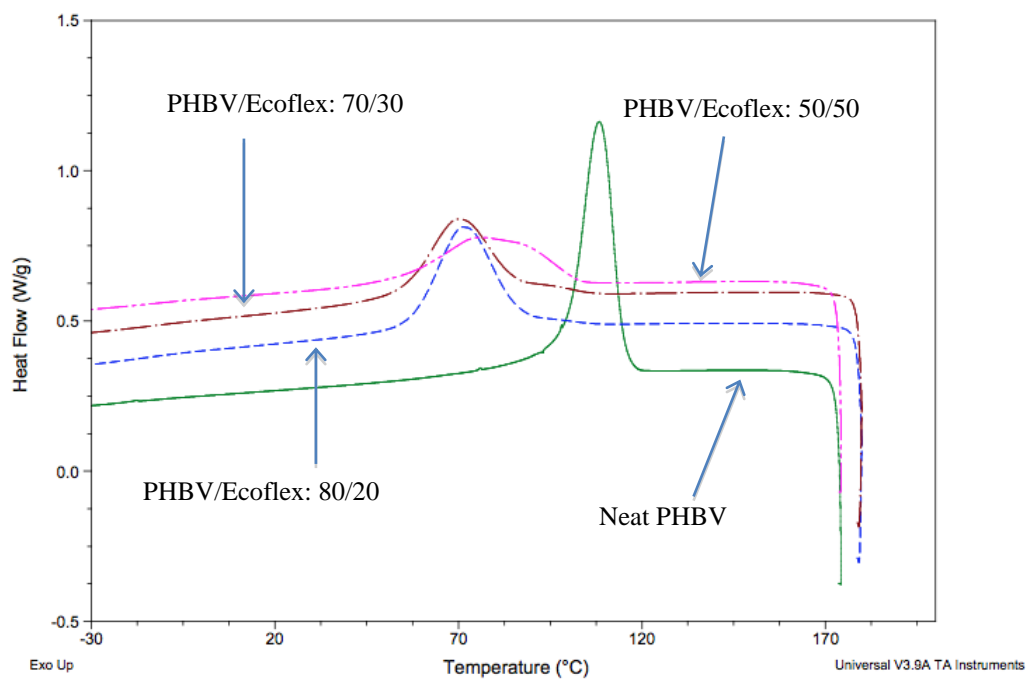
50/50) were lower than the neat PHBV's due to the lesser amount of PHBV in the blends than the neat PHBV. However, the crystallinities of the PHBV/Ecoflex blends were not significantly different from each other and from the neat PHBV, as shown in Table 4.3.

All  $T_c$ s of the blends ( $70.24 \pm 1.05$  °C for 80/20,  $68.77 \pm 1.14$  °C for 70/30, and  $75.83 \pm 0.20$  °C for 50/50) were considerably lower than the  $T_c$  of neat PHBV. The  $T_c$  of the 80/20 and 70/30 PHBV/Ecoflex blends were not statistically different from each other whereas the  $T_c$  of the 50/50 PHBV/Ecoflex blend was higher than those of the 80/20 and 70/30 blends. This result differed from the study of PHBV/PLLA blends by Ferreira et al. who found no  $T_c$  variation of PHBV and PLLA in the blend compared to pure PHBV and pure PLLA. This was because PHBV and PLLA showed a phase separation in which each of them segregated from the blend to form pure domains [137].

Thermal decomposition curves for PHBV and PHBV/Ecoflex blends are shown in Figure 4.11. TGA indicates that PHBV thermally degraded at a lower temperature than PHBV/Ecoflex 50/50. The blends between PHBV and Ecoflex have two thermal degradation steps, which corresponded to the PHBV and Ecoflex components. PHBV in the blends was degraded first, at a lower temperature than that at which neat PHBV degraded, and later Ecoflex degraded at a higher temperature. This thermal behavior of the blend is similar to the polyhydroxyalkanoate (PHA)/epoxidized broccoli oil blend prepared by Audic et al. PHA first degraded and then EBO degraded at a higher temperature. The thermal profile exhibited two different degradation steps [142].



(a)



(b)

Figure 4.10 Endothermic (a) and exothermic (b) profiles of neat PHBV and PHBV/Ecoflex blends

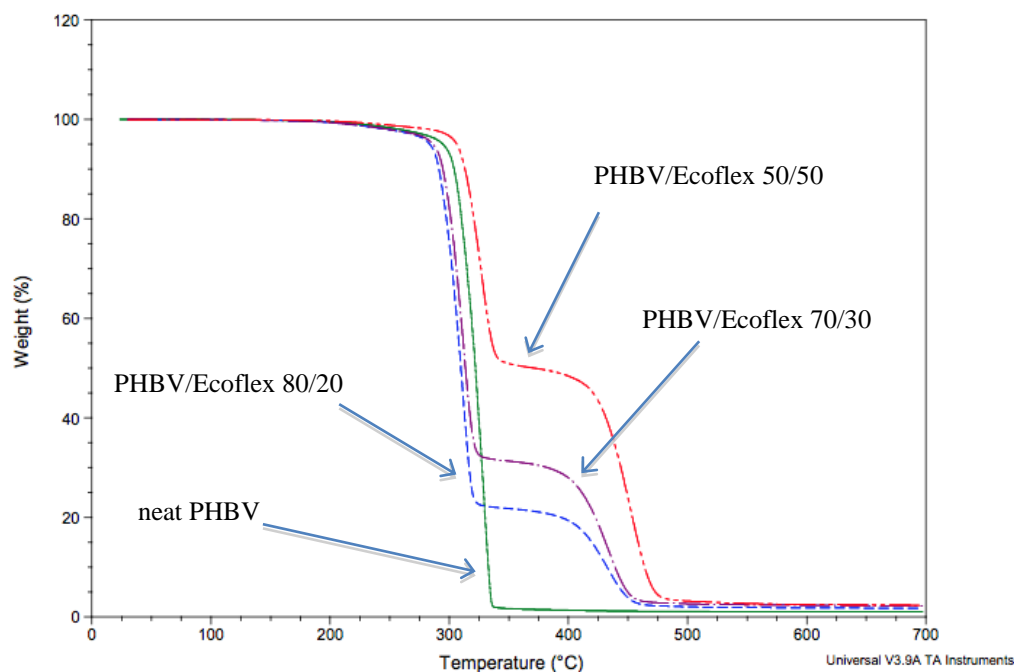
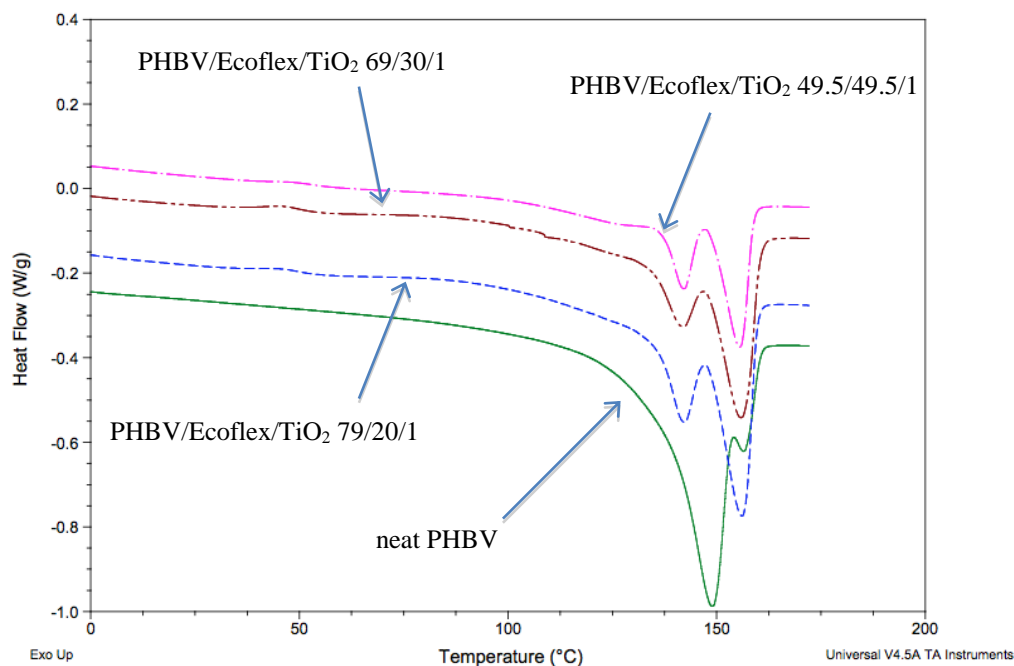


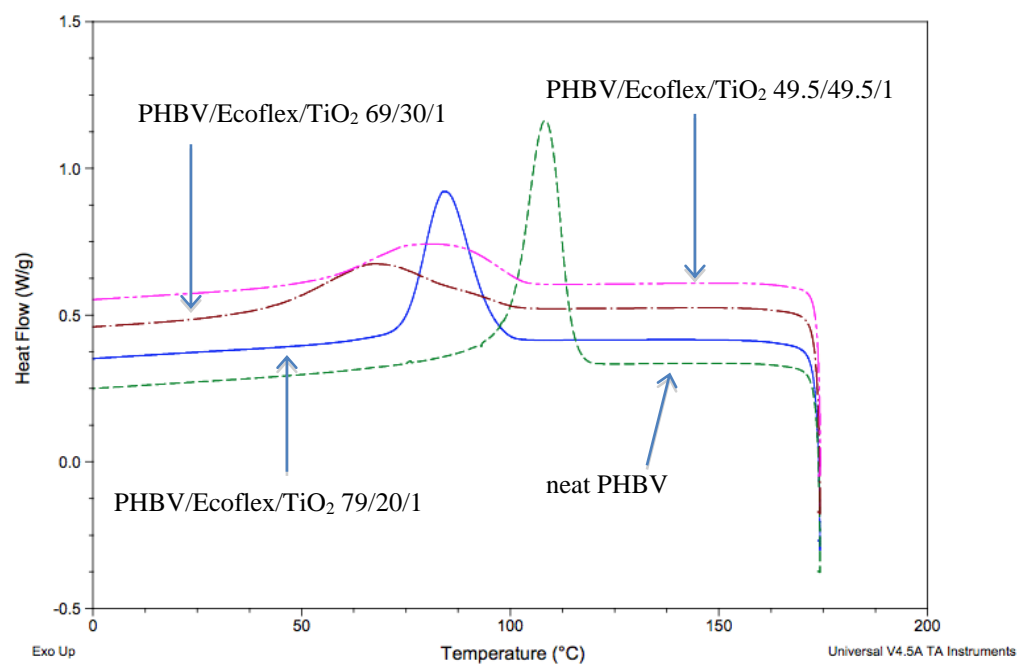
*Figure 4.11 Thermal decomposition profiles of neat PHBV and PHBV/Ecoflex blends*

In the blend of PHBV/Ecoflex/TiO<sub>2</sub> in the third trial, the thermal transition characteristics of all ratios of the blends were different from those of the neat PHBV but not different from each other, as illustrated in Figure 4.12 and Table 4.3. The presence of TiO<sub>2</sub> in the blends did not have an important effect on T<sub>ms</sub>, heat of fusion, or crystallinity of PHBV in the blends when compared to PHBV/Ecoflex blends even though all T<sub>cs</sub> of the PHBV/Ecoflex/TiO<sub>2</sub> blends were slightly higher than those of the PHBV/Ecoflex blends. The thermal decomposition characteristics of the blends were also similar to those of PHBV/Ecoflex blends as shown in Figure 4.13. Table 4.3 indicates thermal properties of the blends. Figure 4.12 shows heating cycle and cooling cycle profiles of PHBV and PHBV/Ecoflex/TiO<sub>2</sub> blends.



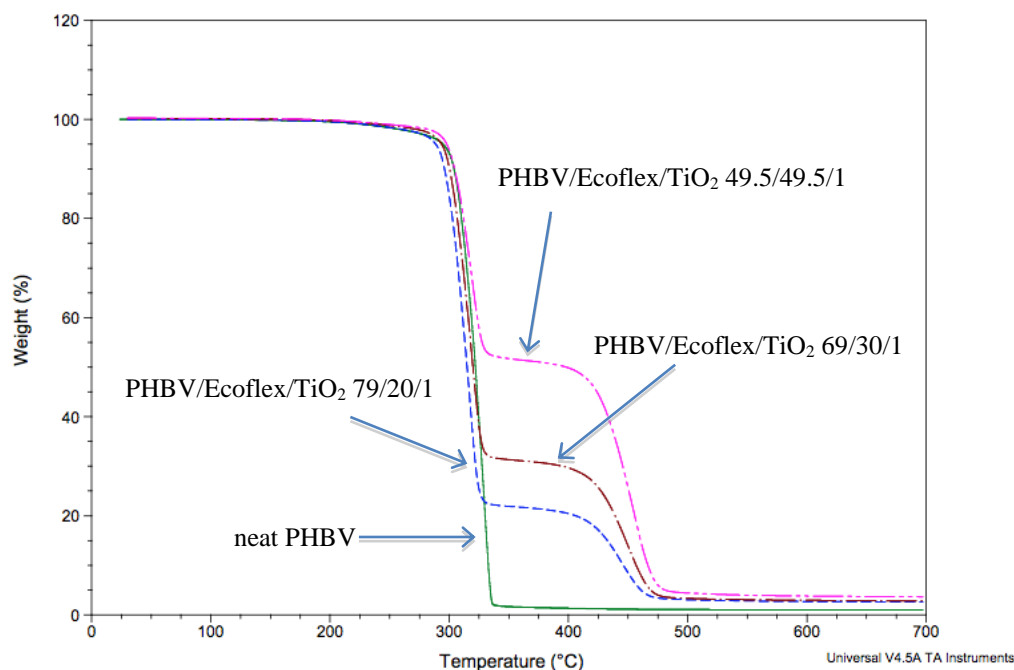


(b)



(b)

Figure 4.12 Endothermic (a) and exothermic (b) profiles of neat PHBV and PHBV/Ecoflex/TiO<sub>2</sub> blends

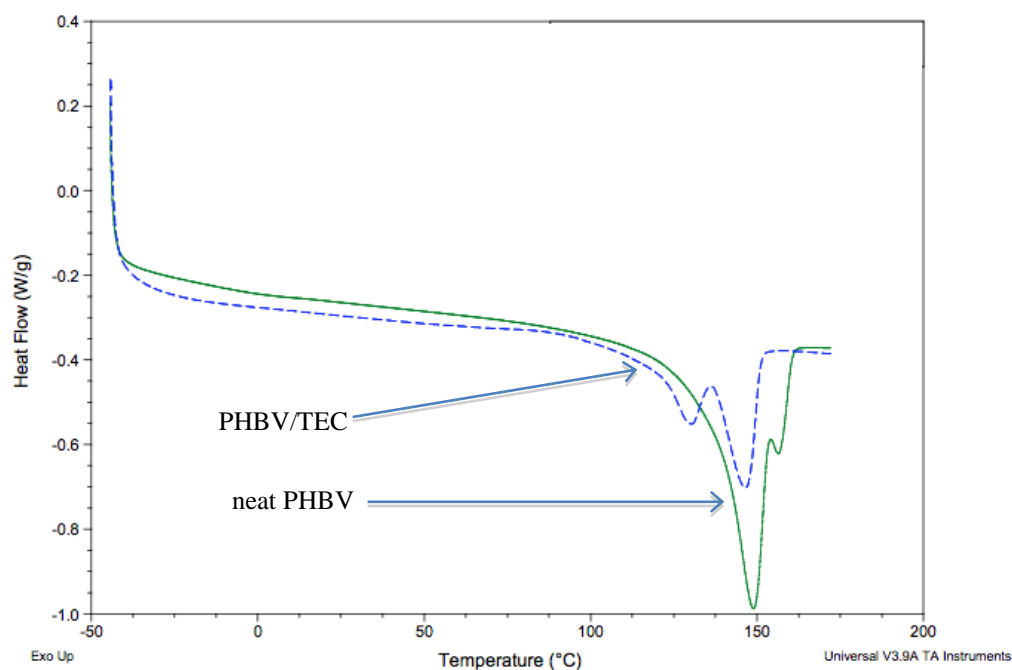


(b)

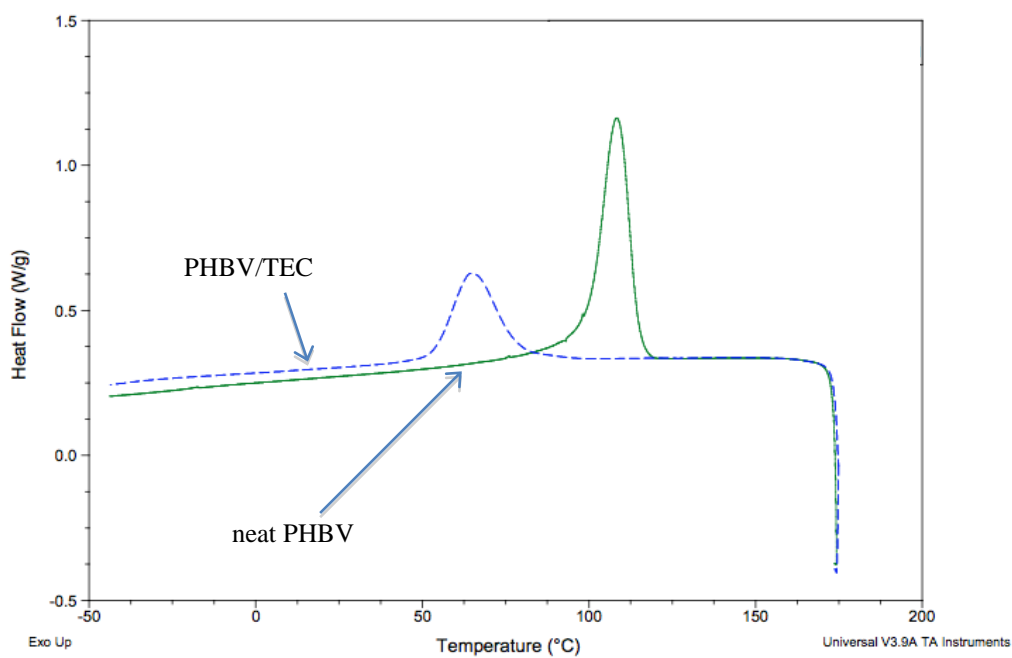
*Figure 4.13 Thermal decomposition profiles of neat PHBV and PHBV/Ecoflex/TiO<sub>2</sub> blends*

As discussed, Triethyl citrate is a plasticizer that is widely used to impart flexibility. Table 4.3 shows the thermal transition properties of the blends. The blend of PHBV/TEC in the fourth trial was found to have different thermal behavior than neat PHBV. The heat flows in the endothermic and exothermic cycle are illustrated in Figure 4.14. The two  $T_m$  points of PHBV/TEC ( $130.98 \pm 0.88$  °C and  $146.51 \pm 0.38$  °C) were lower than those of neat PHBV, as was the heat of fusion. This result is in accordance with the decrease of  $T_m$  of a PLA/starch/methylenediphenyl diisocyanate blend with TEC as a plasticizer found by Ke et al [143]. The  $T_m$  of a PHBV blend with 20% wt. of different plasticizers such as dibutyl phthalate (DBP) and TEC prepared by Choi et al. [144] also decreased. The  $T_m$  is an indicator of the lamella thickness of the crystallites in the polymers and the plasticizer in the blend contributes

to reduction in the thickness [144]. With the inclusion of TEC in the PHBV/TEC blend, then, the  $T_m$  of the blend and heat of fusion of the blend appeared to be lower when compared to those of neat PHBV. This indicates lower crystallinity of the PHBV in the blend. The  $T_c$  also shifted to a lower temperature in the blend, which corresponds to the result obtained in a PLA/starch/maleic anhydride blend with TEC as a plasticizer and a PLA/starch blend with acetyl triethyl citrate (AC) and TEC added as plasticizers [128, 145]. Heat of fusion ( $\Delta H_m$ ) of the PHBV/TEC blend ( $40.54 \pm 2.92$  J/g) was lower than the neat PHBV. The result agreed with the decrease in  $\Delta H_m$  of polyvinyl alcohol (PVA)/glycerin blend. With an increase of glycerin (plasticizer) content in the blend,  $\Delta H_m$  of the PVA/glycerin blend decreased [146]. Figure 4.15 indicates the thermal decomposition profile of the blend. The thermal decomposition temperature of the PHBV/TEC blend was lower than that of neat PHBV due to the presence of TEC in the blend. The PHBV/TEC blend started to slightly degrade at a low temperature, around 150 °C, and reached maximum weight loss at a temperature of about 300 °C. TEC shifted the decomposition temperature of the blend to a lower point. Thus, TEC contributed to decreased thermal stability of the blend compared to neat PHBV.



(a)



(b)

Figure 4.14 Endothermic (a) and exothermic (b) profiles of neat PHBV and PHBV/TEC blends

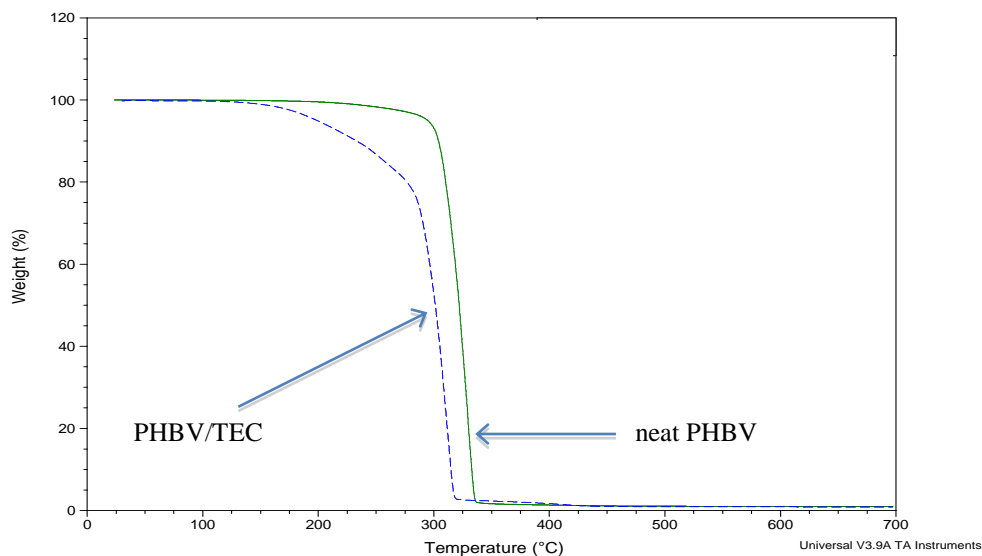
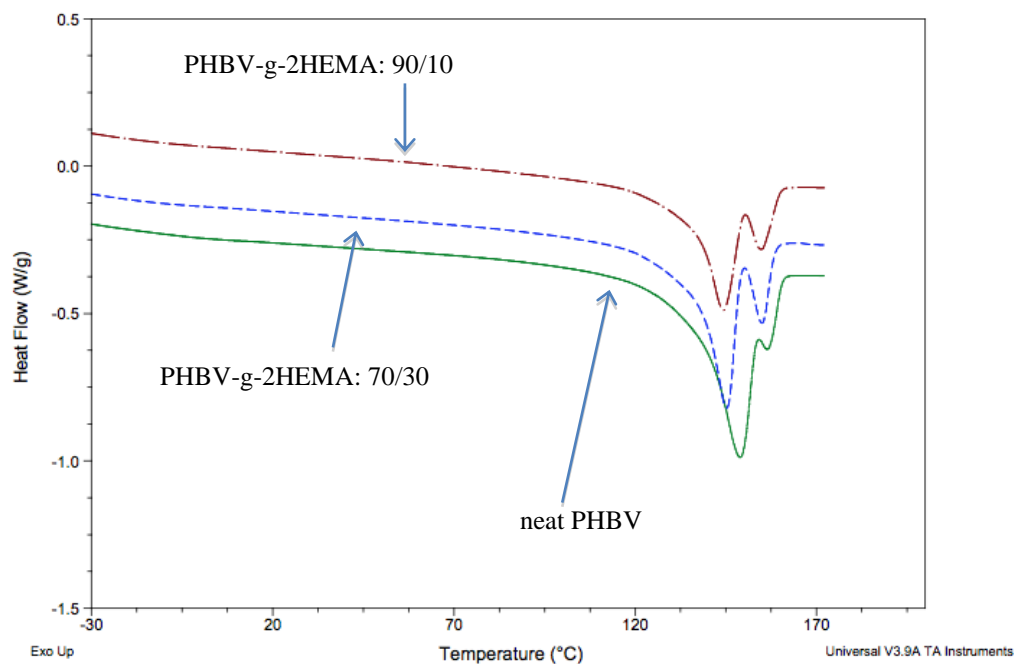


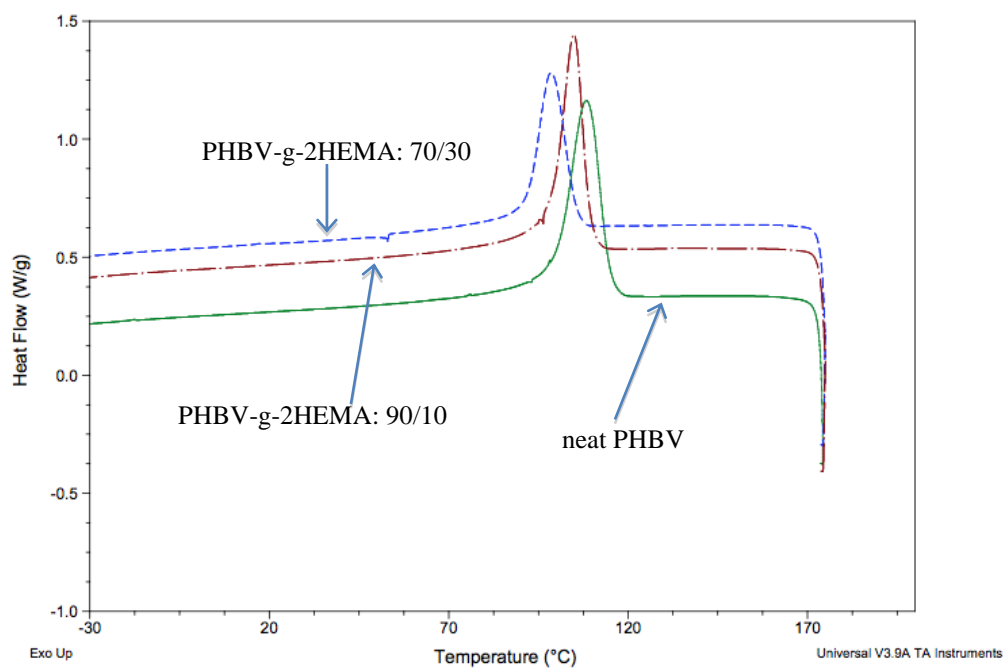
*Figure 4.15 Thermal decomposition profiles of neat PHBV and PHBV/TEC blend*

PHBV grafted with 2HEMA in the fifth trial exhibited two  $T_{ms}$  ( $149.62 \pm 0.23$  °C and  $158.01 \pm 0.44$  °C for PHBV/2HEMA 90/10,  $146.46 \pm 1.84$  °C and  $156.33 \pm 1.22$  °C for 70/30) in the endothermic profile. The  $T_{ms}$  of PHBV-g-2HEMA 70/30 shifted to lower temperatures than neat PHBV whereas the  $T_{ms}$  of PHBV-g-2HEMA 90/10 were not significantly different from the  $T_{ms}$  of neat PHBV, as can be seen in Figure 4.16 (a) and Table 4.3. The exothermic profile is also illustrated in Figure 4.16 (b). In the grafting process, 2HEMA was joined onto the PHBV main chain, resulting in a branched molecular structure in the PHBV-g-2HEMA. The heat of fusion and crystallinity of PHBV in the grafted polymers were also decreased when compared to the neat PHBV. With a higher content of 2HEMA, all thermal transition temperatures decreased. These indicated that 2HEMA grafting introduced in the polymers impeded crystalline formation in the materials [147].

Figure 4.17 shows thermal decomposition profiles of PHBV and two different compositions of PHBV-g-2HEMA. There were two steps of decomposition in the grafted materials. The grafted polymers started to degrade at a lower temperature than PHBV due to 2HEMA in the polymers. According to Demirelli et al., the decomposition product of poly(2HEMA) consists of carbon monoxide, water, ethylene dimethacrylate, ethylene glycol, 3-methyl-5-hydroxy  $\delta$ -valerolactone, 1,2-diisopropenyloxyethane, 1,3-dioxolane, anhydride rings, and other substances. The poly(2HEMA) decomposition was composed of two main steps: depolymerization to monomers and decomposition of esters, which were side chains. The first step occurred at lower temperature and was considered as the main reaction and the second step was at higher temperature [148]. In this study, PHBV-g-2HEMAs began to degrade at a lower temperature of around 150 °C, and reached the maximum weight loss at 320 °C. The second step occurred at a temperature about 325 °C which might be a decomposition of esters and carbon in the backbone structure [118]. The presence of 2HEMA in the grafted PHBV lowered the decomposition temperature of the materials. This indicated that 2HEMA decreased the thermal stability of the grafted PHBV compared to the neat PHBV.



(a)



(b)

Figure 4.16 Endothermic (a) and exothermic (b) profiles of neat PHBV and PHBV-g-2HEMAs

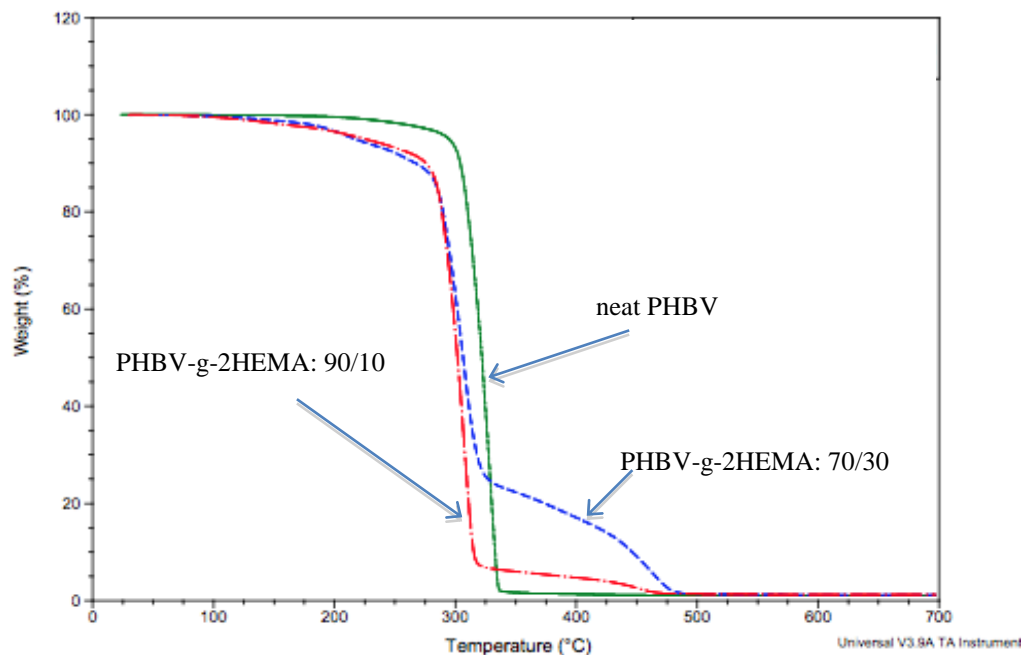
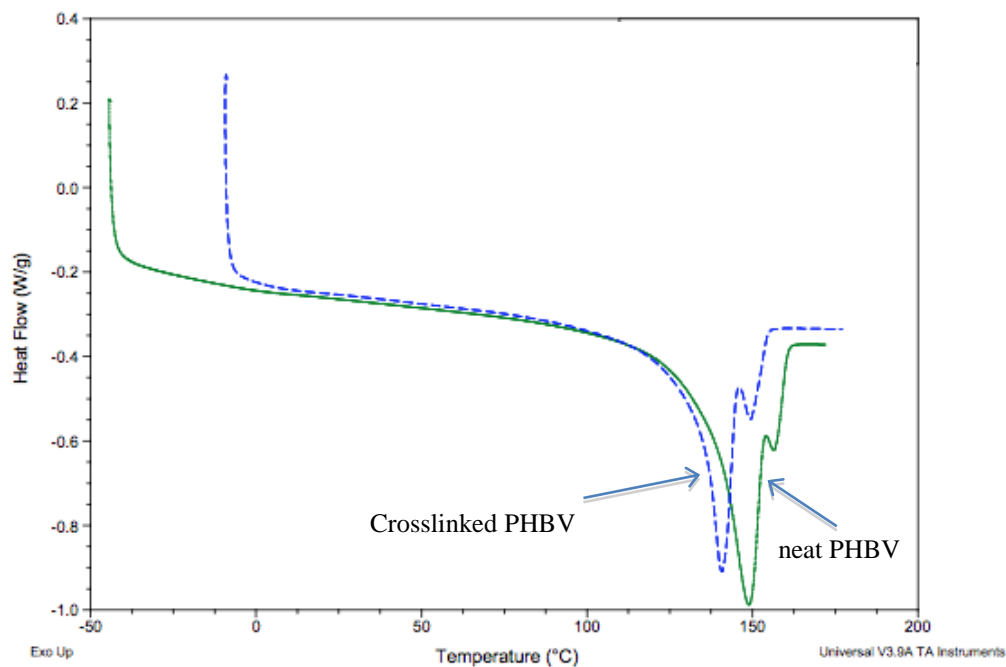


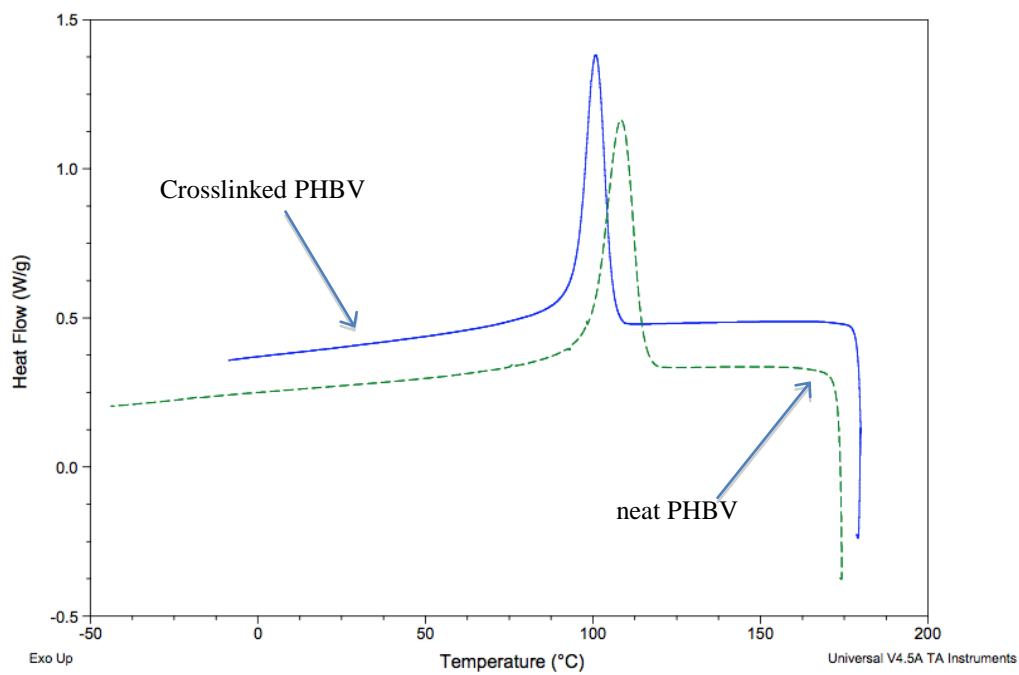
Figure 4.17 Thermal decomposition profiles of neat PHBV and PHBV-g-2HEMAs

Crosslinking is another modification method for improving polymer properties. Table 4.3 shows the thermal properties of the crosslinked PHBV. As can be seen in the endothermic and exothermic curves in Figure 4.18 (a) and 4.18 (b), the melting temperature ( $T_m$ ) of the crosslinked PHBV has two  $T_m$ s ( $140.16 \pm 0.81$  °C and  $148.89 \pm 0.98$  °C) that are lower than those of neat PHBV. The heat of fusion of the crosslinked PHBV was also lower than neat PHBV as can be seen in Table 4.3. This indicated lower crystallinity in the structure. Since the crosslinking process caused PHBV molecular chains to be covalently bonded and become a three-dimensional network, this restricted molecular movement. This network created free volume and interfered with crystallite formation in the material. The result corresponded to the crosslinked PHBV using dicumyl peroxide as an initiator prepared by Fei et al [93]. Also, when crystallinity in the crosslinked structure was hindered, irregular crystalline structures were formed starting at lower temperatures than for PHBV [149].





(a)



(b)

Figure 4.18 Endothermic (a) and exothermic (b) profiles of neat PHBV and crosslinked PHBV

The thermal stability of crosslinked PHBV was investigated using TGA. Figure 4.19 shows the decomposition thermogram of crosslinked PHBV. The thermal decomposition profile of the crosslinked PHBV exhibits one-step weight loss, similar to neat PHBV. The onset and maximum temperature of the crosslinked PHBV were slightly less than neat PHBV. This indicated that crosslinking did not provide thermal stability to the crosslinked PHBV.

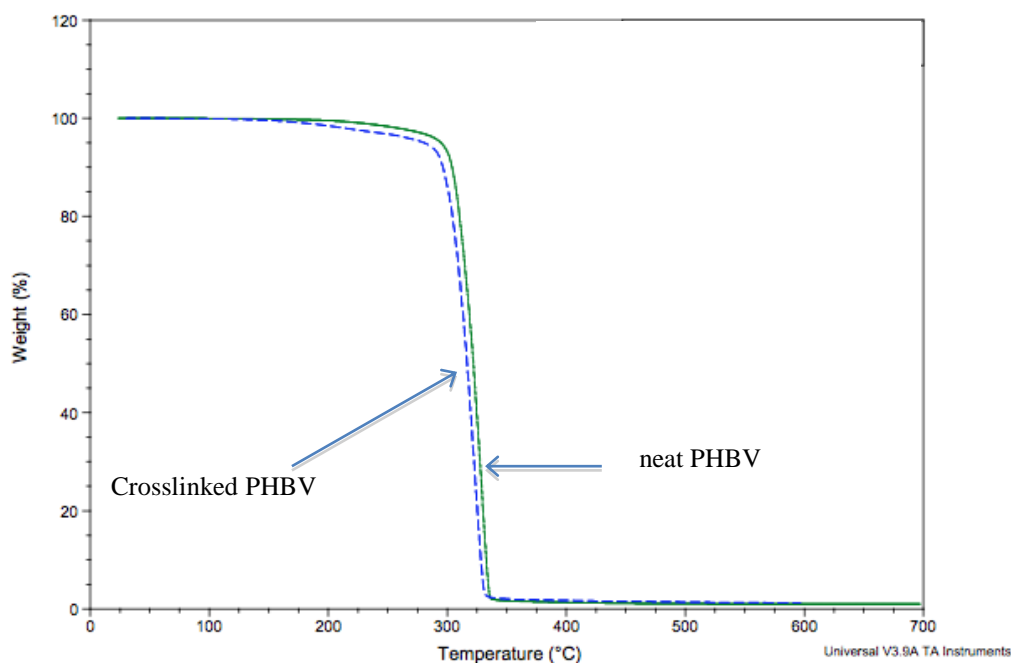


*Figure 4.19 Thermal degradation profiles of neat PHBV and crosslinked PHBV*

#### 4.3.4 Permeation properties of PHBV and modified PHBV

Permeability is an important property for identifying materials that are suitable as good barriers to atmospheric constituents, especially for packaging films. The substances used in barrier testing were water vapor, oxygen, and carbon dioxide. The ability of permeated substances, especially volatiles, to penetrate through a polymer is specific, depending on interactions between the polymer and the penetrant. The diffusion coefficient is an indicating parameter for this specific barrier behavior. It is the penetrant flux within a polymer matrix as a function of the penetrant concentration gradient. The diffusion equation proposed by Fick, Fick's first law, is shown in equation 4.2 for one dimensional mass transfer [59].

$$F = -D \frac{dc}{dx} \quad (4.2)$$

where  $F$  = flow rate

$D$  = diffusion coefficient which is specific for each substance;  $D$  is temperature dependent

$c$  = the concentration of the diffusing substance in the polymer matrix

$x$  = the distance of diffusant travel within the polymer

The diffusion is not the only characteristic involved in permeation of the penetrant through the polymeric materials; solubility is another factor contributing to the permeation characteristics. Solubility is the ability of the polymer to absorb the permeable substances, which can be described by Henry's law for low concentrations of permeants.

The permeation coefficient is a parameter describing permeability. It can be defined as a function of the diffusion and solubility coefficients based on Fick's first law in equation 4.2. This equation is valid for a low concentration of permeant where D and S are independent of concentration and steady state conditions [59, 150].

$$F = D \frac{c_2 - c_1}{L} = DS \frac{p_2 - p_1}{L} \quad (4.3)$$

where  $p$  = the partial pressure of the volatile substance, at low concentration

(Henry's law is valid in this case)

$L$  = thickness of the polymer

$$F = \frac{q}{At} = DS \frac{p_2 - p_1}{L} = P \frac{\Delta p}{L} \quad (4.4)$$

where  $P$  = permeation coefficient

$q$  = the amount of permeant passing through the polymer

$A$  = cross-sectional area through which the permeant travels

$t$  = time

$\Delta p$  = partial pressure difference for the permeant between the two sides  
of the material

In addition, permeability properties of polymeric materials can be affected by various factors. The chemical structure of the polymeric material influences the permeation of volatiles. Polar molecules such as water vapor can be absorbed by polar polymers. The molecular arrangement of polymers also impacts diffusion and absorption of volatiles through the material. Polymer materials with low crystallinity have more amorphous areas where molecules are able to move with respect to one another, creating free volume. This permits a permeant to go through the matrix. Temperature is also a factor affecting permeability. It affects both the solubility and the diffusivity of the permeant through the polymer. This can be described by the Arrhenius equation [59].

$$P = DS = P_0 e^{-E_p/RT}$$

where  $P_0$  = permeability coefficient or pre-exponential factor which is specific  
for a polymer-permeant system

$E_p$  = activation energy

$R$  = gas constant = 8.314 joules per mole

$T$  = temperature in Kelvin

At higher temperature, permeation of permeants in a polymer matrix exponentially increases.

#### 4.3.4.1 Water vapor permeability

The water vapor transmission rate (WVTR) is defined as the quantity of water vapor that penetrates through a unit area of a material in a unit time. Water vapor permeability (WVP) can be obtained by using equation at 4.2 [59].

$$WVP = \frac{WVTR}{\Delta p} \times L \quad (4.5)$$

where  $WVTR = \frac{q}{At}$  in equation 4.4

WVP = P in equation 4.4

$\Delta p$  = water vapor partial pressure difference between the two sides  
of the material film

L = film thickness

WVTR can be measured using a water vapor permeation instrument in accordance with ASTM F1249. Table 4.4 indicates water vapor, oxygen, and carbon dioxide permeability. PHBV has a semicrystalline structure with water insolubility and high crystallinity of  $59.92 \pm 0.30$  %. The water vapor permeability coefficient of PHBV is  $1.74 \times 10^{-6} \pm 0.9 \times 10^{-7}$  kg.m/m<sup>2</sup>.s.Pa. PHBV has a lower WVTR than PLA and polycaprolactone at various temperatures of 6, 25 and 49 °C [150]. This is because PHBV possesses high crystallinity, which decreases water vapor permeability. Crystallites in PHBV are areas in which the molecules are orderly arranged and tightly packed. This packed crystalline structure is the most thermodynamically stable stage.

The ordered pattern of the crystalline array impedes the water vapor path, resulting in a lower cross-sectional area for water vapor to pass through the material [151, 152]. The diffusion of water into PHBV is dependent upon its amorphous area where molecular mobility occurs. The glass transition temperature is a point where polymeric materials change from a glassy to a rubbery form. Water molecules interact with polar molecular groups of the material and plasticize the polymer by altering the glassy to rubbery stage. In other words, amorphous segments allow water vapor to pass through the PHBV matrix [153].

Table 4.4 Permeation properties of all compositions of modified PHBV

| <b>Material</b>   | <b>Water vapor<br/>permeation,<br/>kg.m/m<sup>2</sup>.s.Pa</b> | <b>Oxygen<br/>permeation,<br/>kg.m/m<sup>2</sup>.s.Pa</b> | <b>Carbon dioxide<br/>permeation,<br/>kg.m/m<sup>2</sup>.s.Pa</b> |
|---|--|---|---|
| Neat PHBV   | $1.74 \times 10^{-6} \pm 0.9 \times 10^{-7d}$                  | $2.26 \times 10^{-18} \pm 3.4 \times 10^{-19d,e}$         | $2.06 \times 10^{-17} \pm 8.5 \times 10^{-18c}$                   |
| Blend of PHBV/TiO <sub>2</sub> nanoparticle 1% wt         | $1.70 \times 10^{-6} \pm 1.8 \times 10^{-7d}$                  | $2.60 \times 10^{-18} \pm 1.0 \times 10^{-19d}$           | $2.91 \times 10^{-17} \pm 1.3 \times 10^{-18c}$                   |
| Blend of PHBV/Ecoflex : 50/50 % wt                        | $5.53 \times 10^{-6} \pm 2.4 \times 10^{-7b}$                  | $6.68 \times 10^{-18} \pm 5.3 \times 10^{-19a}$           | $7.23 \times 10^{-17} \pm 1.17 \times 10^{-17a}$                  |
| Blend of PHBV/Ecoflex/TiO <sub>2</sub> : 79/20/1 % wt     | $4.43 \times 10^{-6} \pm 3.8 \times 10^{-7b,c}$                | $5.22 \times 10^{-18} \pm 4.9 \times 10^{-19c}$           | -   |
| Blend of PHBV/Ecoflex/TiO <sub>2</sub> : 69/30/1 % wt     | $5.41 \times 10^{-6} \pm 2.1 \times 10^{-7b,c}$                | $5.38 \times 10^{-18} \pm 5.2 \times 10^{-19b,c}$         | -   |
| Blend of PHBV/Ecoflex/TiO <sub>2</sub> : 49.5/49.5/1 % wt | $5.56 \times 10^{-6} \pm 2.0 \times 10^{-7b}$                  | $6.30 \times 10^{-18} \pm 0.6 \times 10^{-19a,b}$         | $7.95 \times 10^{-17} \pm 9.3 \times 10^{-18a}$                   |

All measurements were performed in triplicate.

Values are reported as mean  $\pm$  standard deviation.

Different letter designations for values in the same column indicate significant differences ( $p \leq 0.05$ ).

Permeability of the PHBV/TEC blend could not be measured since TEC leached out to the polymer surface.



Table 4.4 (Cont'd)

| <b>Material</b>                                     | <b>Water vapor<br/>permeation,<br/>kg.m/m<sup>2</sup>.s.Pa</b> | <b>Oxygen<br/>permeation,<br/>kg.m/m<sup>2</sup>.s.Pa</b> | <b>Carbon dioxide<br/>permeation,<br/>kg.m/m<sup>2</sup>.s.Pa</b> |
|---|--|---|---|
| Grafted PHBV with 2HEMA : 90/20 % wt (L101 0.1% wt) | $2.11 \times 10^{-6} \pm 2.6 \times 10^{-7d}$                  | $1.40 \times 10^{-18} \pm 4.0 \times 10^{-19e}$           | $3.06 \times 10^{-17} \pm 0.1 \times 10^{-18c}$                   |
| Grafted PHBV with 2HEMA : 70/30 % wt (L101 0.1% wt) | $4.13 \times 10^{-6} \pm 8.0 \times 10^{-7c}$                  | $2.88 \times 10^{-18} \pm 2.3 \times 10^{-19d}$           | $5.13 \times 10^{-17} \pm 0.3 \times 10^{-18b}$                   |
| Crosslinked PHBV (L101 2% wt)                       | $8.18 \times 10^{-6} \pm 9.8 \times 10^{-7a}$                  | -   | $2.39 \times 10^{-17} \pm 3.6 \times 10^{-18c}$                   |

All measurements were performed in triplicate.

Values are reported as mean  $\pm$  standard deviation.

Different letter designations for values in the same column indicate significant differences ( $p \leq 0.05$ ).

The residence time in the extruder of crosslinked PHBV was 1 min.

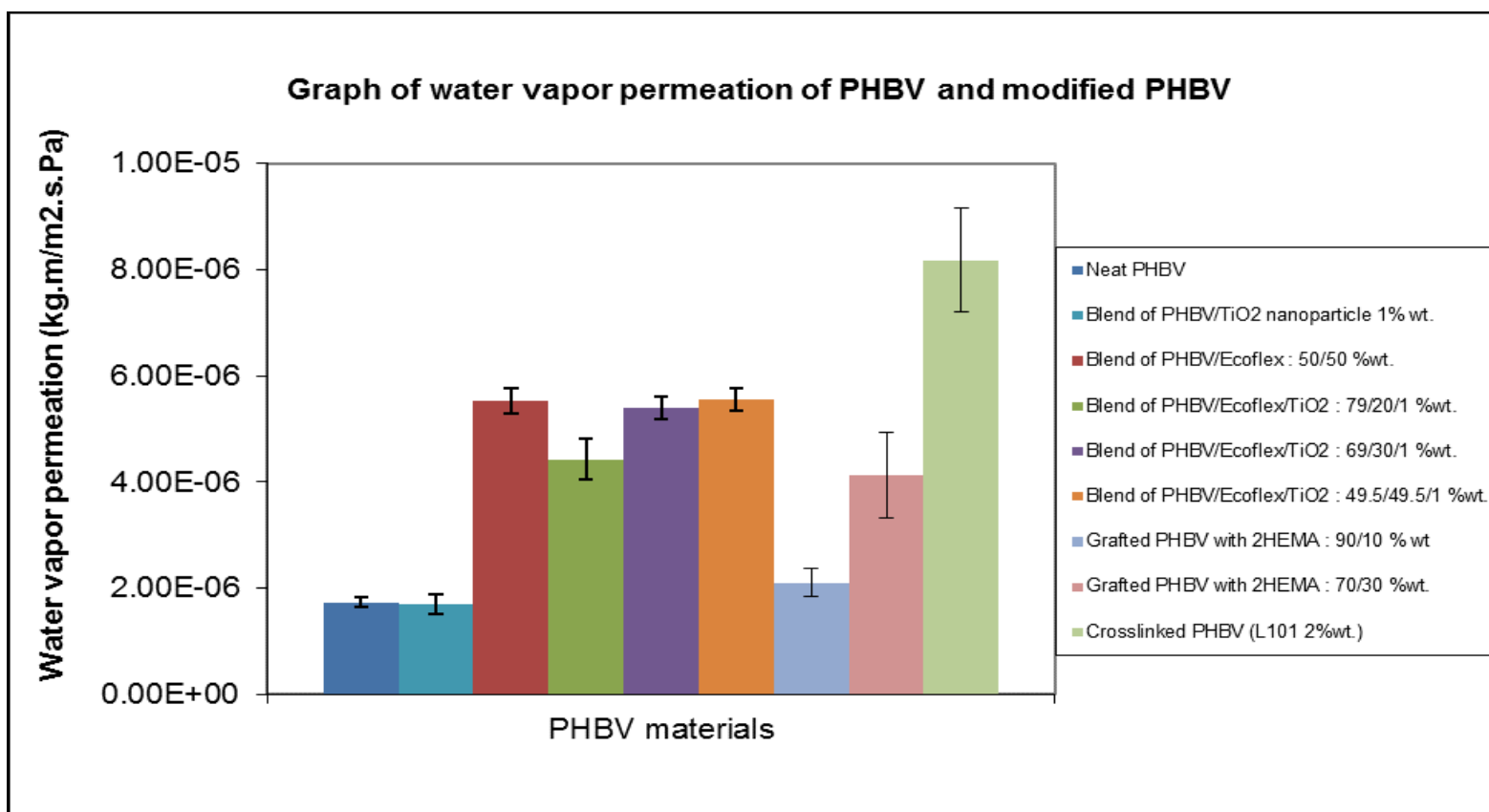


*Figure 4.20 Water vapor permeation of PHBV material sheets*

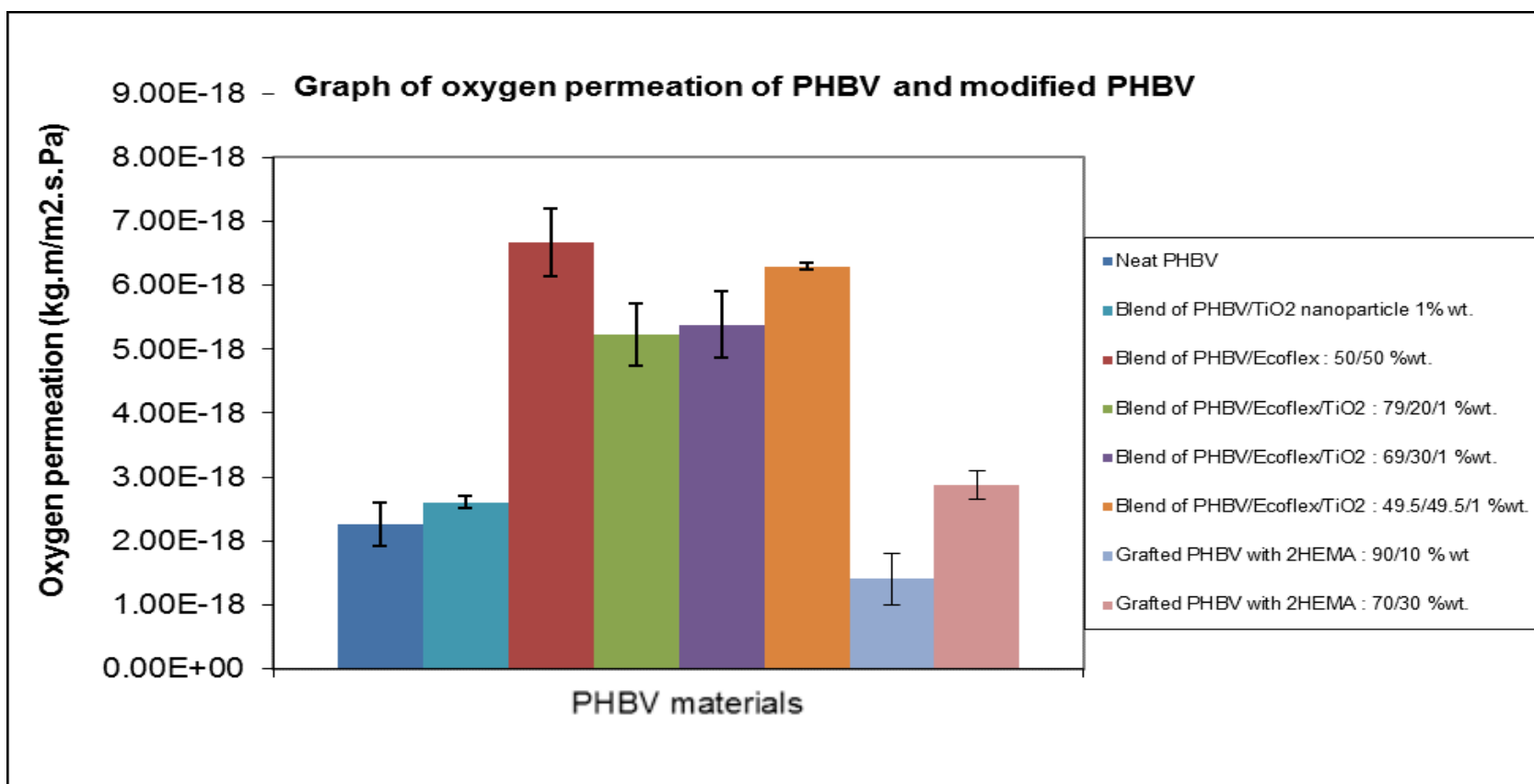


*Figure 4.21 Oxygen permeation of PHBV material sheets*

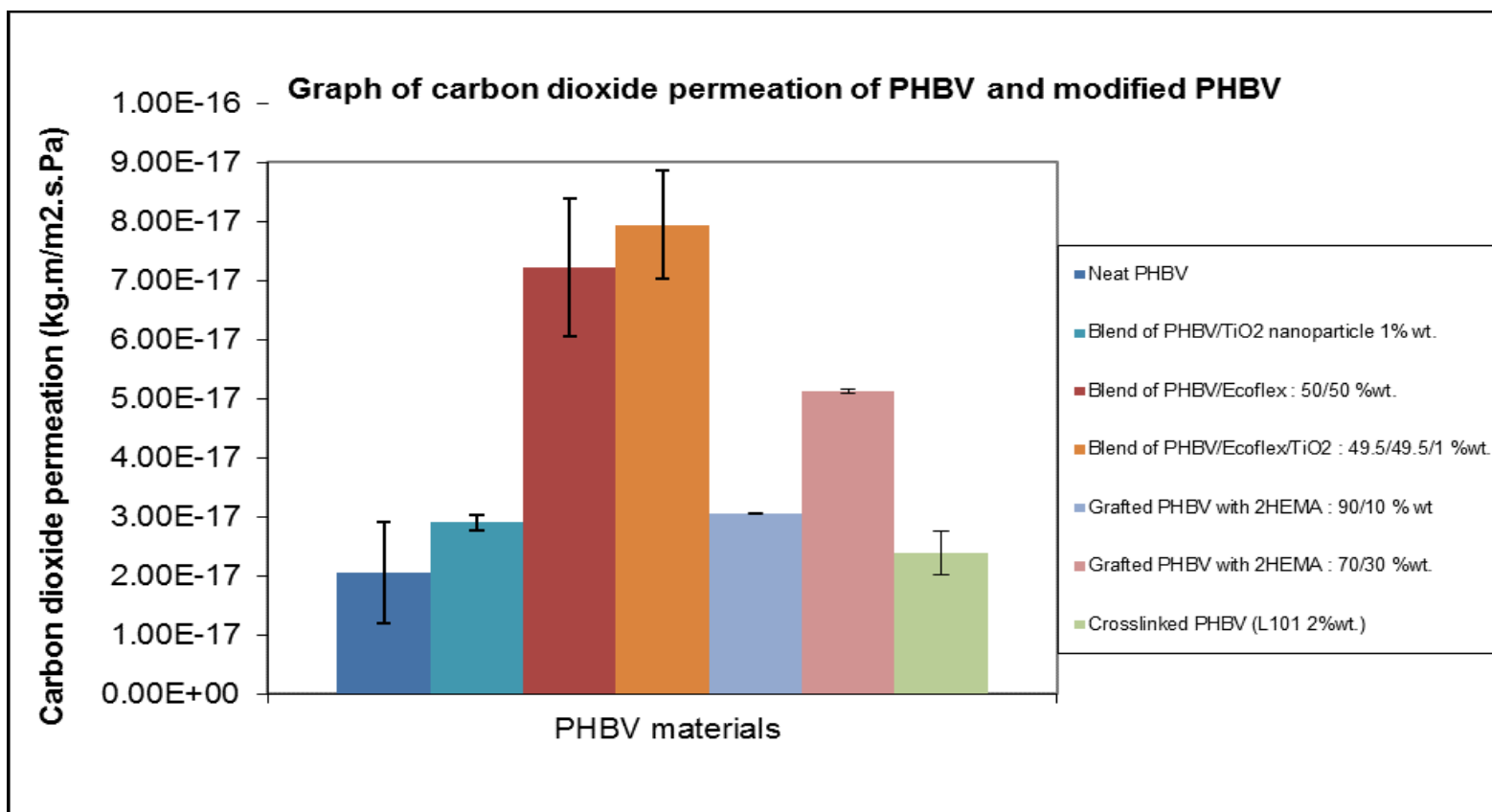


*Figure 4.22 Carbon dioxide permeation of PHBV material sheets*

Incorporation of other substances has an impact on WVP. PHBV with TiO<sub>2</sub> in this study had WVP insignificantly lower than the neat PHBV. WVP of PHBV/TiO<sub>2</sub> was  $1.70 \times 10^{-6} \pm 1.8 \times 10^{-7}$  kg.m/m<sup>2</sup>.s.Pa. This result corresponded with PHBV/fiber blends prepared by Sanchez-Garcia et al. Fiber inclusion in PHBV slightly decreased WVP at a low fiber content of 1% wt. With higher content of fiber, WVP increased due to agglomeration of the fiber. This behavior caused a lack of polymer homogeneity and cohesion in the matrix and created pathways (voids) for permeation [152]. In addition, according to Rhim et al., nanoclay added to PLA improved water vapor barrier when compared to PLA [154]. The PHBV/TiO<sub>2</sub> blend had a better barrier to water vapor than the neat PHBV. This was attributed to the tortuous path created by TiO<sub>2</sub> resulting in low WVP.

Blending with other polymeric material also modified WVP. The inclusion of Ecoflex in the PHBV/Ecoflex blend worsened the water vapor barrier. The WVP of PHBV/Ecoflex 50/50 %wt. of this study was  $5.53 \times 10^{-6} \pm 2.4 \times 10^{-7}$  kg.m/m<sup>2</sup>.s.Pa whereas WVP for PHBV/Ecoflex 70/30 and 80/20 could not be measured since the amount of water vapor detected was so large it was beyond the measuring range of the machine. The repeated failure of the test occurred also for oxygen and carbon dioxide permeation measurements for these blends and was attributed to minor cracks in the material. Ecoflex is a biopolymer with higher hydrophilicity than PHBV, which might compromise the barrier property. This factor has a detrimental effect on WVP [108]. Furthermore, similar behavior was observed by Suyatma et al. PLA, a hydrophobic polymer, was incorporated in chitosan decreasing WVP. With an increase of PLA to 10% wt., water vapor barrier was better than the blends with PLA contents of 20% and 30% [155].

Additionally, the effect of incorporation of both  $\text{TiO}_2$  and Ecoflex was studied. The PHBV/Ecoflex/ $\text{TiO}_2$  blends, with PHBV/Ecoflex/ $\text{TiO}_2$  ratios of 79/20/1, 69/30/1, and 49.5/49.5/1, had WVP of  $4.43 \times 10^{-6} \pm 3.8 \times 10^{-7}$ ,  $5.41 \times 10^{-6} \pm 2.1 \times 10^{-7}$ , and  $5.56 \times 10^{-6} \pm 2.0 \times 10^{-7}$  kg.m/m<sup>2</sup>.s.Pa, respectively. WVPs of the blends were not significantly different from each other or from the PHBV/Ecoflex 50/50 blend. However, they were much higher than for the neat PHBV. Adding  $\text{TiO}_2$  in the PHBV/Ecoflex/ $\text{TiO}_2$  79/20/1 and 69/30/1 blends did result in sheets for which the permeability coefficient could be measured, unlike the blends without  $\text{TiO}_2$  for which measurements failed, as discussed earlier.

Plasticizers in polymers also influence permeability of the material. In this study, the permeability of the PHBV/TEC blend could not be measured. This is because TEC leached out to the surface of the material, resulting in an oily surface and inability to attach to the aluminum mask for the permeation test. However, the study of Munoz et al., showed that the incorporation of glycerol as a plasticizer in glutenin-rich film strikingly increased WVP of the film at higher than 40%wt of glycerol. The plasticizer in the blend created free volume and increased molecular movement and the matrix was less dense [156].

Grafting also can alter the permeability of the polymer. WVPs of the grafted PHBV with 2HEMA are indicated in Table 4.4. The presence of 2HEMA content of 20 % wt. did not significantly increased WVP of the grafted PHBV compared to the neat PHBV. However, sheets with 30 wt. % 2HEMA (30 %wt.) in the grafted material had significantly higher WVP than both neat PHBV and grafted PHBV with 20 % wt. of 2HEMA. Grafting of 2HEMA created a branched chain PHBV matrix, which hindered the crystallization of PHBV,

contributing to free volume for water vapor passing through [147]. Additionally, 2HEMA is a water-soluble monomer, which has polar affinity [157]. Thus, the grafted PHBV is more water-favorable. With an increase of 2HEMA, the WVP barrier was compromised. This result was in agreement with the chitosan/HEMA membrane produced by Li et al. HEMA in the material increased hydrophilicity of chitosan leading to higher permeation [158].

Other than the modifications reported earlier, crosslinking is another way to modify polymers for suitable applications. WVP of the crosslinked PHBV with a help of L101 as an initiator in this study was  $8.18 \times 10^{-6} \pm 9.8 \times 10^{-7}$  kg.m/m<sup>2</sup>.s.Pa, which is higher than that of the neat PHBV. In general, crosslinking decreases permeation since molecular chains are restricted and linked by covalent bonds in a three-dimensional array, contributing to limited movement of the molecules and a dense structure. This decreases the permeability. According to Frederick, crosslinked protein-pullulan films with alginate derivative propyleneglycol alginate (PGA) as a crosslinker had decreased WVP when compared to the un-crosslinked [159]. In addition, crosslinked gliadin-rich fraction film prepared by Hernandez-Munoz et al. had significantly higher water barrier than the un-crosslinked film [160]. In this study, in contrast, higher WVP of the crosslinked PHBV might be because covalent bonds in the crosslinking network impeded the crystallinity of the PHBV, creating free volume (voids), which was a preferable path for water vapor.

#### 4.3.4.2 Oxygen and carbon dioxide permeability

Oxygen and carbon dioxide are common gases used in measuring gas barrier properties of polymeric materials. Oxygen and carbon dioxide permeation through materials are crucial to food shelf life. So, oxygen and carbon dioxide permeation are essential to plastic packaging selection. Oxygen and carbon dioxide permeation of PHBV in this study were  $2.26 \times 10^{-18} \pm 3.4 \times 10^{-19}$  and  $2.06 \times 10^{-17} \pm 8.5 \times 10^{-18}$  kg.m/m<sup>2</sup>.s.Pa, respectively. According to Thellen et al., PHBV possesses high barrier to oxygen [161]. This could be due to high crystallinity and less amorphous area creating fewer pathways for the gases to pass through. In addition, according to Costamagna, et al., a crystalline structure is an impermeable barrier. It takes longer for gases to travel along the interface of crystalline and amorphous regions (tortuous path) than in amorphous regions, resulting in lower gas permeability [162]. Inclusion of both the inorganic compound and the polymer in PHBV also affected the permeation of oxygen and carbon dioxide. According to Ray et al. PLA-layered silicate nanocomposite was prepared by adding montmorillonite modified with octadecylammonium cation in PLA in melt extrusion. The PLA nanocomposite blend had lower O<sub>2</sub> permeation than the neat PLA [163]. Fabrication of PLA/TiO<sub>2</sub> nanocomposite films as reported by Zhu et al. had a lower O<sub>2</sub> permeability coefficient than pure PLA [126]. Matteucci et al. stated that gas (CO<sub>2</sub> H<sub>2</sub>, N<sub>2</sub> and CH<sub>4</sub>) permeation of poly(1-trimethylsilyl-1-propyne) added with TiO<sub>2</sub> was lower at low TiO<sub>2</sub> content whereas the permeation increased with a high content of TiO<sub>2</sub> due to the higher void fraction in the material [164]. In this study, PHBV/TiO<sub>2</sub> had O<sub>2</sub> and CO<sub>2</sub> permeation of  $2.60 \times 10^{-18} \pm 1.0 \times 10^{-19}$  and  $2.91 \times 10^{-17} \pm 1.3 \times 10^{-18}$  kg.m/m<sup>2</sup>.s.Pa, respectively. These values were not significantly greater than PHBV. This indicates the presence of TiO<sub>2</sub>. 1%wt. did not affect



O<sub>2</sub> and CO<sub>2</sub> permeability of the neat PHBV. In contrast, the presence of Ecoflex in PHBV/Ecoflex 50/50 %wt. decreased the O<sub>2</sub> and CO<sub>2</sub> barrier properties when compared to the neat PHBV. This might be due to the fact that Ecoflex somewhat impeded the crystalline formation of PHBV, leading to a less dense matrix and gases could travel through the free volume of the polymer. For PHBV/Ecoflex 80/20 and 70/30 %wt%, the gas permeation, both O<sub>2</sub> and CO<sub>2</sub>, could not be measured, as stated earlier.

In the PHBV/Ecoflex/TiO<sub>2</sub> systems, the O<sub>2</sub> and CO<sub>2</sub> permeation were also higher than PHBV, as shown in Table 4.4. CO<sub>2</sub> permeation for PHBV/Ecoflex/TiO<sub>2</sub> 79/20/1 and 69/30/1 %wt. could not be measured as the CO<sub>2</sub> quantity was beyond the range of the instrument. A possible explanation is minor cracks occurred in the test samples but that did not occur for the WVP and O<sub>2</sub> samples so the cause is uncertain. O<sub>2</sub> and CO<sub>2</sub> permeation of PHBV/Ecoflex/TiO<sub>2</sub> 49.5/49.5/1 %wt. were not statistically different from those of PHBV/Ecoflex 50/50 %wt.

The O<sub>2</sub> and CO<sub>2</sub> permeation coefficients of PHBV-g-2HEMA 90/10 and 70/30%wt are shown in table 4.4. It was found that O<sub>2</sub> permeation coefficient for PHBV-g-2HEMA 90/10 and 70/30 were not significantly different from that of the neat PHBV. However, there was a difference between PHBV-g-2HEMA 90/10 and 70/30. Grafting with a low content of 2HEMA decreased O<sub>2</sub> permeation compared to the neat PHBV, as opposed to grafting with a higher 2HEMA load. CO<sub>2</sub> permeation in the neat PHBV and PHBV-g-2HEMA 90/10 were not significantly different whereas PHBV-g-2HEMA 70/30 had greater CO<sub>2</sub> permeation than both the neat PHBV and PHBV-g-2HEMA 90/10. According to Costamagna et al. [162], grafting poly(acrylic acid) onto LDPE decreased O<sub>2</sub> permeation when compared to the ungrafted

polymer [162]. Huang and Kanitz stated that polyethylene-styrene graft copolymer fabricated by  $\gamma$  radiation of LDPE in a styrene-methanol solution had a decrease in O<sub>2</sub> and CO<sub>2</sub> permeability with increase in grafting from 20-30% and both gas permeabilities increased again above 30%. This was because, in low grafting, the free volume decreased due to less mobility of LDPE chains creating cohesion forces resulting in lower permeability. Above 30%, polystyrene chains disrupted crystalline areas of LDPE [165]. In this study, at lower 2HEMA of 10% wt., grafting did not influence the permeability of either of the gases. With an increase of 2HEMA, greater CO<sub>2</sub> permeability was obtained even though the increase in O<sub>2</sub> permeation was not significant, compared to the neat PHBV. This is because grafting initiated branching of the molecules in the polymer matrix and made the polymer matrix less crystalline. Thus, gases were able to diffuse through the polymer.

For gas permeation of the crosslinked PHBV in this study, O<sub>2</sub> permeation could not be measured due to failure in the O<sub>2</sub> permeation tester. In this case, the O<sub>2</sub> transmission level increased and did not level off, resulting in a “failed” test. However, CO<sub>2</sub> permeation of the crosslinked PHBV was  $2.39 \times 10^{-17} \pm 3.6 \times 10^{-18}$  kg.m/m<sup>2</sup>.s.Pa, which was not statistically different from PHBV. Thus, crosslinking did not influence the CO<sub>2</sub> permeation in the crosslinked material.

#### **4.4 Conclusion**

In the effort to modify PHBV, many methods were used for improving PHBV to be effective for use in flexible packaging. The main property that needs to be improved is elongation, which indicates flexibility. PHBV has inherent brittleness, tackiness, high crystallinity, and low melt strength. These drawbacks lead to inability to process in conventional processes such as extrusion cast film and blown film. To overcome the drawbacks, inorganic compound incorporation, blending, incorporation of plasticizer, grafting and crosslinking were applied in order to fabricate a modified PHBV. The resulting modified PHBV materials had lower tensile strength and elongation at break than the neat PHBV except for the crosslinked PHBV. The crosslinked PHBV had elongation at break much greater than the neat PHBV even though its tensile strength was only slightly higher than the neat PHBV. Crosslinking, therefore, was the selected modification method for improving flexibility of PHBV in this study.

## **5. INFLUENCE OF THE AMOUNT OF INITIATOR ON THE DEGREE OF PHBV CROSSLINKING AND ITS PROPERTIES**

### **5.1 Introduction**

The previous study showed that crosslinking is the best way to improve the ductility including flexibility of PHBV thin sheet for packaging applications. Elongation is the crucial property that is of concern in this study. Elongation is the ability of a material to be plastically deformed under load. It is the change in length before failure. The goal was to obtain the optimum content of initiator resulting in the maximum elongation of the crosslinked PHBV. Crosslinking is a potential modification method for polymer materials in order to impart useful properties for suitable applications. It is polymer chain extension by covalently bonding in multiple directions creating a crosslinked network. The covalent bonds in crosslinking can be intramolecular or intermolecular bonds, or both. The crosslinking process is irreversible. Molecular chains in a crosslinked polymer are restricted so that they are unable to move past one another, resulting in elasticity in amorphous areas and reduced crystallinity as well as reduction of free volume. Crosslinking impedes the orderly arrangement of molecular chains in crystalline formations, contributing to elastic behavior at a low degree of crosslinking. Polymeric materials become softer. Crosslinking changes polymer properties to become more durable and resistant to heat, light, chemicals, mechanical load, etc. [60].

## **5.2 Fabrication of crosslinked polyhydroxybutyrate-co-valerate with different amounts of initiator**

PHBV neat resin was placed in the mini twin-screw extruder with L101 as an initiator for the crosslinking reaction. The amount of initiator was varied: 0.5, 1, 2, 3 and 4% wt. The extruder was set at a screw speed of 150 rpm, and temperature of 165 °C in all three temperature zones. In the beginning of the process, the polymer was sticky and hard to mix in the extruder. The force increased sharply as cross-linking began to occur. At the maximum shearing force, the materials were well mixed and the reaction reached a maximum. When the reaction proceeded beyond this point, PHBV experienced thermal degradation and the shear force declined. Therefore the point of maximum shear force was used as a guideline to obtain the maximum extent of cross-linking. The residence time (at the maximum shear force) was 1 min. Figure 5.1 shows the shearing force profile of molten PHBV in the extruder. The crosslinked extrudates were discharged from the extruder in a strand form with low melt strength, stickiness and elastomeric behavior [77]. The extrudates were left at room temperature until they solidified. The solid strands were pelletized. Then, the crosslinked PHBV pellets were placed in a 180×180 mm<sup>2</sup> aluminum frame of thickness 0.25 mm. and sandwiched between aluminum platens in order to form compression molded sheets. The pellets were compression molded at a temperature of 165 °C and 20,000 psi for 5 min. and cooled by tap water flow through the platens for 15 min. The crosslinked PHBV sheets obtained were pre-conditioned at 23 °C, 50 %RH for 48 hrs. and then investigated visually, and tested for mechanical, thermal and permeability properties. Figure 5.2 shows the crosslinked PHBV resins produced with L101 initiator content at 0.5, 1, 2, 3, and 4 %wt.

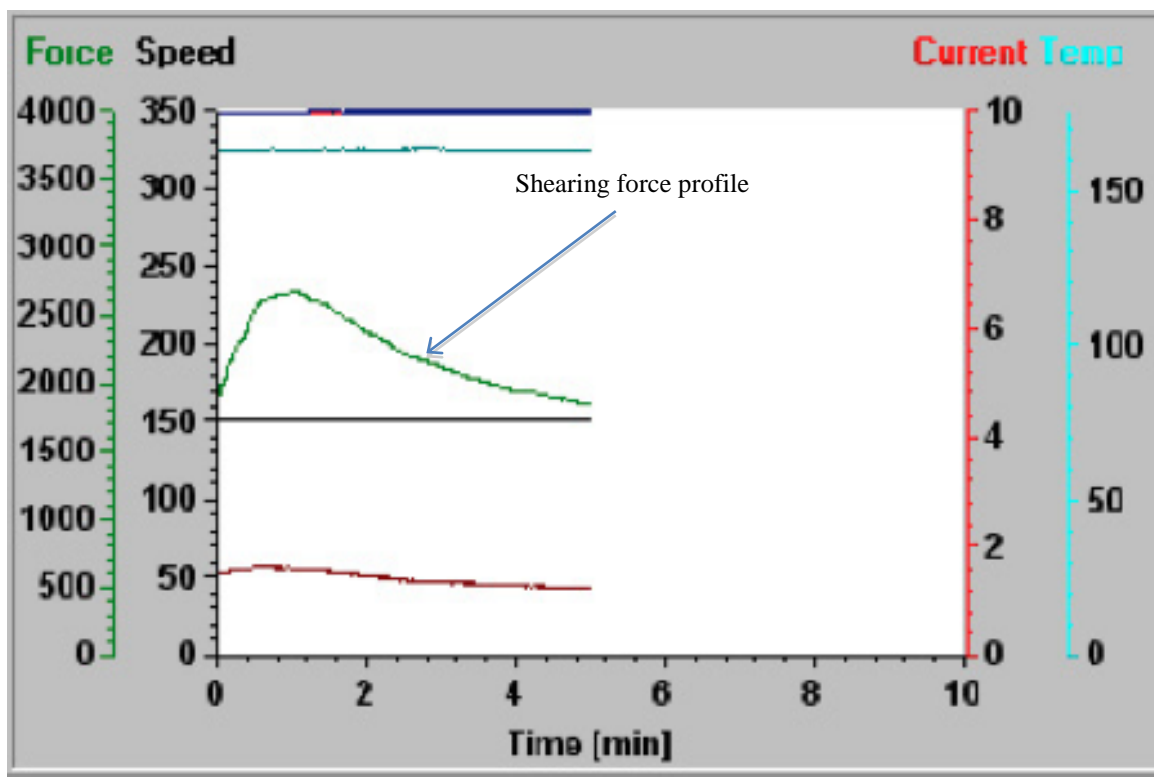


*Figure 5.1 Shearing force profile of the molten PHBV crosslinked with a presence of L101 vs. time in the mini twin screw extruder indicating the maximum force of molten polymer reached the highest at reaction time of 1 min.*



(a)



(b)



(c)



(d)



(e)



(f)

*Figure 5.2 PHBV neat resin (a) and crosslinked PHBV with L101 of 0.5 (b), 1 (c), 2 (d), 3 (e), and 4 (f) %wt.*

### 5.3 Results and discussion

#### *5.3.1 Visual characteristics of the crosslinked poly(hydroxybutyrate-co-valerate)s*

The PHBV extrudates with L101 at 0.5, 1, and 2 %wt. had low melt strength, elastomeric behavior and tackiness, causing them to stick to surfaces such as the die. The PHBV extrudates with L101 at 3 and 4 %wt., on the other hand, had better melt strength and less tackiness than PHBV and those with L101 at 0.5, 1, and 2 %wt. After cooling down and pelletization, the pellets of PHBV with L101 at 0.5, 1, and 2 %wt., visually similar to neat PHBV, were yellowish in color, had a smooth surface, and were rigid and soft when compressed, similar to rubber. Meanwhile, the pellets of crosslinked PHBV with L101 at 3, 4 %wt. were pale yellow and had air pockets inside, resulting in a structure that resembled a sponge, as can be seen in Figure 5.2. This characteristic was similar to that of crosslinked PHBV with dicumyl peroxide (DCP) as an initiator prepared by Fei et al. The crosslinked PHBV with 3%wt DCP had many bubbles distributed in the material [93]. The pellets were rigid and harder than neat PHBV when compressed. After being molded into sheet form, all the crosslinked PHBV sheets looked similar to one another and to the neat PHBV sheet as well. All the visual characteristics of the crosslinked PHBV polymers are shown in Table 5.1



Table 5.1 Visual characteristics of PHBV and crosslinked PHBV with L101 of 0.5, 1, 2, 3, and 4 % wt.

| Material                        | Extrudate  | Disk form                  | Sheet form                                       |
|---------------------------------|--|----------------------------|--|
| Neat PHBV                       | -  | -                          | Yellow,<br>flexible but brittle when folded      |
| Crosslinked PHBV (L101 0.5% wt) | Low melt strength,<br>Sticky when heated,<br>Rigid when cooled | Rigid but soft like rubber | Yellow,<br>flexible but brittle when folded      |
| Crosslinked PHBV (L101 1% wt)   |  |                            |  |
| Crosslinked PHBV (L101 2% wt)   |  |                            |  |
| Crosslinked PHBV (L101 3% wt)   |  |                            | Pale yellow,<br>flexible but brittle when folded |
| Crosslinked PHBV (L101 4% wt)   |  |                            |  |

The residence time of all crosslinked PHBV was 1 min.

### 5.3.2 Mechanical properties of crosslinked poly(hydroxybutyrate-co-valerate)s

As mentioned earlier, elongation is the property of most concern in this study. It indicates ductility and flexibility of the material. The tensile strength and elongation at break of neat PHBV and crosslinked PHBVs are shown in Table 5.2, Figure 5.3 and Figure 5.4. Tensile strength is the ability of a polymeric material to withstand load. The crosslinked PHBV with L101 at 0.5 and 1 %wt. had lower tensile strength than the neat PHBV whereas tensile strengths of both crosslinked PHBVs with L101 at 2 and 4 %wt. were not statistically significantly different from the neat PHBV. Meanwhile, elongation at break in the crosslinked PHBV was significantly improved. When the amount of L101 was increased, the elongation at break increased until reaching the maximum at L101 2% wt. With an increase of L101 greater than 2 %wt., elongation at break decreased. The crosslinked PHBV with L101 2 % wt. had statistically greater elongation than the neat PHBV, more than two times that of the neat material. L101 in the reaction acts as an initiator or crosslinker for the crosslinking reaction. It initiates free radicals on the PHBV molecular chains, which promptly covalently react to form a multi directional network and the network rapidly grows. The covalent bonds can be intra- and/or intermolecular bonds resulting in molecular chain restriction, so that the molecular chains are unable to move pass one another. In the crosslinked PHBV with L101 less than 2 %wt., the elongation at break increased with an increase of L101 content. This might be because the crosslinker induced more free radicals, which resulted in more molecular chain restriction and more elongation. At PHBV with L101 more than 2 %wt., on the other hand, the large number of free radicals may have led to more restrictions due to a higher crosslink density. PHBV with L101 at 3 and 4 %wt. appeared to be a rigid and hard material. According

to Haene et al., branched PHBV was obtained with a small amount of dicumyl peroxide (DCP) of 0.025-0.3 %wt. as an initiator. At DCP more than 0.2 %wt., elongational viscosity in the crosslinked PHBV melt steeply increased indicating long chain branching [166]. An increase in elongation at break of the crosslinked PHBV in this study agreed with the results of PHBV sheets crosslinked with DCP. At DCP 1 %wt., elongation improved from 4 to 8.9%, and the elongation was far higher with crosslinked PHBV at DCP of 2 and 3%wt. Moreover, the tensile strengths of crosslinked PHBV produced with various amount of DCP were not much different from one another [93]. This corresponds to the tensile strength results for crosslinked PHBV in this study.

Moreover, many studies indicate that crosslinking alters the mechanical properties of polymers. Bigi et al. reported that glutaraldehyde (GTA) crosslinked gelatin film possessed high stress at break and elongation at GTA more than 1%wt as well as low deformation of the film [167]. The crosslinked starch-PVC blend with borax as a crosslinker was fabricated for improving tensile strength and flexibility of the gelatinized starch. Borax initiated covalent bonds in the blend, which promoted intermolecular H-bonds previously present in the blend. The crosslinked material had higher tensile strength than the non-crosslinked starch-PVC blend [168].

Table 5.2 Mechanical properties of crosslinked PHBV at various initiator contents compared to neat PHBV

| Material                        | Tensile strength (MPa)      | Elongation at break (%)   |
|---------------------------------|-----------------------------|---------------------------|
| Neat PHBV                       | 19.84±0.54 <sup>a,b</sup>   | 15.04±0.59 <sup>c</sup>   |
| Crosslinked PHBV (L101 0.5% wt) | 15.42±0.88 <sup>d</sup>     | 16.37±1.76 <sup>c</sup>   |
| Crosslinked PHBV (L101 1% wt)   | 17.78±0.63 <sup>c</sup>     | 28.80±1.35 <sup>b</sup>   |
| Crosslinked PHBV (L101 2% wt)   | 20.45±0.66 <sup>a</sup>     | 37.20±2.25 <sup>a</sup>   |
| Crosslinked PHBV (L101 3% wt)   | 18.27±0.62 <sup>b,c</sup>   | 28.47±0.85 <sup>b</sup>   |
| Crosslinked PHBV (L101 4% wt)   | 19.00±0.16 <sup>a,b,c</sup> | 32.77±3.07 <sup>a,b</sup> |

All measurements were performed in triplicate.

Values are reported as mean ± standard deviation.

Different letter designations for values in the same column indicate significant differences ( $p \leq 0.05$ ).

The residence time of all crosslinked PHBV was 1 minute

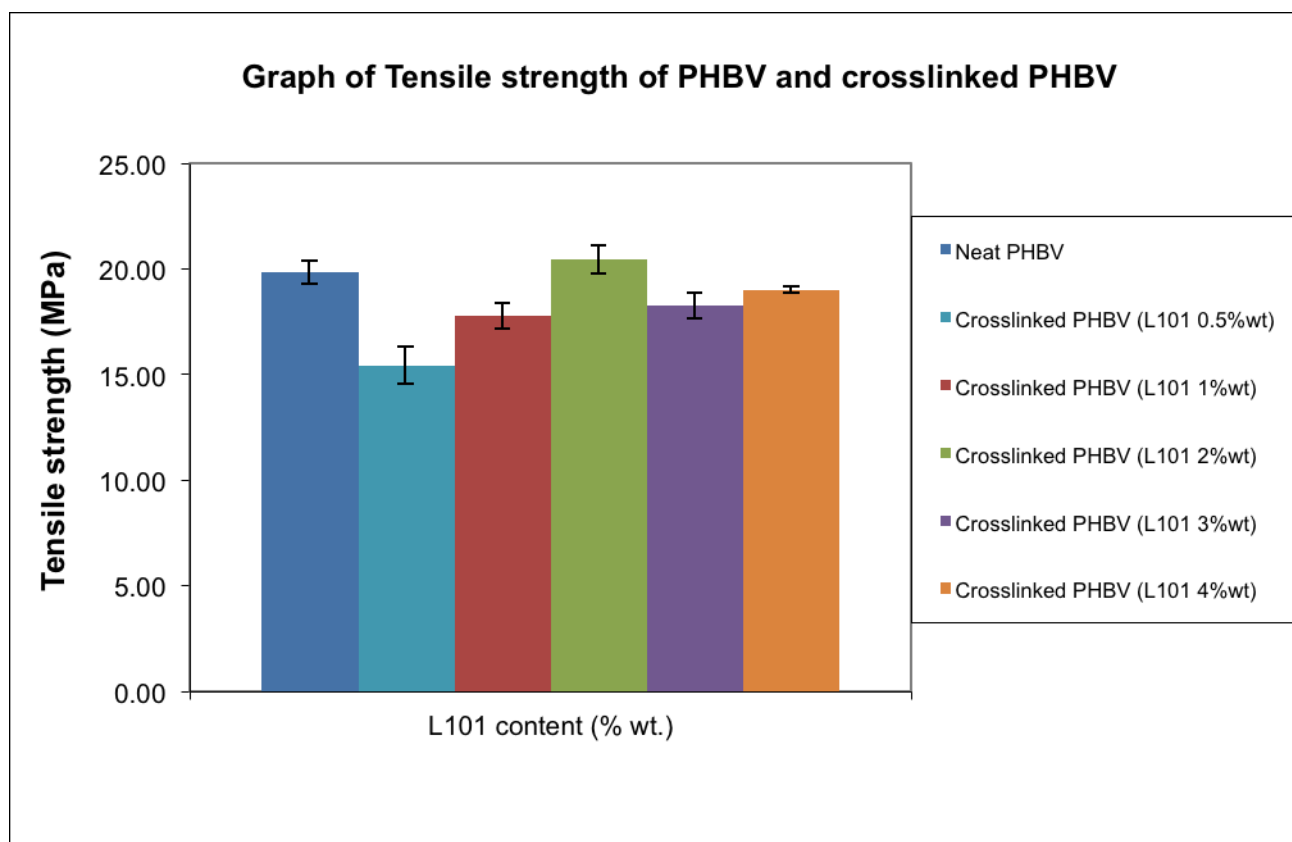


*Figure 5.3 Tensile strength of neat PHBV and crosslinked PHBV sheets*

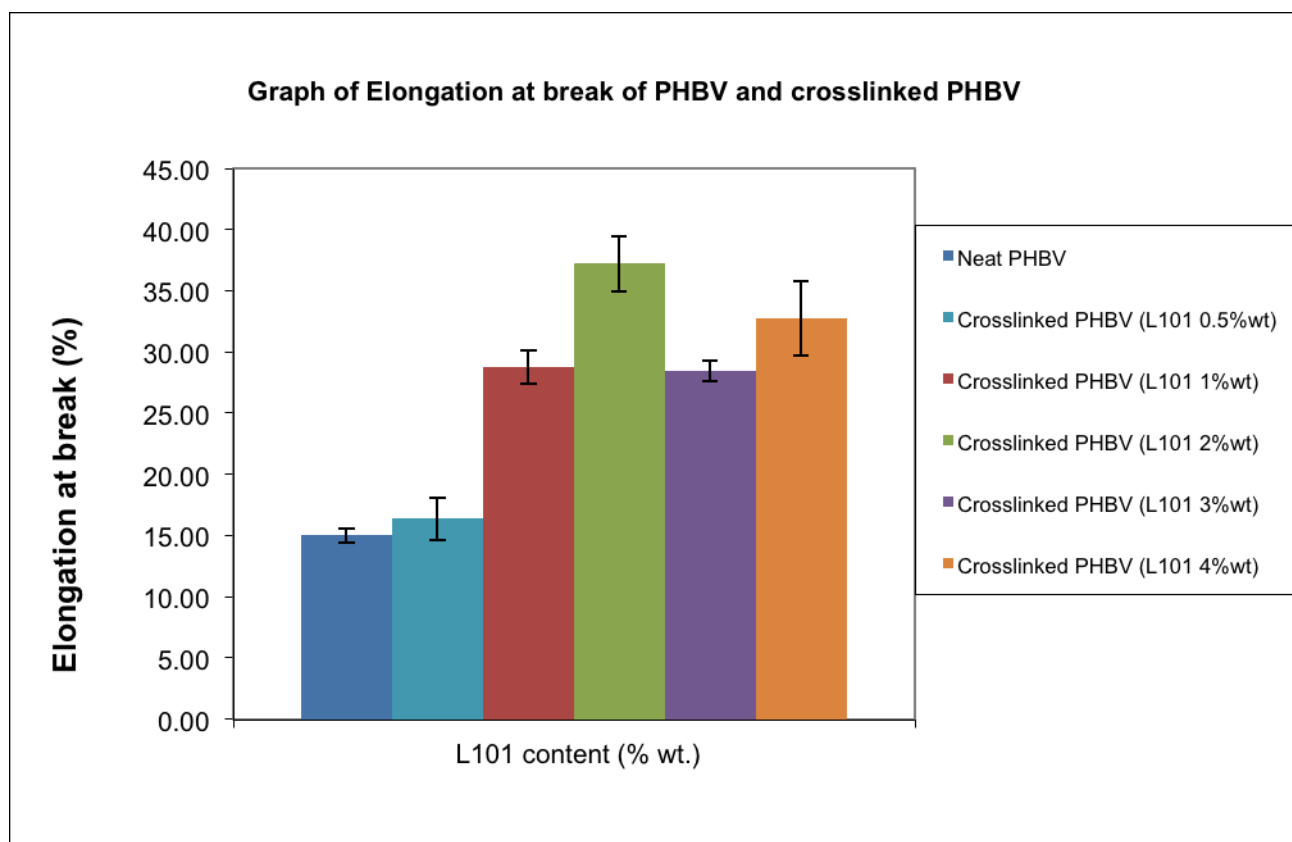


*Figure 5.4 Elongation at break of neat PHBV and crosslinked PHBV sheets*

### 5.3.3 Thermal properties of crosslinked poly(hydroxybutyrate-co-valerate)

Thermal properties of crosslinked PHBV were identified by DSC thermograms as shown in Figure 5.5 and Table 5.2. DSC showed that the  $T_c$  and  $T_m$  of the crosslinked PHBVs were significantly lower than the neat PHBV. The  $T_g$ s of PHBV and the crosslinked PHBV were not observed in this study. The crosslinked PHBVs had a covalent network that restricted the molecular movement. This array pattern impeded crystalline formation and decreased crystallinity, as shown in Table 5.2. In addition, the decrease of crystallinity contributed to imperfect and small size crystallite formation beginning at a lower temperature ( $T_c$ ). The two  $T_m$ s were also lower with an increase of L101 content due to higher crosslink density [149, 169]. This result was consistent with crosslinked PHBV with dicumyl peroxide (DCP) as a crosslinker.  $T_c$  and  $T_m$  of the materials decreased compared to non-crosslinked PHBV [93]. In the work of Yang et al., crosslinked PLA was prepared by adding triallyl isocyanurate (TAIC) and DCP as an initiator. The crosslinked PLA showed a decrease in  $T_c$  and  $T_m$  when the crosslinker increased resulting in lower crystallinity due to molecular chain motion inhibition [149]. Crosslinked poly( $\epsilon$ -caprolactone) with benzoyl peroxide (BPO) also had the same trend. The presence of BPO decreased  $T_m$  and crystallinity of the crosslinked material. However, the  $T_c$  of the crosslinked PLA was unexpectedly higher since other substances such as impurities from the processing and catalyst residue acted as nucleating agents, probably initiate crystallization [170].

The heat of fusion ( $\Delta H_m$ ) indicates the energy required by the polymer material in order to melt the crystallites. The heat of fusion of all crosslinked PHBVs was statistically significantly lower than the neat PHBV than the neat PHBV. At lower content of L101 of 0.5 and 1 %wt.,  $\Delta H_m$ s were not significantly different. In addition,  $\Delta H_m$ s of crosslinked PHBV with L101 at 2, 3 and 4 %wt. were not statistically different but were significantly lower than those of the crosslinked PHBV with L101 0.5 and 1 %wt. This shows that the crosslinking had an influence on the crystallinity of PHBV. With an increase of L101 content in the crosslinked PHBV, crystallinity was slightly decreased. An abrupt decrease in  $\Delta H_m$  and crystallinity occurred at L101 2%wt. At a content of L101 more than 2%wt. any further decrease in  $\Delta H_m$  and crystallinity was insignificant. This behavior of crosslinked PHBV indicated that crosslinking disturbed crystallite formation. The decrease in crystallinity in a crosslinked polymer was also reported by Krumova et al. DSC showed that  $\Delta H_m$  and  $T_m$  of poly(vinyl alcohol), PVA, crosslinked with hexamethylene diisocyanate dramatically decreased indicating less crystallinity in the structure [171]. Moreover,  $\Delta H_m$  and  $T_m$  of a crosslinked polyethylene/ethylene vinyl acetate blend with *tert*-butyl cumyl peroxide (BCUP) as an initiator were found to be lower when BCUP increased [172].

The thermal stability of the crosslinked PHBV was investigated using TGA. In this study, the crosslinked PHBV had slightly lower thermal stability than the neat PHBV as can be seen in Figure 5.6. Both experienced one stage weight loss. The onset temperature for the crosslinked PHBVs was around 295 °C which was slightly less than neat PHBV (300°C) and the decomposition was complete at about 330 °C which was lower than the 340 °C for neat PHBV. Generally, the crosslinking process increases thermal stability. According to Yang et



al., the thermal degradation temperature of crosslinked PLA was higher than that of neat PLA. The different in onset temperature was about 70 °C and of the ending decomposition temperature was 65 °C [149]. In addition, crosslinked poly(isobornyl methacrylate-co-butyl acrylate) copolymer possessed greater thermal stability than linear poly(isobornyl methacrylate-co-butyl acrylate) copolymer [173]. However, the thermal stability of the crosslinked PHBVs in this study was not enhanced. The TGA result in Figure 5.6 agreed with TGA of crosslinked PHBV with DCP as a crosslinker prepared by Fei et al [93]. There was no difference observed between PHBV and crosslinked PHBV in thermal decomposition [93].

One possible explanation for this behavior was suggested by Khonakdar et al. Crosslinking reactions induce covalent bonds at tertiary carbons in the polymer molecules, where are more likely to have thermal decomposition [169, 174]. According to Ke et al., benzophenone (BP) was used as an initiator in the presence of UV light, which induced photografting polymerization of polyacrylamide (PAM) onto PHBV. The tertiary hydrogen was abstracted from the PHBV main chain. Thus, PAM was attached onto the PHBV [175].

Table 5.3 Thermal properties of crosslinked PHBV at various initiator contents compared to neat PHBV

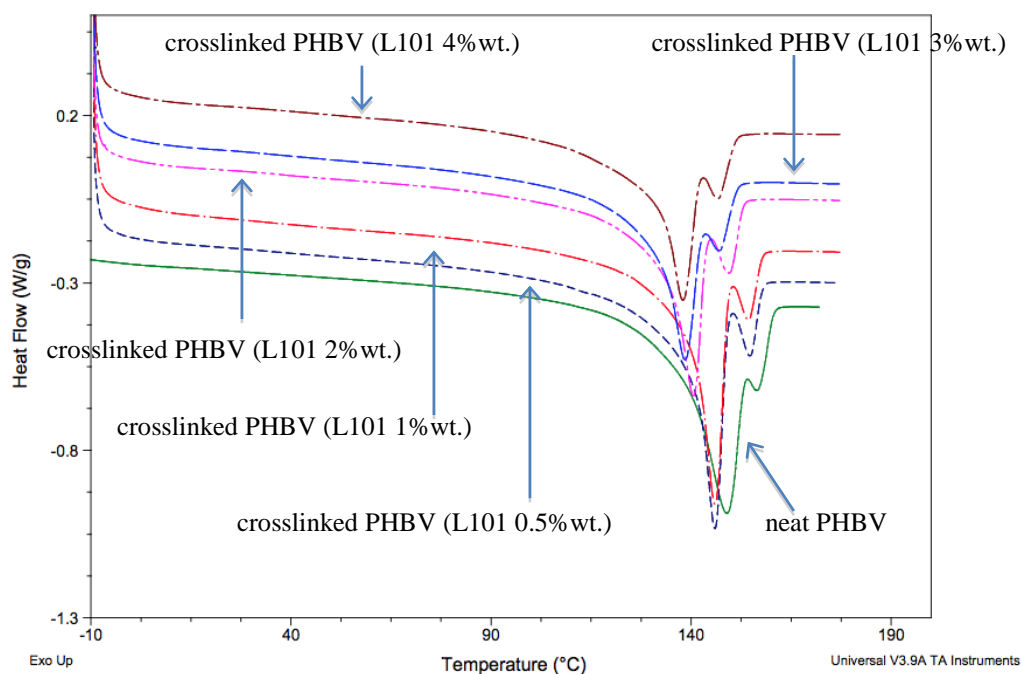
| Material                        | T <sub>c</sub> (°C)      | T <sub>m</sub> (°C)      |                            | Heat of fusion,<br>ΔH <sub>m</sub> (J/g) | PHBV<br>Crystallinity (%) |
|---------------------------------|--------------------------|--------------------------|----------------------------|--|---------------------------|
|                                 |                          |                          |                            |  |                           |
| Neat PHBV                       | 107.71±0.40 <sup>a</sup> | 149.31±0.67 <sup>a</sup> | 156.82±0.56 <sup>a</sup>   | 65.31±0.33 <sup>a</sup>                  | 59.92±0.30 <sup>a</sup>   |
| Crosslinked PHBV (L101 0.5% wt) | 105.33±0.52 <sup>b</sup> | 146.98±1.04 <sup>b</sup> | 155.44±0.85 <sup>a,b</sup> | 60.84±1.86 <sup>b</sup>                  | 55.81±1.71 <sup>b</sup>   |
| Crosslinked PHBV (L101 1% wt)   | 104.48±0.30 <sup>b</sup> | 145.33±0.61 <sup>b</sup> | 153.78±0.63 <sup>b</sup>   | 59.28±1.17 <sup>b</sup>                  | 54.38±1.08 <sup>b</sup>   |
| Crosslinked PHBV (L101 2% wt)   | 100.00±1.24 <sup>c</sup> | 140.16±0.81 <sup>c</sup> | 148.89±0.98 <sup>c</sup>   | 51.42±0.32 <sup>c</sup>                  | 47.17±0.29 <sup>c</sup>   |
| Crosslinked PHBV (L101 3% wt)   | 99.21±0.89 <sup>c</sup>  | 139.53±1.17 <sup>c</sup> | 148.34±1.32 <sup>c</sup>   | 50.01±0.66 <sup>c</sup>                  | 45.88±0.60 <sup>c</sup>   |
| Crosslinked PHBV (L101 4% wt)   | 99.08±0.54 <sup>c</sup>  | 138.60±0.54 <sup>c</sup> | 147.06±0.48 <sup>c</sup>   | 49.69±0.68 <sup>c</sup>                  | 45.59±0.62 <sup>c</sup>   |

All measurements were performed in triplicate.

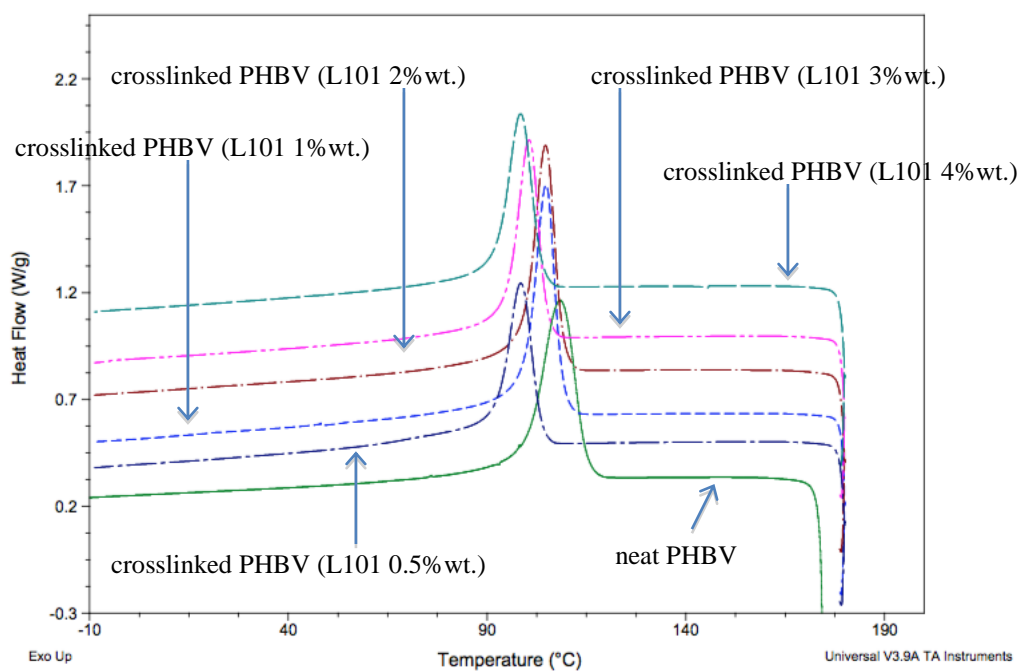
Values are reported as mean ± standard deviation.

Different letter designations for values in the same column indicate significant differences ( $p \leq 0.05$ ).

The residence time of all crosslinked PHBV was 1 minute.



(a)



(b)

Figure 5.5 Endothermic (a) and exothermic (b) profiles of neat PHBV and crosslinked PHBVs with L101 at 0.5, 1, 2, 3 and 4 %wt.

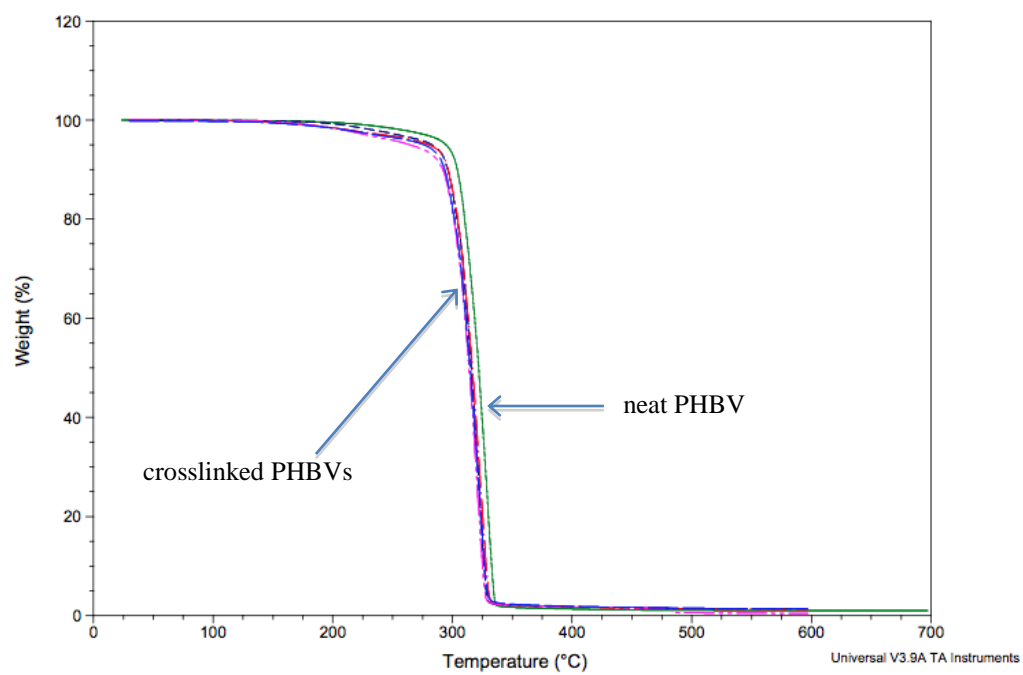


Figure 5.6 Thermal decomposition profiles of neat PHBV and crosslinked PHBVs with L101 at 0.5, 1, 2, 3 and 4 %wt.

#### 5.3.4 Permeation properties of crosslinked poly(hydroxybutyrate-co-valerate)s

Permeability of water vapor, oxygen, and carbon dioxide was used in identifying whether the selected flexible material is suitable to be effectively used in packaging applications. Water vapor permeability (WVP) of all the crosslinked PHBVs was higher than that of neat PHBV as shown in Table 5.4 and Figure 5.7. However, the result in this study was different from many studies. According to Ouattara et al., crosslinked milk protein film by irradiation had lower WVP when compared to the non-crosslinked film [176]. Hernandez-Munoz et al. reported that crosslinked gliadin-rich fraction film had significantly higher water barrier when compared to the un-crosslinked film [160]. Additionally, Coma et al. stated that moisture barrier of crosslinked hydroxypropyl methyl cellulose (HPMC) with citric acid, compared to the un-crosslinked HPMC, was improved from  $269 \pm 14$  g/m<sup>2</sup>.day to  $221 \pm 2$  g/m<sup>2</sup>.day at 23 °C 50%RH [177]. In this study, PHBV inherently has a high water vapor barrier. The result showed that WVPs of the crosslinked PHBVs with L101 at 1 and 2%wt. were slightly higher than that of the neat PHBV, and WVPs of the crosslinked PHBVs with L101 at 0.5, 3 and 4%wt. were significantly greater than that of the neat PHBV. In fact, the crystalline structure of polymer is impermeable to water vapor and gases [178]. Crosslinking involves reduction of crystallinity as can be seen in Table 5.3 since the crosslinking network contributed to chain restriction, which impeded the crystallinity of the PHBV, creating free volume (voids) for water vapor permeation; further, thermal processing in the extruder may cause some thermal degradation involving chain scission. Then crosslinking did not contribute to improving water vapor barrier.

Table 5.4 Permeability properties of crosslinked PHBV at various initiator contents compared to neat PHBV

| <b>Material</b>                 | <b>Water vapor<br/>permeation, kg.m/m<sup>2</sup>.s.Pa</b> | <b>Oxygen<br/>permeation, kg.m/m<sup>2</sup>.s.Pa</b> | <b>Carbon dioxide<br/>permeation, kg.m/m<sup>2</sup>.s.Pa</b> |
|---------------------------------|--|---|---|
| Neat PHBV                       | $1.74 \times 10^{-6} \pm 0.9 \times 10^{-7c}$              | $2.26 \times 10^{-18} \pm 3.4 \times 10^{-19}$        | $2.06 \times 10^{-17} \pm 8.5 \times 10^{-18b}$               |
| Crosslinked PHBV (L101 0.5% wt) | $1.01 \times 10^{-5} \pm 3.2 \times 10^{-6b}$              | -   | $2.44 \times 10^{-17} \pm 3.1 \times 10^{-18b}$               |
| Crosslinked PHBV (L101 1% wt)   | $6.33 \times 10^{-6} \pm 1.3 \times 10^{-7b,c}$            | -   | $2.04 \times 10^{-17} \pm 2.8 \times 10^{-18b}$               |
| Crosslinked PHBV (L101 2% wt)   | $8.18 \times 10^{-6} \pm 9.8 \times 10^{-7b,c}$            | -   | $2.39 \times 10^{-17} \pm 4.0 \times 10^{-18b}$               |
| Crosslinked PHBV (L101 3% wt)   | $8.95 \times 10^{-6} \pm 1.75 \times 10^{-6b}$             | -   | $5.00 \times 10^{-17} \pm 4.8 \times 10^{-18a}$               |
| Crosslinked PHBV (L101 4% wt)   | $2.20 \times 10^{-5} \pm 4.5 \times 10^{-6a}$              | -   | -   |

All measurements were performed in triplicate.

Values are reported as mean  $\pm$  standard deviation.

Different letter designations for values in the same column indicate significant differences ( $p \leq 0.05$ ).

The residence time of the crosslinked PHBV was 1 min.

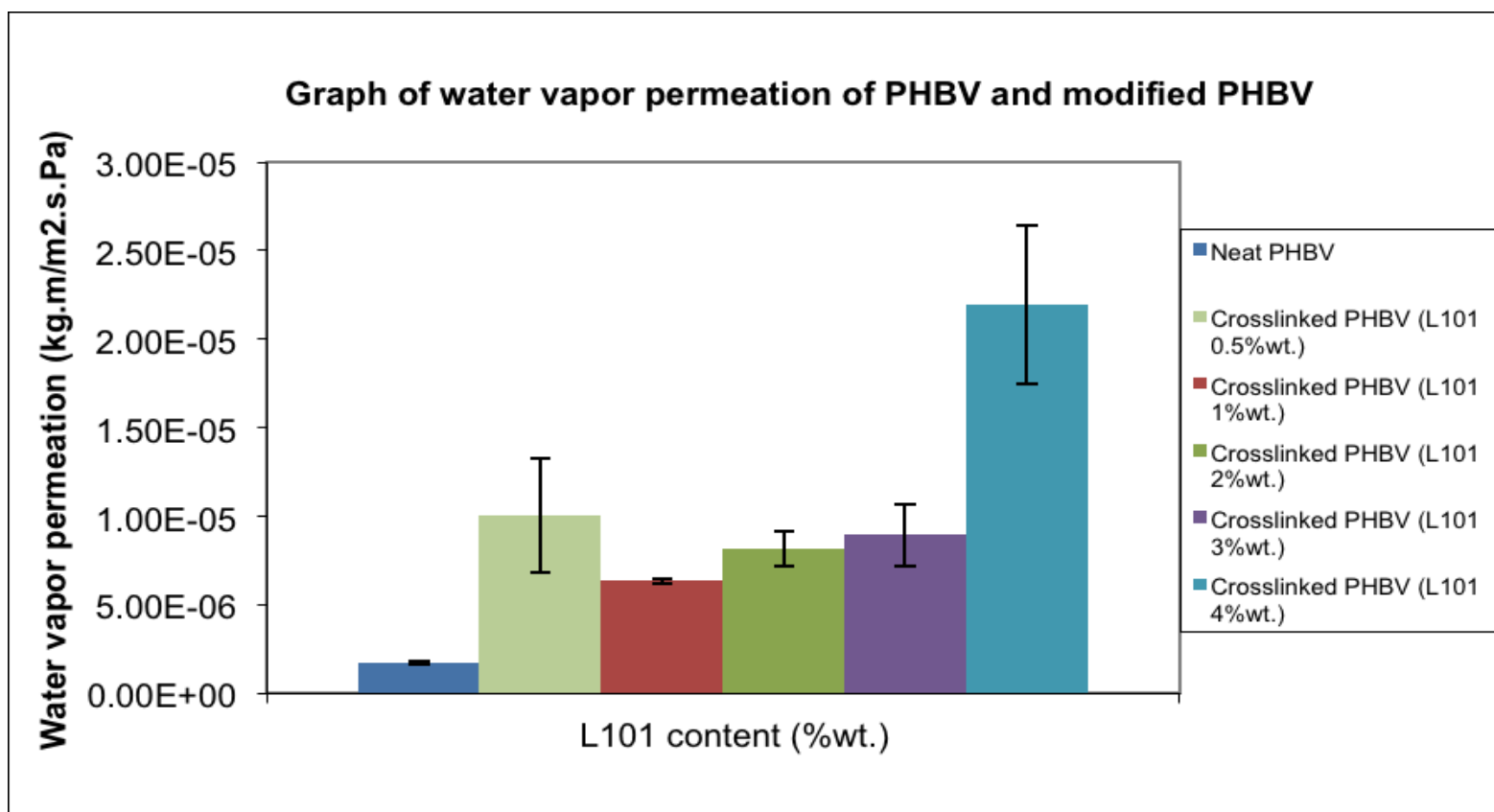


*Figure 5.7 Water vapor permeation of neat PHBV and crosslinked PHBV sheets*

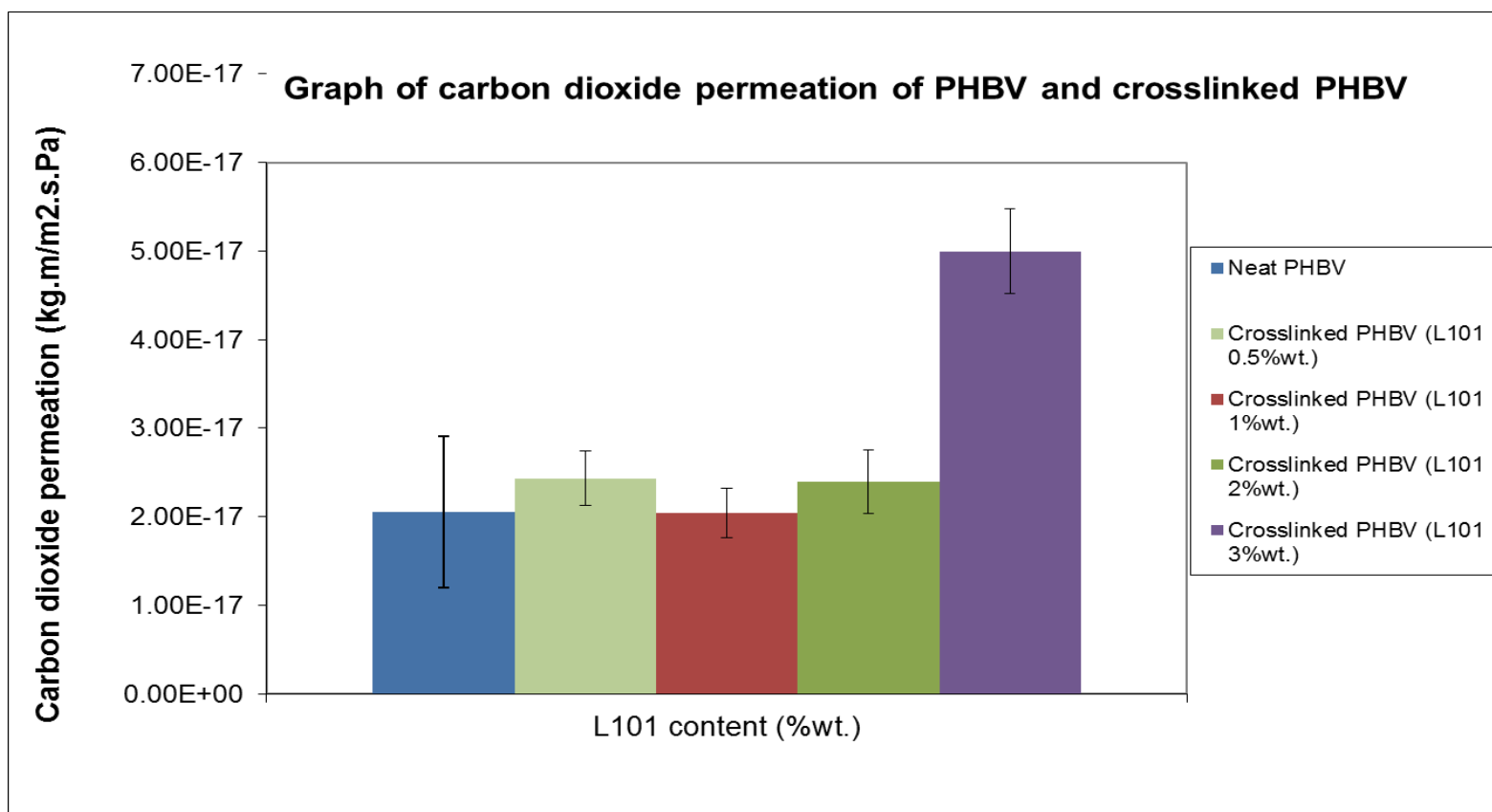


*Figure 5.8 Carbon dioxide permeation of neat PHBV and crosslinked PHBV sheets*



Oxygen permeation of the crosslinked PHBV could not be determined since the oxygen permeation machine (Mocon Oxtran 2/21) failed to perform the test. This was due to the fact that a high quantity of O<sub>2</sub> passed through the sheet and the measuring values were too high for the machine to quantify. Another possible reason for machine failure was that the crosslinked samples had a defect (small crack) due to its brittleness. In addition, carbon dioxide permeation (CO<sub>2</sub>P) for the crosslinked PHBV with L101 4%wt. could not be measured because the amount of CO<sub>2</sub> passing through the sheet was beyond the measuring range of the machine. Generally, crosslinking decreases the CO<sub>2</sub>P of polymers since the covalent network blocks free volume resulting in less gas permeation [179]. In this study, CO<sub>2</sub>P of the neat PHBV and the crosslinked PHBVs with L101 at 0.5, 1 and 2 %wt. were not statistically significantly different. Meanwhile, CO<sub>2</sub>P of the crosslinked PHBV with L101 at 3 %wt. was significantly higher than the neat PHBV and the crosslinked PHBV with L101 at 0.5, 1 and 2 %wt. Thus, crosslinking did not have significant effect on CO<sub>2</sub> permeability of PHBV at L101 content less than 3%wt. The greater CO<sub>2</sub>P of crosslinked PHBV with L101 3 %wt., on the other hand, was attributed to chain restriction in the crosslinked network that interfered with the crystallization of the PHBV, creating voids for CO<sub>2</sub> passing through. Therefore, crosslinking worsened the CO<sub>2</sub> barrier of the PHBV at L101 3%wt.

## **5.4 Conclusion**

Crosslinking is a modification method for improving PHBV properties, which tends to be inherently brittle and sticky. In this study, the crosslinking process (chemical reaction) required an initiator or crosslinker (catalyst), L101, in order to drive the reaction. The increase of L101 content in the crosslinked PHBV changed mechanical, thermal and permeability properties of PHBV.

## 6: CONCLUSIONS AND RECOMMENDATIONS FOR FUTURE WORK

### 6.1 Summary and conclusions

Poly(hydroxybutyrate-co-valerate), PHBV, is a biodegradable polymer which has potential to be used in many areas, especially in packaging applications. However, it has serious inherent drawbacks such as brittleness and lack of elongation. To overcome its downsides, PHBV was modified by various methods in order to permit its use in flexible applications.

#### *6.1.1 Selection of modification method for improving polyhydroxybutyrate-co-valerate properties for compression molding thin sheet*

PHBV was blended with titanium dioxide ( $\text{TiO}_2$ ) 1% by weight in order to obtain a toughening effect. The PHBV/ $\text{TiO}_2$ , compression molded into sheet, exhibited cracks all over the sheet. The sheet had tensile strength and elongation at break of  $18.64 \pm 0.55$  MPa and  $10.60 \pm 0.50\%$ , respectively, which were less than those of PHBV ( $19.84 \pm 0.54$  MPa and  $15.04 \pm 0.59\%$ ). Thermal properties of PHBV/ $\text{TiO}_2$  showed lower crystallinity than PHBV due to  $\text{TiO}_2$  interfering with the PHBV structure. Permeability of all three gases evaluated (water vapor, oxygen and carbon dioxide) of PHBV/ $\text{TiO}_2$  was slightly higher than PHBV since  $\text{TiO}_2$  aggregations created voids that gasses can get through. In the second trial, PHBV was blended with poly(butylene adipate-co-terephthalate) (PBAT or Ecoflex) at various ratios of PHBV/Ecoflex (80/20, 70/30, and 50/50 by weight) for flexibility. The compression molded sheets had lower tensile strength and elongation at break at every ratio of the blend ( $9.64 \pm 1.34$

MPa and  $5.43 \pm 1.27\%$  for 80/20,  $8.58 \pm 0.89$  MPa and  $8.37 \pm 1.74\%$  for 70/30,  $4.16 \pm 0.45$  MPa and  $4.47 \pm 0.12\%$  for 50/50) when compared to PHBV. Thermal properties indicated that all blends of PHBV/Ecoflex had lower crystallinity than PHBV because Ecoflex impeded PHBV crystalline formation. Permeability of the blend (50/50) for all three gases was greater than PHBV. In the third trial, PHBV was blended with Ecoflex and  $\text{TiO}_2$  at different ratios of PHBV/Ecoflex/ $\text{TiO}_2$  (79/20/1, 69/30/1 and 49.5/49.5/1 by weight) to obtain combined effects of  $\text{TiO}_2$  and Ecoflex. The compression molded sheets had lower tensile strength and elongation at break than PHBV in all ratios of the blend ( $12.54 \pm 1.02$  MPa and  $3.57 \pm 0.65\%$  for 79/20/1,  $11.30 \pm 1.20$  MPa and  $3.83 \pm 1.29\%$  for 69/30/1,  $6.31 \pm 0.56$  MPa and  $6.47 \pm 1.07\%$  for 49.5/49.5/1). The PHBV blends had lower crystallinity than PHBV since Ecoflex in the blend interfered with crystallinity as well as  $\text{TiO}_2$  aggregation creating non-uniformity, which diminished the crystallinity. The permeability of gasses in all blends was higher than PHBV corresponding to lower crystallinity in the blends. In the fourth trial, PHBV was blended with triethyl citrate (TEC) at a ratio of PHBV/TEC of 80/20 by weight to impart flexibility. The sheet was appeared to have clear liquid on the surface of the sheet due to TEC migration. Tensile strength and elongation at break of the compression molded sheet was lower than PHBV ( $4.82 \pm 1.19$  MPa and  $2.57 \pm 0.31\%$ ). PHBV/TEC had less crystallinity than PHBV. Permeability of the blend was not measured due to TEC migration. In the fifth trial, PHBV was grafted with 2-Hydroxyethyl methacrylate (2HEMA) at ratios of PHBV/2HEMA of 90/10 and 70/30 by weight. The sheets had lower tensile strength and elongation at break than PHBV ( $10.91 \pm 0.16$  MPa and  $7.51 \pm 0.02\%$  for 90/10,  $12.54 \pm 0.21$  MPa and  $11.40 \pm 1.51\%$  for 70/30). Thermal analysis showed lower crystallinity in the blend than PHBV since the grafting process creates branched molecules in PHBV, which impede crystallization.

Permeability of the blends was higher than PHBV due to the branched chains in the matrix. In the final trial, PHBV was crosslinked in the presence of 2,5-Bis(tert-butylperoxy)-2,5-dimethylhexane (L101). The sheet had significant greater elongation at break than PHBV and tensile strength was slightly higher than PHBV ( $20.45 \pm 0.66$  MPa and  $37.20 \pm 2.25\%$ ). The crosslinked PHBV had lower crystallinity than PHBV since the crosslinked network impeded crystalline formation, creating voids for favorable paths for gases resulting in higher permeation.

#### *6.1.2 Influence of the amount of initiator on the degree of polyhydroxybutyrate-co-valerate crosslinking and its properties*

Crosslinking was selected for modifying PHBV since it resulted in better elongation at break. In the second part, the amount of L101 in the crosslinking reaction was varied in order to obtain crosslinked material with higher elongation at break. L101 was added for the crosslinking reaction of PHBV at 0.5, 1, 2, 3, and 4 % by weight. The neat PHBV and crosslinked PHBVs sheets were not significantly different in tensile strength. However, elongation at break of crosslinked PHBVs was much greater than for PHBV, especially at a L101 content of 2%wt. where it was two times higher than neat PHBV. Thermal analysis showed that crystallinity of the crosslinked PHBVs were lower than neat PHBV when L101 content increased. Also, the permeability of gases decreased with an increase in L101 content

## **6.2 Problems and recommendations for future work**

PHBV has an advantage of being biodegraded in damp conditions and exposure to microorganisms and its drawback of lack of elongation was improved by a crosslinking process in the presence of an initiator, L101. However, the modified PHBV might change the biodegradation behavior of the neat PHBV. Therefore the biodegradability of the modified PHBV needs to be studied and compared to that of the neat PHBV in order to evaluate the ability to maintain biodegradability of the modified PHBV.

## **APPENDICES**

## Appendix A- Mechanical properties of neat PHBV and modified PHBV material sheets

**Table A-1 Tensile strength of all compositions of modified PHBV material sheets**

| Material  | Tensile strength (MPa) |             |             |
|---|------------------------|-------------|-------------|
|   | Replicate 1            | Replicate 2 | Replicate 3 |
| Neat PHBV   | 20.4402                | 19.6542     | 19.4170     |
| Blend of PHBV/TiO <sub>2</sub> nanoparticle 1% wt         | 18.2131                | 19.2536     | 18.4455     |
| Blend of PHBV/Ecoflex : 80/20 % wt                        | 11.1444                | 9.2290      | 8.5519      |
| Blend of PHBV/Ecoflex : 70/30 % wt                        | 7.5528                 | 9.0766      | 9.1117      |
| Blend of PHBV/Ecoflex : 50/50 % wt                        | 4.6721                 | 3.8074      | 3.9957      |
| Blend of PHBV/Ecoflex/TiO <sub>2</sub> : 79/20/1 % wt     | 13.7211                | 11.9125     | 11.9939     |
| Blend of PHBV/Ecoflex/TiO <sub>2</sub> : 69/30/1 % wt     | 9.9633                 | 12.2717     | 11.6732     |
| Blend of PHBV/Ecoflex/TiO <sub>2</sub> : 49.5/49.5/1 % wt | 6.9391                 | 6.0979      | 5.8856      |
| Blend of PHBV/Triethyl citrate : 80/20 % wt               | 4.6052                 | 3.7461      | 6.0966      |
| Grafted PHBV with 2HEMA : 90/10 % wt (L101 0.1% wt)       | 11.0747                | 10.7521     | 10.8969     |
| Grafted PHBV with 2HEMA : 70/30 % wt (L101 0.1% wt)       | 12.7578                | 12.3455     | 12.5020     |
| Crosslinked PHBV (L101 2% wt) rxn time 1 min              | 20.7967                | 19.6838     | 20.8691     |

**Table A-2 Elongation at break of all compositions of modified PHBV material sheets**

| Material  | Elongation at break (%) |             |             |
|---|-------------------------|-------------|-------------|
|   | Replicate 1             | Replicate 2 | Replicate 3 |
| Neat PHBV   | 14.89                   | 15.69       | 14.53       |
| Blend of PHBV/TiO <sub>2</sub> nanoparticle 1% wt         | 10.10                   | 11.10       | 10.60       |
| Blend of PHBV/Ecoflex : 80/20 % wt                        | 6.80                    | 4.30        | 5.20        |
| Blend of PHBV/Ecoflex : 70/30 % wt                        | 9.70                    | 6.40        | 9.00        |
| Blend of PHBV/Ecoflex : 50/50 % wt                        | 4.40                    | 4.40        | 4.60        |
| Blend of PHBV/Ecoflex/TiO <sub>2</sub> : 79/20/1 % wt     | 4.20                    | 2.90        | 3.60        |
| Blend of PHBV/Ecoflex/TiO <sub>2</sub> : 69/30/1 % wt     | 2.90                    | 3.30        | 5.30        |
| Blend of PHBV/Ecoflex/TiO <sub>2</sub> : 49.5/49.5/1 % wt | 5.80                    | 5.90        | 7.70        |
| Blend of PHBV/Triethyl citrate : 80/20 % wt               | 2.50                    | 2.30        | 2.90        |
| Grafted PHBV with 2HEMA : 90/10 % wt (L101 0.1% wt)       | 7.50                    | 7.41        | 7.62        |
| Grafted PHBV with 2HEMA : 70/30 % wt (L101 0.1% wt)       | 10.90                   | 10.20       | 13.10       |
| Crosslinked PHBV (L101 2% wt) rxn time 1 min              | 39.40                   | 37.30       | 34.90       |



**Table A-3 Tensile strength of crosslinked PHBV at various initiator contents compared to neat PHBV**

| Material                        | Tensile strength (MPa) |             |             |
|---------------------------------|------------------------|-------------|-------------|
|                                 | Replicate 1            | Replicate 2 | Replicate 3 |
| Neat PHBV                       | 20.4402                | 19.6542     | 19.4170     |
| Crosslinked PHBV (L101 0.5% wt) | 14.4600                | 15.6100     | 16.2000     |
| Crosslinked PHBV (L101 1% wt)   | 18.4700                | 17.2400     | 17.6200     |
| Crosslinked PHBV (L101 2% wt)   | 20.7967                | 19.6838     | 20.8691     |
| Crosslinked PHBV (L101 3% wt)   | 18.7900                | 18.4300     | 17.5900     |
| Crosslinked PHBV (L101 4% wt)   | 18.8261                | 19.0295     | 19.1384     |

**Table A-4 Elongation at break of crosslinked PHBV at various initiator contents compared to neat PHBV**

| Material                        | Elongation at break (%) |             |             |
|---------------------------------|-------------------------|-------------|-------------|
|                                 | Replicate 1             | Replicate 2 | Replicate 3 |
| Neat PHBV                       | 14.89                   | 15.69       | 14.53       |
| Crosslinked PHBV (L101 0.5% wt) | 18.40                   | 15.40       | 15.30       |
| Crosslinked PHBV (L101 1% wt)   | 28.40                   | 30.30       | 27.70       |
| Crosslinked PHBV (L101 2% wt)   | 39.40                   | 37.30       | 34.90       |
| Crosslinked PHBV (L101 3% wt)   | 29.30                   | 27.60       | 28.50       |
| Crosslinked PHBV (L101 4% wt)   | 29.50                   | 33.20       | 35.60       |

## Appendix B- Thermal properties of neat PHBV and modified PHBV material sheets

**Table B-1 Crystallization temperature of all compositions of modified PHBV material sheets**

| Material  | Crystallization temperature, T <sub>c</sub> (°C) |             |             |
|---|--|-------------|-------------|
|   | Replicate 1                                      | Replicate 2 | Replicate 3 |
| Neat PHBV   | 107.58   | 107.39      | 108.16      |
| Blend of PHBV/TiO <sub>2</sub> nanoparticle 1%wt          | 110.02   | 109.57      | 110.05      |
| Blend of PHBV/Ecoflex : 80/20 % wt                        | 70.95  | 70.73       | 69.04       |
| Blend of PHBV/Ecoflex : 70/30 % wt                        | 67.46  | 69.51       | 69.35       |
| Blend of PHBV/Ecoflex : 50/50 % wt                        | 75.63  | 76.03       | 75.83       |
| Blend of PHBV/Ecoflex/TiO <sub>2</sub> : 79/20/1 % wt     | 84.15  | 84.78       | 85.12       |
| Blend of PHBV/Ecoflex/TiO <sub>2</sub> : 69/30/1 % wt     | 81.94  | 81.01       | 81.75       |
| Blend of PHBV/Ecoflex/TiO <sub>2</sub> : 49.5/49.5/1 % wt | 82.80  | 81.16       | 83.42       |
| Blend of PHBV/Triethyl citrate : 80/20 % wt               | 64.45  | 74.89       | 71.84       |
| Grafted PHBV with 2HEMA : 90/10 % wt (L101 0.1% wt)       | 104.95   | 105.20      | 104.84      |
| Grafted PHBV with 2HEMA : 70/30 % wt (L101 0.1% wt)       | 98.62  | 102.11      | 102.38      |
| Crosslinked PHBV (L101 2%wt) rxn time 1 min               | 100.56   | 98.57       | 100.86      |

**Table B-2 The first melting temperature of all compositions of modified PHBV material sheets**

| Material  | Melting temperature, T <sub>m1</sub> (°C) |             |             |
|---|---|-------------|-------------|
|   | Replicate 1                               | Replicate 2 | Replicate 3 |
| Neat PHBV   | 148.87                                    | 150.09      | 148.98      |
| Blend of PHBV/TiO <sub>2</sub> nanoparticle 1%wt          | 153.12                                    | 153.50      | 152.99      |
| Blend of PHBV/Ecoflex : 80/20 % wt                        | 143.13                                    | 143.38      | 142.37      |
| Blend of PHBV/Ecoflex : 70/30 % wt                        | 142.87                                    | 143.12      | 145.11      |
| Blend of PHBV/Ecoflex : 50/50 % wt                        | 143.55                                    | 142.92      | 143.55      |
| Blend of PHBV/Ecoflex/TiO <sub>2</sub> : 79/20/1 % wt     | 146.01                                    | 145.61      | 145.88      |
| Blend of PHBV/Ecoflex/TiO <sub>2</sub> : 69/30/1 % wt     | 146.15                                    | 145.87      | 146.00      |
| Blend of PHBV/Ecoflex/TiO <sub>2</sub> : 49.5/49.5/1 % wt | 146.54                                    | 146.29      | 146.94      |
| Blend of PHBV/Triethyl citrate : 80/20 % wt               | 130.28                                    | 131.97      | 130.70      |
| Grafted PHBV with 2HEMA : 90/10 % wt (L101 0.1% wt)       | 149.87                                    | 149.42      | 149.56      |
| Grafted PHBV with 2HEMA : 70/30 % wt (L101 0.1% wt)       | 144.34                                    | 147.42      | 147.62      |
| Crosslinked PHBV (L101 2%wt) rxn time 1 min               | 140.55                                    | 139.23      | 140.70      |

**Table B-3 The second melting temperature of all compositions of modified PHBV material sheets**

| Material  | Melting temperature, T <sub>m2</sub> (°C) |             |             |
|---|---|-------------|-------------|
|   | Replicate 1                               | Replicate 2 | Replicate 3 |
| Neat PHBV   | 156.40                                    | 157.45      | 156.61      |
| Blend of PHBV/TiO <sub>2</sub> nanoparticle 1% wt         | 159.55                                    | 159.98      | 159.77      |
| Blend of PHBV/Ecoflex : 80/20 % wt                        | 156.93                                    | 157.02      | 155.97      |
| Blend of PHBV/Ecoflex : 70/30 % wt                        | 156.15                                    | 156.81      | 157.47      |
| Blend of PHBV/Ecoflex : 50/50 % wt                        | 156.69                                    | 156.13      | 156.54      |
| Blend of PHBV/Ecoflex/TiO <sub>2</sub> : 79/20/1 % wt     | 157.87                                    | 157.66      | 157.66      |
| Blend of PHBV/Ecoflex/TiO <sub>2</sub> : 69/30/1 % wt     | 158.08                                    | 157.68      | 157.87      |
| Blend of PHBV/Ecoflex/TiO <sub>2</sub> : 49.5/49.5/1 % wt | 158.20                                    | 158.27      | 158.71      |
| Blend of PHBV/Triethyl citrate : 80/20 % wt               | 146.55                                    | 146.86      | 146.11      |
| Grafted PHBV with 2HEMA : 90/10 % wt (L101 0.1% wt)       | 158.50                                    | 157.87      | 157.66      |
| Grafted PHBV with 2HEMA : 70/30 % wt (L101 0.1% wt)       | 154.92                                    | 157.03      | 157.03      |
| Crosslinked PHBV (L101 2% wt) rxn time 1 min              | 149.45                                    | 147.76      | 149.45      |

**Table B-4 Heat of fusion of all compositions of modified PHBV material sheets**

| Material  | Heat of fusion, ΔH <sub>m</sub> (J/g) |             |             |
|---|---------------------------------------|-------------|-------------|
|   | Replicate 1                           | Replicate 2 | Replicate 3 |
| Neat PHBV   | 65.50                                 | 65.50       | 64.93       |
| Blend of PHBV/TiO <sub>2</sub> nanoparticle 1% wt         | 59.66                                 | 59.25       | 59.57       |
| Blend of PHBV/Ecoflex : 80/20 % wt                        | 50.90                                 | 50.58       | 50.83       |
| Blend of PHBV/Ecoflex : 70/30 % wt                        | 46.98                                 | 46.09       | 45.28       |
| Blend of PHBV/Ecoflex : 50/50 % wt                        | 31.89                                 | 31.54       | 31.77       |
| Blend of PHBV/Ecoflex/TiO <sub>2</sub> : 79/20/1 % wt     | 49.24                                 | 48.77       | 49.06       |
| Blend of PHBV/Ecoflex/TiO <sub>2</sub> : 69/30/1 % wt     | 43.51                                 | 44.11       | 44.22       |
| Blend of PHBV/Ecoflex/TiO <sub>2</sub> : 49.5/49.5/1 % wt | 31.95                                 | 31.69       | 31.91       |
| Blend of PHBV/Triethyl citrate : 80/20 % wt               | 37.18                                 | 42.46       | 41.97       |
| Grafted PHBV with 2HEMA : 90/10 % wt (L101 0.1% wt)       | 51.59                                 | 54.23       | 53.39       |
| Grafted PHBV with 2HEMA : 70/30 % wt (L101 0.1% wt)       | 39.44                                 | 41.99       | 41.22       |
| Crosslinked PHBV (L101 2% wt) rxn time 1 min              | 51.07                                 | 51.70       | 51.49       |

**Table B-5 Crystallization temperature of crosslinked PHBV at various initiator contents compared to neat PHBV**

| Material                        | Crystallization temperature, $T_c$ (°C) |             |             |
|---------------------------------|---|-------------|-------------|
|                                 | Replicate 1                             | Replicate 2 | Replicate 3 |
| Neat PHBV                       | 107.58                                  | 107.39      | 108.16      |
| Crosslinked PHBV (L101 0.5% wt) | 104.85                                  | 105.89      | 105.26      |
| Crosslinked PHBV (L101 1% wt)   | 104.66                                  | 104.65      | 104.14      |
| Crosslinked PHBV (L101 2% wt)   | 100.56                                  | 98.57       | 100.86      |
| Crosslinked PHBV (L101 3% wt)   | 98.45                                   | 98.99       | 100.19      |
| Crosslinked PHBV (L101 4% wt)   | 98.48                                   | 99.21       | 99.54       |

**Table B-6 The first melting temperature of crosslinked PHBV at various initiator contents compared to neat PHBV**

| Material                        | Melting temperature, $T_{m1}$ (°C) |             |             |
|---------------------------------|------------------------------------|-------------|-------------|
|                                 | Replicate 1                        | Replicate 2 | Replicate 3 |
| Neat PHBV                       | 148.87                             | 150.09      | 148.98      |
| Crosslinked PHBV (L101 0.5% wt) | 145.96                             | 148.04      | 146.95      |
| Crosslinked PHBV (L101 1% wt)   | 145.94                             | 145.32      | 144.72      |
| Crosslinked PHBV (L101 2% wt)   | 140.55                             | 139.23      | 140.70      |
| Crosslinked PHBV (L101 3% wt)   | 138.49                             | 139.31      | 140.79      |
| Crosslinked PHBV (L101 4% wt)   | 137.99                             | 139.00      | 138.81      |

**Table B-7 The second melting temperature of crosslinked PHBV at various initiator contents compared to neat PHBV**

| Material                        | Melting temperature, $T_{m2}$ (°C) |             |             |
|---------------------------------|------------------------------------|-------------|-------------|
|                                 | Replicate 1                        | Replicate 2 | Replicate 3 |
| Neat PHBV                       | 156.40                             | 157.45      | 156.61      |
| Crosslinked PHBV (L101 0.5% wt) | 154.73                             | 156.39      | 155.21      |
| Crosslinked PHBV (L101 1% wt)   | 154.26                             | 154.02      | 153.07      |
| Crosslinked PHBV (L101 2% wt)   | 149.45                             | 147.76      | 149.45      |
| Crosslinked PHBV (L101 3% wt)   | 147.15                             | 148.10      | 149.76      |
| Crosslinked PHBV (L101 4% wt)   | 146.50                             | 147.34      | 147.34      |

**Table B-8 Heat of fusion of crosslinked PHBV at various initiator contents compared to neat PHBV**

| Material                        | Heat of fusion, $\Delta H_m$ (J/g) |             |             |
|---------------------------------|------------------------------------|-------------|-------------|
|                                 | Replicate 1                        | Replicate 2 | Replicate 3 |
| Neat PHBV                       | 65.50                              | 65.50       | 64.93       |
| Crosslinked PHBV (L101 0.5% wt) | 58.72                              | 62.21       | 61.58       |
| Crosslinked PHBV (L101 1% wt)   | 58.05                              | 60.39       | 59.39       |
| Crosslinked PHBV (L101 2% wt)   | 51.07                              | 51.70       | 51.49       |
| Crosslinked PHBV (L101 3% wt)   | 49.39                              | 50.70       | 49.95       |
| Crosslinked PHBV (L101 4% wt)   | 49.03                              | 50.38       | 49.66       |

## Appendix C- Permeation properties of neat PHBV and modified PHBV material sheets

**Table C-1 Water vapor permeation of all compositions of modified PHBV material sheets**

| Material  | Water vapor permeation (kg.m/m <sup>2</sup> .s.Pa) |                         |                         |
|---|--|-------------------------|-------------------------|
|   | Replicate 1  | Replicate 2             | Replicate 3             |
| Neat PHBV   | 1.7137×10 <sup>-6</sup>                            | 1.6556×10 <sup>-6</sup> | 1.8382×10 <sup>-6</sup> |
| Blend of PHBV/TiO <sub>2</sub> nanoparticle 1% wt         | 1.8638×10 <sup>-6</sup>                            | 1.5144×10 <sup>-6</sup> | 1.7363×10 <sup>-6</sup> |
| Blend of PHBV/Ecoflex : 50/50 % wt                        | 5.7988×10 <sup>-6</sup>                            | 5.3421×10 <sup>-6</sup> | 5.4455×10 <sup>-6</sup> |
| Blend of PHBV/Ecoflex/TiO <sub>2</sub> : 79/20/1 % wt     | 4.8423×10 <sup>-6</sup>                            | 4.3439×10 <sup>-6</sup> | 4.1044×10 <sup>-6</sup> |
| Blend of PHBV/Ecoflex/TiO <sub>2</sub> : 69/30/1 % wt     | 5.1935×10 <sup>-6</sup>                            | 5.6159×10 <sup>-6</sup> | 5.4142×10 <sup>-6</sup> |
| Blend of PHBV/Ecoflex/TiO <sub>2</sub> : 49.5/49.5/1 % wt | 5.7446×10 <sup>-6</sup>                            | 5.5777×10 <sup>-6</sup> | 5.3460×10 <sup>-6</sup> |
| Grafted PHBV with 2HEMA : 90/10 % wt (L101 0.1% wt)       | 2.3726×10 <sup>-6</sup>                            | 1.8465×10 <sup>-6</sup> | 2.1066×10 <sup>-6</sup> |
| Grafted PHBV with 2HEMA : 70/30 % wt (L101 0.1% wt)       | 3.2242×10 <sup>-6</sup>                            | 4.4369×10 <sup>-6</sup> | 4.7425×10 <sup>-6</sup> |
| Crosslinked PHBV (L101 2% wt) rxn time 1 min              | 8.9446×10 <sup>-6</sup>                            | 8.5172×10 <sup>-6</sup> | 7.0841×10 <sup>-6</sup> |

**Table C-2 Oxygen permeation of all compositions of modified PHBV material sheets**

| Material  | Oxygen permeation (kg.m/m <sup>2</sup> .s.Pa) |                          |                          |
|---|---|--------------------------|--------------------------|
|   | Replicate 1                                   | Replicate 2              | Replicate 3              |
| Neat PHBV   | 2.5043×10 <sup>-18</sup>                      | 2.4029×10 <sup>-18</sup> | 1.8702×10 <sup>-18</sup> |
| Blend of PHBV/TiO <sub>2</sub> nanoparticle 1% wt         | 2.4966×10 <sup>-18</sup>                      | 2.6211×10 <sup>-18</sup> | 2.6892×10 <sup>-18</sup> |
| Blend of PHBV/Ecoflex : 50/50 % wt                        | 6.8898×10 <sup>-18</sup>                      | 6.0747×10 <sup>-18</sup> | 7.0663×10 <sup>-18</sup> |
| Blend of PHBV/Ecoflex/TiO <sub>2</sub> : 79/20/1 % wt     | 5.7426×10 <sup>-18</sup>                      | 5.1542×10 <sup>-18</sup> | 4.7701×10 <sup>-18</sup> |
| Blend of PHBV/Ecoflex/TiO <sub>2</sub> : 69/30/1 % wt     | 5.9086×10 <sup>-18</sup>                      | 4.8650×10 <sup>-18</sup> | 5.3653×10 <sup>-18</sup> |
| Blend of PHBV/Ecoflex/TiO <sub>2</sub> : 49.5/49.5/1 % wt | 6.2619×10 <sup>-18</sup>                      | 6.2645×10 <sup>-18</sup> | 6.3630×10 <sup>-18</sup> |
| Grafted PHBV with 2HEMA : 90/10 % wt (L101 0.1% wt)       | 1.8337×10 <sup>-18</sup>                      | 1.0318×10 <sup>-18</sup> | 1.3464×10 <sup>-18</sup> |
| Grafted PHBV with 2HEMA : 70/30 % wt (L101 0.1% wt)       | 2.8285×10 <sup>-18</sup>                      | 3.1267×10 <sup>-18</sup> | 2.6770×10 <sup>-18</sup> |

**Table C-3 Carbon dioxide permeation of all compositions of modified PHBV material sheets**

| Material  | Carbon dioxide permeation (kg.m/m <sup>2</sup> .s.Pa) |                          |                          |
|---|---|--------------------------|--------------------------|
|   | Replicate 1   | Replicate 2              | Replicate 3              |
| Neat PHBV   | 1.5858×10 <sup>-17</sup>                              | 1.5437×10 <sup>-17</sup> | 3.0438×10 <sup>-17</sup> |
| Blend of PHBV/TiO <sub>2</sub> nanoparticle 1% wt         | 2.9089×10 <sup>-17</sup>                              | 3.0316×10 <sup>-17</sup> | 2.7815×10 <sup>-17</sup> |
| Blend of PHBV/Ecoflex : 50/50 % wt                        | 7.7334×10 <sup>-17</sup>                              | 8.0598×10 <sup>-17</sup> | 5.8830×10 <sup>-17</sup> |
| Blend of PHBV/Ecoflex/TiO <sub>2</sub> : 49.5/49.5/1 % wt | 8.1706×10 <sup>-17</sup>                              | 6.9323×10 <sup>-17</sup> | 8.7477×10 <sup>-17</sup> |
| Grafted PHBV with 2HEMA : 90/10 % wt (L101 0.1% wt)       | 3.0511×10 <sup>-17</sup>                              | 3.0696×10 <sup>-17</sup> | 3.0488×10 <sup>-17</sup> |
| Grafted PHBV with 2HEMA : 70/30 % wt (L101 0.1% wt)       | 5.1475×10 <sup>-17</sup>                              | 5.1051×10 <sup>-17</sup> | 5.1084×10 <sup>-17</sup> |
| Crosslinked PHBV (L101 2% wt) rxn time 1 min              | 2.7303×10 <sup>-17</sup>                              | 2.4278×10 <sup>-17</sup> | 2.0140×10 <sup>-17</sup> |

**Table C-4 Water vapor permeation of crosslinked PHBV at various initiator contents compared to neat PHBV**

| Material                        | Water vapor permeation (kg.m/m <sup>2</sup> .s.Pa) |                          |                          |
|---------------------------------|--|--------------------------|--------------------------|
|                                 | Replicate 1  | Replicate 2              | Replicate 3              |
| Neat PHBV                       | 1.7137×10 <sup>-6</sup>                            | 1.6556×10 <sup>-6</sup>  | 1.8382×10 <sup>-6</sup>  |
| Crosslinked PHBV (L101 0.5% wt) | 8.5133×10 <sup>-6</sup>                            | 7.8943×10 <sup>-6</sup>  | 1.37628×10 <sup>-5</sup> |
| Crosslinked PHBV (L101 1% wt)   | 6.2113×10 <sup>-6</sup>                            | 6.2959×10 <sup>-6</sup>  | 6.4711×10 <sup>-6</sup>  |
| Crosslinked PHBV (L101 2% wt)   | 8.9446×10 <sup>-6</sup>                            | 8.5172×10 <sup>-6</sup>  | 7.0841×10 <sup>-6</sup>  |
| Crosslinked PHBV (L101 3% wt)   | 1.03819×10 <sup>-5</sup>                           | 6.9995×10 <sup>-6</sup>  | 9.4594×10 <sup>-6</sup>  |
| Crosslinked PHBV (L101 4% wt)   | 1.87391×10 <sup>-5</sup>                           | 2.71214×10 <sup>-5</sup> | 2.01022×10 <sup>-5</sup> |

**Table C-5 Carbon dioxide permeation of crosslinked PHBV at various initiator contents compared to neat PHBV**

| Material                        | Carbon dioxide permeation (kg.m/m <sup>2</sup> .s.Pa) |                          |                          |
|---------------------------------|---|--------------------------|--------------------------|
|                                 | Replicate 1   | Replicate 2              | Replicate 3              |
| Neat PHBV                       | 1.5858×10 <sup>-17</sup>                              | 1.5437×10 <sup>-17</sup> | 3.0438×10 <sup>-17</sup> |
| Crosslinked PHBV (L101 0.5% wt) | 2.1176×10 <sup>-17</sup>                              | 2.4524×10 <sup>-17</sup> | 2.7356×10 <sup>-17</sup> |
| Crosslinked PHBV (L101 1% wt)   | 1.7586×10 <sup>-17</sup>                              | 2.3138×10 <sup>-17</sup> | 2.0518×10 <sup>-17</sup> |
| Crosslinked PHBV (L101 2% wt)   | 2.7303×10 <sup>-17</sup>                              | 2.4278×10 <sup>-17</sup> | 2.0140×10 <sup>-17</sup> |
| Crosslinked PHBV (L101 3% wt)   | 4.5930×10 <sup>-17</sup>                              | 5.5278×10 <sup>-17</sup> | 4.8726×10 <sup>-17</sup> |

## REFERENCES



## REFERENCES

1. Nadal, M., Schuhmacher, M., and Domingo, J.L. "Metal pollution of soils and vegetation in an area with petrochemical industry." *Science of the Total Environment*. 321: 59–69, 2004.
2. Luzier, W.D., "Materials derived from biomass/biodegradable materials," *Proceedings of the National Academy of Sciences of the United States of America*. 89: 839-842, 1992.
3. Scott G., *Degradable polymers: principles and applications*, 2<sup>nd</sup> ed., Kluwer Academic Publishers, Dordrecht, Netherlands, 238, 256 pp., 2002.
4. Gao, C., Stading, M., Wellner, N., Parker, M. L., Noel, T.R., Mills, E.N.C., and Belton, P.S. "Plasticization of a Protein-Based Film by Glycerol: A Spectroscopic, Mechanical, and Thermal Study." *Journal of Agricultural and Food Chemistry*. 54: 4611-4616, 2006.
5. Chieng, B.W., Ibrahim, N.A., Yunus, W.M.Z.W., and Hussein, M.Z. "Plasticized Poly(lactic acid) with Low Molecular Weight Poly(ethylene glycol): Mechanical, Thermal, and Morphology Properties." *Journal of Applied Polymer Science*. 4576-4580, 2013.
6. Farhoodi, M., Dadashi, S., Mousavi, S.M.A., Sotudeh-Gharebagh, R., Emam-Djomeh, Z., Oromiehie, A., and Hemmati, F. "Influence of TiO<sub>2</sub> Nanoparticle Filler on the Properties of PET and PLA Nanocomposites." *Polymer-Korea*. 36(6): 745-755, 2012.
7. Rio, T.G., Rodriguez, J., Pearson, R.A. "Compressive properties of nanoparticle modified epoxy resin at different strain rates." *Composites: Part B*. 57: 173–179, 2014.
8. Jiang, L., Wolcott, M.P., and Zhang, J. "Study of Biodegradable Polylactide/Poly(butylene adipate-co-terephthalate) Blends." *Biomacromolecules*. 7: 199-207, 2006.
9. Vroman, I., and Tighzert, L. "Review Biodegradable Polymers" *Materials*. 2: 307-344, 2009.
10. Chabba, S., Matthews, G.F., and Netravali, A.N. "'Green' composites using cross-linked soy flour and flax yarns." *Green Chemistry*. 7: 576–581, 2005.
11. Semba, T., Kitagawa, K., Ishiaku, U.S., and Hamada, H. "The Effect of Crosslinking on the Mechanical Properties of Polylactic Acid/Polycaprolactone Blends." *Journal of Applied Polymer Science*. 101: 1816 –1825, 2006.
12. US. Environmental Protection Agency, "Municipal Solid Waste Generation, Recycling, and Disposal in the United States: Facts and Figures for 2010,"

- [http://www.epa.gov/wastes/nonhaz/municipal/pubs/2012\\_msw\\_fs.pdf](http://www.epa.gov/wastes/nonhaz/municipal/pubs/2012_msw_fs.pdf), accessed March 9, 2014.
13. US. Environmental Protection Agency, "Municipal Solid Waste in the United States: 2009 Facts and Figures," <http://www.epa.gov/wastes/nonhaz/municipal/pubs/msw2009rpt.pdf>, accessed July 7, 2013.
  14. Waste Online, "Plastics recycling information sheet," <http://www.wasteonline.org.uk/resources/InformationSheets/Plastics.htm>, accessed Nov. 27, 2007.
  15. US. Environmental Protection Agency, "Basic Facts: Municipal Solid Waste (MSW)," <http://www.epa.gov/garbage/facts.htm>, accessed Nov. 27, 2007.
  16. Grossman, E.L., Cifuentes, L.A. and Cozzarelli, I.M., "Anaerobic Methane Oxidation in a Landfill-Leachate Plume," *Environmental Science & Technology*. 36: 2436-2442, 2002.
  17. Narayan, R. and Pettigrew, C.A., "ASTM Standards help define and grow a new biodegradable plastics industry," *ASTM STANDARDIZATION NEWS*. pp. 36-42, 1999.
  18. Smith, R., *Biodegradable Polymers for Industrial Applications*, 1<sup>st</sup> ed., Woodhead Publishing Limited, Cambridge, England, 3, 25 and 230-237 pp., 2005.
  19. Okada, M. "Chemical synthesis of biodegradable polymers," *Progress in Polymer Science*. 27(1): 87-133, 2002.
  20. Lofgren, A., Albertsson, A.C., Dubois, P., and Herome, R., "Recent advances in ring opening polymerization of lactones and related compounds," *Journal of Macromolecular Science, Part C: Polymer Reviews*. 35(3): 379-418, 1995.
  21. Fujimaki, T., 'Processability and properties of aliphatic polyesters, "Bionolle", synthesized by polycondensation reaction," *Polymer Degradation and Stability*. 59: 209-214, 1998.
  22. Takiyama, E., and Fujimaki, T., *Biodegradable Plastics and Polymers*, Elsevier, Amsterdam, Netherlands, 12, 150 pp., 1994.
  23. Ishioka, R., Kitakuni, E., and Ichikawa, Y., *Aliphatic polyesters: "Bionolle"*, Wiley VCH, Weinheim, Germany, 275-297 pp., 2002.
  24. Mochizuki, M., and Hiram, M., "Structure effects on the biodegradation of aliphatic polyesters." *Polymers for Advanced Technologies*. 8: 203-209, 1997.
  25. Nair, L.S., and Laurencin, C.T., "Biodegradable Polymers as biomaterials." *Progress in Polymer Science*. 32: 762-798, 2007.

26. Middleton, J.C., and Tipton, A.I., "Synthetic biodegradable polymers as medical devices." *Medical Plastics Biomaterials*. 5: 30-39, 1998.
27. Zhu, K.J., Hendren, R.W., Jensen, K., and Pitt, C.G. "Synthesis, properties and biodegradation of poly(1,3-trimethylene carbonate)." *Macromolecules*. 24: 1736-1740. 1991.
28. Witt, U., Muller, R.J., and Deckwer, W.D., "Biodegradation behavior and material properties of aliphatic/aromatic polyesters of commercial importance." *Journal of Environmental Polymer Degradation*. 5: 81-89. 1997.
29. Witt, U., Eining, T., Yamamoto, M., Kleeberg, I., Deckwer, M.D., and Muller, R.J. "Biodegradation of aliphatic-aromatic copolyesters: evaluation of the final biodegradability and ecotoxicological impact of degradation intermediates." *Chemosphere*. 44: 289-299. 2001.
30. Mohanty, A.K., Misra, M., and Hinrichsen, G., "Biofibres, biodegradable polymers and biocomposites: An overview." *Macromolecular Materials and Engineering*. 276-277: 1-24. 2000.
31. Tester, R.F., Karkalas, J., and Qi, X., "Starch – composition, fine structure and architecture: Review." *Journal of Cereal Science*. 39: 151-165, 2004.
32. Buleon, A., Colonna, P., Planchot, V., and Ball, S., "Starch granules: structure and biosynthesis." *International Journal of Biological Macromolecules*. 23: 85-112, 1998.
33. McWilliams, M., *Foods, Experimental Perspectives*. 5<sup>th</sup> ed. 5005: Pearson Prentice Hall.
34. Miao, Chuanwei., Hamad, W.Y. "Cellulose reinforced polymer composites and nanocomposites: a critical review." *Cellulose*. 20: 2221-2262, 2013.
35. Mohanty, A.K., Misra, M., and Drzal, L.T. "Sustainable Bio-Composites from Renewable Resources: Opportunities and Challenges in the Green Materials World." *Journal of Polymers and the Environment*. 10: 19-26, 2002.
36. Swain, S.N., Biswal, S.S., Nanda, P.K., and Nayak, P.L. "Biodegradable Soy-Based Plastics: Opportunities and Challenges." *Journal of Polymers and the Environment*. 12(1), 35-42, 2004.
37. Félix, M., Martin-Alfonso, J.E., and Romero, A. "Development of albumen/soy biobased plastic materials processed by injection molding." *Journal of Food Engineering*. 125: 7-16, 2014.
38. Zhou, X., Mohanty, A., and Misra, M. "A New Biodegradable Injection Moulded Bioplastic from Modified Soy Meal and Poly(butylene adipate-co-terephthalate): Effect of

- Plasticizer and Denaturant.” *Journal of Polymers and the Environment*. 21(3), 615-622, 2013.
39. Momany, F.A., Sessa, D.J., Lawton, J.W., Selling, G.W., Hamaker, S.A.H., and Willett, J.L. “Structural Characterization of r-Zein.” *Journal of Agricultural and Food Chemistry*. 54, 543-547, 2006.
  40. Du, X., Li, Y., Liu, X., Wang, X., Huselstein, C., Zhao, Y., Chang, P.R., and Chen, Y. “Fabrication and evaluation of physical properties and cytotoxicity of zein-based polyurethanes.” *Journal of Materials Science-Materials in Medicine*. 25(3), 823-833, 2014.
  41. Luecha, J., Sozer, N., and Kokini, J.L. “Synthesis and properties of corn zein/montmorillonite nanocomposite films.” *Journal of Materials Science*. 45(13), 3529-3537, 2010.
  42. Bastioli, C., *Handbook of Biodegradable Polymers*. Rapra Technology Limited, 2005.
  43. Garlotta, D., “A Literature Review of Poly(lactic acid).” *Journal of Polymers and the Environment*. 9, 63-84, 2001.
  44. Dicker, M.P.M., Duckworth, P.F., Baker, A.B., Francois, G., Hazzard, M.K., and Weaver, P.M. “Green Composites: A Review of Material Attributes and Complementary Applications.” *Composites: Part A*. 56, 280-289, 2014.
  45. Jamshidian, M., Tehrany, E.A., Imran, M., Jacquot, M., and Desobry, S. “Poly-Lactic Acid: Production, Applications, Nanocomposites, and Release Studies.” *Comprehensive Reviews in Food Science and Food Safety*. 9(5), 552-571, 2010.
  46. Bastioli, C. “Global Status of the Production of Biobased Packaging Materials.” *Starch-starke*. 53, 351-355, 2001.
  47. Qin, Y., Yang, J., Yuan, M., Xue, J., Chao, J., Wu, Y., and Yuan, M. “Mechanical, Barrier, and Thermal Properties of Poly(lactic acid)/Poly(trimethylene carbonate)/Talc Composite Films.” *Journal of Applied Polymer Science*. 131(6), 2014.
  48. Emad, A., Al-Mulla, J., Ibrahim, N.A., Shameli, K., Ahmad, M.B., and Yunus, Z.W. “Effect of epoxidized palm oil on the mechanical and morphological properties of a PLA–PCL blend.” *Research on Chemical Intermediates*. 40(2), 689-698, 2014.
  49. Lenz, R.W., and Marchessault, R.H. “Bacterial Polyesters: Biosynthesis, Biodegradable Plastics and Biotechnology.” *Biomacromolecules*. 6(1), 1-7, 2005.
  50. Robeson, L.M., *Polymer blends: a comprehensive review*, HANSER, 11-18 pp., 2007.

51. Vasile, C., and Kulshreshtha, A.K., *Handbook of Polymer Blends and Composites*, Volume 3A, Rapra Technology, 21-22 pp., 2003.
52. Michler, G.H., and Calleja, F.J.B., Glass Transition Temperature and Microhardness of Compatible and Incompatible Elastomer/Plastomer Blends.” *Journal of Bangladesh Academy of Science*. 33(1): 15-24, 2009.
53. Baird, D.G., and Collias, D.I. “Polymer Processing Principles and Design.” *New York: Butterworth-Heinemann, 1995*.
54. Chen, C.C., and White, J.L. “Compatibilizing agents in polymer blends : interfacial tension, phase morphology, and mechanical properties.” *Polymer Engineering and Science*. 33, 923-930, 1993.
55. Baker, W., Scott, C., and Hu, G.H. *Reactive Polymer Blending*. Carl Hanser Verlag, 2001.
56. Paul, D.R., and Bucknall, C.B. *Polymer Blends Volume 1: Formulation*. John Wiley & Son, Inc., 2000.
57. Utracki, L.A., and Abdelah, A. “Interphase and Compatibilization of Polymer Blends.” *Polymer Engineering and Science*. 1574-1585, 1996.
58. Robeson, L.M. *Polymer Blends: A Comprehensive Review*. Carl Hanser Verlag, 2007.
59. Selke, S.E.M., Culter, J.D., and Hernandez, R.J. *Plastics Packaging: Properties, Processing, Applications, and Regulations*, 2<sup>nd</sup> ed., HANSER, 28, 79-81, 342-362 pp., 2004.
60. Bhattacharya, A., Rawlins, J.W., and Ray, P., *Polymer Grafting and Crosslinking*, Wiley, 4-8 pp, 2009.
61. Meister, J.J., *Polymer Modification: Principles, Techniques, and Applications*, Marcel Dekker, Inc., 57 pp. 2000.
62. Fares, M.M., El-faqeeh, A.S., and Osman, M.E. “Graft copolymerization onto starch–I. Synthesis and optimization of starch grafted with N-tert-butylacrylamide copolymer and its hydrogels.” *Journal of Polymer Research*. 10, 119–125, 2003.
63. Kalla, S., and Sabaa, M.W. *Polysaccharide Based Graft Copolymers*. Springer, 4 pp., 2013.
64. Arora, M.G., Singh, M., and Yadav, M.S., *Polymer Chemistry*. Anmol Publications PVT. LTD., New Delhi, India., 429 pp. 2000.

65. Suchao-in, K., Koombhongse, P., and Chirachanchai, S. "Starch grafted poly(butylene succinate) via conjugating reaction and its role on enhancing the compatibility." *Carbohydrate Polymers*. 102, 95-102, 2014.
66. Vlcek, P., Janata, M., Latalova, P., Kriz, J., Cadova, E., and Toman, L. "Controlled grafting of cellulose diacetate." *Polymer*. 47, 2587-2595, 2006.
67. Wan, Y.J., Tang, L.C., Gong, L.X., Yan, D., Li, Y.B., Wu, L.B., Jiang, J.X., and Lai, G.Q. "Grafting of epoxy chains onto graphene oxide for epoxy composites with improved mechanical and thermal properties." *Carbon*. 69, 467-480, 2014.
68. Jacquel, N., Lo, C.W., Wei, Y.H., Wu, H.S., and Wang, H.S. "Isolation and purification of bacterial poly(3-hydroxyalkanoates)." *Biochemical Engineering Journal*. 39(1), 15-27, 2008.
69. Parulekar Y. and Mohanty A.K., "Extruded Biodegradable Cast Films from Polyhydroxyalkanoate and Thermoplastic Starch Blends: Fabrication and Characterization," *Macromolecular Materials and Engineering*. 292: 1218-1228, 2007.
70. Liu, F., Li, W., Ridgway, D. and Gu, T., "Production of poly- $\beta$ -hydroxybutyrate on molasses by recombinant *Escherichia coli*," *Biotechnology Letters*. 20: 4: 345-348, 1998.
71. Salehizadeh, H. and Loosdrecht, M.C.M.V., "Production of polyhydroxyalkanoates by mixed culture: recent trends and biotechnological importance," *Biotechnology Advances*. 22: 261-279, 2004.
72. Griffin G.J.L., *Chemistry and Technology of Biodegradable Polymers*, 1<sup>st</sup> ed., BLACKIE ACADEMIC & PROFESSIONAL, 78 pp., 1994.
73. Chen, G.Q. and Wu, Q., "The application of polyhydroxyalkanoates as tissue engineering materials," *Biomaterials*. 26: 6565-6578, 2005.
74. Kai, W., He, Y. and Inoue Y., "Fast Crystallization of poly(3-hydroxybutyrate) and poly(3-hydroxybutyrate-co-3-hydroxyvalerate) with talc and boron nitride as nucleating agents," *Polymer International*. 54: 780-789, 2005.
75. Chen, G.X., Hao, G.J., Guo, T.Y., Song, M.D, and Zhang, B.H., "Structure and mechanical properties of poly(3-hydroxybutyrate co-3-hydroxyvalerate) (PHBV)/clay nanocomposites," *Journal of Materials Science Letters*. 21: 1587-1589, 2002.
76. Liu, W.J., Yang, H.L., Wang, Z., Dong, L.S., and Lui, J.J., "Effect of Nucleating Agents on the Crystallization of Poly(3-Hydroxybutyrate-co-3-Hydroxyvalerate)." *Journal of Applied Polymer Science*. 86:2145-2152, 2002.
77. Wang, J.H., and Schertz, D.M., "Grafted Biodegradable Polymer Blend Compositions." US Patent No. 7,053,151 B2, 2006.

78. Wang, X., Chen, Z., Chen, X., Pan J., and Xu, K., "Miscibility, crystallization kinetics, and mechanical properties of poly(3-hydroxybutyrate-co-3-hydroxyvalerate)(PHBV)/poly(3-hydroxybutyrate-co-4-hydroxybutyrate)(P3/4HB) blends." *Journal of Applied Polymer Science*. 117:838-848, 2002.
79. Sombatmankhong, K., Sanchavanakit, N., Pavasant, P., and Supaphol, P., "Bone scaffolds from electrospun fiber mats of poly(3-hydroxybutyrate), poly(3-hydroxybutyrate-co-3-hydroxyvalerate) and their blend." *Polymer*. 48:1419-1427, 2007.
80. Yoshie, N., Asaka, A., and Inoue, Y., "Cocrystallization and Phase Segregation in Crystalline/Crystalline Polymer Blends of Bacterial Copolyesters" *Macromolecules*. 37(10):3770-3779, 2004.
81. Park, E.S., Kim, H.K., Shim, J.H., Kim, H.S., Jang, L.W., and Yoon, J.S., "Compatibility of poly(butadiene-co-acrylonitrile) with poly(L-lactide) and poly(3-hydroxybutyrate-co-3-hydroxyvalerate)" *Journal of Applied Polymer Science*. 92:3508-3513, 2004.
82. Buzarovska, A., and Grozdanov, A., "Crystallization kinetics of poly(hydroxybutyrate-co-hydroxyvalerate) and poly(dicyclohexylitaconate) PHBV/PDCHI blends: thermal properties and hydrolytic degradation." *Journal of Materials Science*. 44(7):1844-1850, 2009.
83. Li, J., Lai, M.F., and Liu, J.J., "Effect of Poly(propylene carbonate) on the Crystallization and Melting Behavior of Poly(B-hydroxybutyrate-co-B-hydroxyvalerate)." *Journal of Applied Polymer Science*. 92:2514-2521, 2004.
84. Miao, L., Qiu, Z., Yang, Wantai., and Ikehara, T., "Fully biodegradable poly(3-hydroxybutyrate-co-hydroxyvalerate)/poly(ethylene succinate) blends: Phase behavior, crystallization and mechanical properties." *Reactive & Functional Polymers*. 68:446-457, 2008.
85. Imam, S.H., Chen, L., Gordon, S.H., Shogren, R.L., and Weisleder, D., "Biodegradation of Injection Molded Starch-Poly (3-hydroxybutyrate-co-3-hydroxyvalerate) Blends in a Natural Compost Environment." *Journal of Environmental Polymer Degradation*. 6(2):91-98, 1998.
86. Goncalves, S.P.C., Martins-Franchetti, S.M., and Chinaglia, D.L., "Biodegradation of the Films of PP, PHBV and Its Blend in Soil." *Journal of Polymers and the Environment*. 17(4):280-285, 2009.
87. Lao, H.K., Renard, E., Langlois, V., Vallee-Rehel, K., and Linossier, I., "Surface functionalization of PHBV by HEMA grafting via UV treatment: Comparison with thermal free radical polymerization." *Journal of Applied Polymer Science*. 116:288-297, 2010.

88. Wang, J.H., and Schertz, D.M., "Reactive Extrusion Process for Making Modified Biodegradable Compositions." US Patent No. 6,579,934 B1, 2003.
89. Wang, W., Zhang, Y., Zhu, M., and Chen, Y., "Effect of graft modification with poly(*N*-vinylpyrrolidone) on thermal and mechanical properties of poly (3-hydroxybutyrate-*co*-3-hydroxyvalerate)." *Journal of Applied Polymer Science*. 109(3):1699-1707, 2008.
90. Wang, Y., Ke, Y., Wu, G., and Chen, X., "Photografting polymerization of polyacrylamide on poly(3- hydroxybutyrate-*co*-3-hydroxyvalerate) films. II. Wettability and crystallization behaviors of poly(3-hydroxybutyrate- *co*-3-hydroxyvalerate)-*graft*-polyacrylamide films." *Journal of Applied Polymer Science*. 107(6):3765-3772, 2008.
91. Grondahl, L., Chandler-Temple, A., and Trau, Matt., "Polymeric Grafting of Acrylic Acid onto Poly(3-hydroxybutyrate-*co*-3-hydroxyvalerate): Surface Functionalization for Tissue Engineering Applications." *Biomacromolecules*. 6:2197-2203, 2005.
92. Fei, B., Chen, C., Wu, H., Peng, S., Wang, X., and Dong, L., "Comparative study of PHBV/TBP and PHBV/BPA blends." *Polymer International*. 53(7):903-910, 2004.
93. Fei, B., Chen, C., Chen, S., Peng, S., Zhuang, Y., An, Y., and Dong, L., "Crosslinking of poly[(3-hydroxybutyrate)-*co*-(3-hydroxyvalerate)] using dicumyl peroxide as initiator." *Polymer International*. 53:937-943, 2004.
94. Muller, R.J. *Biodegradability of Polymers: Regulations and Methods for Testing*. Biopolymers online, 366-368 pp., 2005.
95. Grima, S., Bellon-Maurel, V., Feuilloley, P., and Silvestre, F. "Aerobic Biodegradation of Polymers in Solid-State Conditions: A Review of Environmental and Physicochemical Parameter Settings in Laboratory Simulations." *Journal of Polymers and the Environment*. 8(4), 183-195, 2002.
96. Leejarkpai, T., Suwanmanee, U., Rudeekit, Y., and Mungcharoen. T. "Biodegradable kinetics of plastics under controlled composting conditions." *Waste Management*. 32, 1153-1161, 2011.
97. Sang, B.I., Hori, K., Tanji, Y., and Unno, H. "A kinetic analysis of the fungal degradation process of poly(3-hydroxybutyrate-*co*-3-hydroxyvalerate) in soil." *Biochemical Engineering Journal*. 9, 175-184, 2001.
98. Shah, A.A., Hasan, F., and Hameed, A. "Degradation of poly(3-hydroxybutyrate-*co*-3-hydroxyvalerate) by a newly isolated *Actinomadura* sp. AF-555, from soil." *International Biodeterioration & Biodegradation*. 64, 281-285, 2010.
99. Weng, Y.X., Wang, Y., Wang, X.L., and Wang, Y.Z. "Biodegradation behavior of PHBV films in a pilot-scale composting condition." *Polymer Testing*. 29, 579-587, 2010.



100. Reischwitz, A., Stoppok, E., and Buchholz, K. "Anaerobic degradation of poly-3-hydroxybutyrate and poly-3-hydroxybutyrate-co-3-hydroxyvalerate." *Biodegradation*. 8, 313-319, 1998.
101. Abou-Zeid, D.M., Muller, R.J., and Deckwer, W.D. "Degradation of natural and synthetic polyesters under anaerobic conditions." *Journal of Biotechnology*. 86, 113-126, 2001.
102. ASTM D882 Standard Test Method for Tensile Properties of Thin Plastic Sheeting, 2012.
103. ASTM D618 Standard Practice for Conditioning Plastics for Testing, 2013.
104. ASTM D3418 Standard Test Method for Transition Temperatures and Enthalpies of Fusion and Crystallization of Polymers by Differential Scanning Calorimetry, 2003.
105. ASTM D3985 Standard Test Method for Oxygen Gas Transmission Rate Through Plastic Film and Sheeting Using a Coulometric Sensor, 2005.
106. ASTM F1249 Standard Test Method for Water Vapor Transmission Rate Through Plastic Film and Sheeting Using a Modulated Infrared Sensor, 2005.
107. Carballeira, P., and Hauptert, F. "Toughening Effects of Titanium Dioxide Nanoparticles on TiO<sub>2</sub>/Epoxy Resin Nanocomposites." *Polymer Composites*. 31(7): 1241-1246, 2010.
108. Wang, A., Gan, Y., Yu, H., Liu, Y., Zhang, M., Cheng, B., Wang, F., Wang, H., and Yan, J. "Improvement of the cytocompatibility of electrospun poly[(R)-3-hydroxybutyrate-co-(R)-3-hydroxyvalerate] mats by Ecoflex." *Journal of Biomedical Materials Research Part A*. 100A(6): 1505-1511, 2012.
109. Zhang, N., Wang, Q., Ren, J., and Wang, L. "Preparation and properties of biodegradable poly(lactic acid)/poly(butylene adipate-co-terephthalate) blend with glycidyl methacrylate as reactive processing agent." *Journal of Materials Science*. 44(1): 250-256, 2009.
110. Mondal, D., Bhowmick, B., Mollick, Md. M.R., Maity, D., Saha, N.R., Rangarajan, V., Rana, D., Sen, R., and Chattopadhyay, D. "Antimicrobial Activity and Biodegradation Behavior of Poly(butylene adipate-co-terephthalate)/Clay Nanocomposites." *Journal of Applied Polymer Science*. 1-9, 2014.
111. Evstatiev, M., Simeonova, S., Friedrich, K., Pei, X.Q., and Formanek, P. "MFC-structured biodegradable poly(L-lactide)/poly(butylene adipate-co-terephthalate) blends with improved mechanical and barrier properties." *Journal of Materials Science*. 48(18): 6312-6330, 2013.
112. Rieger, B., Kunkel, A., and Coates, G.W. *Synthetic Biodegradable Polymers*. Springer, 112, 2012.

113. Shahlari, M., and Lee, S. "Mechanical and Morphological Properties of Poly(butylene adipate-co-terephthalate) and Poly(lactic acid) Blended With Organically Modified Silicate Layers." *Polymer Engineering and Science*. 1420-1428, 2012.
114. Jiang, L., Liu, B., and Zhang, J. "Properties of Poly(lactic acid)/Poly(butylene adipate-co-terephthalate)/Nanoparticle Ternary Composites." *Industrial & Engineering Chemistry Research*. 48: 7594–7602, 2009.
115. Jiang, L., and Zhang, J. "Toughening of Polylactic Acid." *Encyclopedia of Polymer Composites: Properties, Performance and Applications*. Book Series: Polymer Science and Technology Series, 991-1007 pp., 2010.
116. Wypach G. *Handbook of Plasticizers*. ChemTec Publishing, William Andrew Inc., Toronto, Ontario, Canada, 3 pp., 2012.
117. Hauser, R., Duty, S., Godfrey-Bailey, L., and Calafat, A.M. "Medications as a Source of Human Exposure to Phthalates." *Environmental Health Perspectives*. 112(6): 751–753, 2004.
118. Zhao, Q., Gu, X.Y., Zhang, S., Dong, M.Z., Jiang, P., and Hu, Z.W. "Surface modification of polyamide 66 fabric by microwave induced grafting with 2-hydroxyethyl methacrylate." *Surface & Coatings Technology*. 240: 197–203, 2014.
119. Kodama, Y., Barsbay, M., and Guven, O. "Radiation-induced and RAFT-mediated grafting of poly(hydroxyethylmethacrylate) (PHEMA) from cellulose surfaces." *Radiation Physics and Chemistry*. 94: 98-104, 2014.
120. Tsukada, M., Khan, M.R., Miura, T., Postle, R., and Sakaguchi, A. "Mechanical performance of wool fabrics grafted with methacrylamide and 2-hydroxyethyl methacrylate by the Kawabata Evaluation System for Fabric method." *Textile Research Journal*. 83(12): 1242-1250, 2013.
121. Luperox® 101, 2,5-Bis(tert-butylperoxy)-2,5-dimethylhexane : Material Safety Data Sheet, Sigma-Aldrich.
122. Mendes, J.B.E., Riekes, M.K., Oliveira, V.M., Michel, M.D., Stulzer, H.K., Khalil, N.M., Zawadzki, S.F., Mainardes, R.M., and Farago, P.V. "PHBV/PCL Microparticles for Controlled Release of Resveratrol: Physicochemical Characterization, Antioxidant Potential, and Effect on Hemolysis of Human Erythrocytes." *The Scientific World Journal*. 2012.
123. Avella, M., Martuscelli, E., and Raimo, M. "Review Properties of blends and composites based on poly(3-hydroxy)butyrate (PHB) and poly(3-hydroxybutyrate-hydroxyvalerate) (PHBV) copolymers." *Journal of Materials Science*. 35: 523-545, 2000.

124. Szegda, D., Duangphet, S., Song, J., and Tarverdi, K. "Extrusion foaming of PHBV." *Journal of Cellular Plastics*. 50: 145, 2014.
125. Li, H., Khor, K.A., and Cheang, P. "Titanium dioxide reinforced hydroxyapatite coatings deposited by high velocity oxy-fuel (HVOF) spray." *Biomaterials*. 23: 85–91, 2002.
126. Zhu, Y., Buonocore, G.G., Lavorgna, M., and Ambrosio, L. "Poly(lactic acid)/Titanium Dioxide Nanocomposite Films: Influence of Processing Procedure on Dispersion of Titanium Dioxide and Photocatalytic Activity." *Polymer Composites*. 32(4): 519-528, 2011.
127. Eslami, H., and Kamal, M.R. "Effect of a Chain Extender on the Rheological and Mechanical Properties of Biodegradable Poly(lactic acid)/Poly[(butylene succinate)-co-adipate] Blends." *Journal of Applied Polymer Science*. 129(5): 2418-2428, 2013.
128. Zhang, J.F., and Sun, X. "Physical Characterization of Coupled Poly(lactic acid)/Starch/Maleic Anhydride Blends Plasticized by Acetyl Triethyl Citrate." *Macromolecular Bioscience*. 4(11): 1053-1060, 2004.
129. Yang, D., Peng, X., Zhong, L., Cao, X., Chen, W., Zhang, X., Liu, S., and Sun, R. "Green" films from renewable resources: Properties of epoxidized soybean oil plasticized ethyl cellulose films." *Carbohydrate polymers*. 103: 198-206, 2013.
130. Wang, D., Xuan, Y., Huang, Y., and Shen, J. "Synthesis and Properties of Graft Copolymer of Cellulose Diacetate with Poly(caprolactone monoacrylate)." *Journal of Applied Polymer Science*. 89(1): 85-90, 2003.
131. Samui, S., Ghosh, A.K., Ali, M.A., and Chowdhury, P. "Synthesis, characterization and kinetic studies of PEMA grafted acacia gum." *Indian Journal of Chemical Technology*. 14(2): 126-133, 2007.
132. Ten, E., Turtle, J., Bahr, D., Jiang, L., and Wolcott, M. "Thermal and mechanical properties of poly(3-hydroxybutyrate-co-3-hydroxyvalerate)/cellulose nanowhiskers composites." *Polymer*. 51: 2652-2660, 2010.
133. Jiang, L., Morelius, E., Zhang, J., Wolcott, M. "Study of the Poly(3-hydroxybutyrate-co-3-hydroxyvalerate)/Cellulose Nanowhisker Composites Prepared by Solution Casting and Melt Processing." *Journal of Composite Materials*. 42(24): 2629-2645, 2008.
134. Chen, C.W., Don, T.M., and Yen, H.F. "Enzymatic extruded starch as a carbon source for the production of poly(3-hydroxybutyrate-co-3-hydroxyvalerate) by *Haloferax mediterranei*." *Process Biochemistry*. 41: 2289–2296, 2006.
135. Buzarovska, A., Grozdanov, A., Avella, M., Gentile, G., and Errico, M. "Poly(hydroxybutyrate-co-hydroxyvalerate)/Titanium Dioxide Nanocomposites: A Degradation Study." *Journal of Applied Science*. 114(5): 3118-3124, 2009.

136. Wang, Y., Chen, R., Cai, J., Liu, Z., and Zheng, Y. "Biosynthesis and Thermal Properties of PHBV Produced from Levulinic Acid by *Ralstonia eutropha*." *PLOS ONE*, April 4, 2013.
137. Ferreira, B.M.P., Zavaglia, C.A.C., and Duek, E.A.R. "Thermal, morphologic and mechanical characterization of poly (L-lactic acid) / poly (hydroxybutyrate-co-hydroxyvalerate) blends." *Revista Brasileira de Engenharia Biomédica*. 19(1): 21-27, 2003.
138. Srikanth, P. "Microcellular processing of polylactide-hyperbranched polyester-nanoclay composites." *Journal of Materials Science*. 45(10), 2732-2746, 2010.
139. Qiu, Z., Yang, W., Ikehara, T., and Nishi, T. "Miscibility and crystallization behavior of biodegradable blends of two aliphatic polyesters. Poly(3-hydroxybutyrate-co-hydroxyvalerate) and poly(3-caprolactone)." *Polymer*. 46: 11814–11819, 2005.
140. Titanium dioxide : product information from sigma-aldrich.com
141. Duangphet, S., Szegda, D., Song, J., and Tarverdi, K. "The Effect of Chain Extender on Poly(3-hydroxybutyrate-co-3-hydroxyvalerate): Thermal Degradation, Crystallization, and Rheological Behaviours." *Journal of Polymers and the Environment*. 22(1), 1-8, 2014.
142. Audic, J.L., Lemiegre, L., and Corre, Y.M. "Thermal and Mechanical Properties of a Polyhydroxyalkanoate Plasticized with Biobased Epoxidized Broccoli Oil." *Journal of Applied Polymer Science*. 131(6), 2014.
143. Ke, T., and Sun, X. "Thermal and Mechanical Properties of Poly(lactic acid)/Starch/Methylenediphenyl Diisocyanate Blending with Triethyl Citrate." *Journal of Applied Polymer Science*. 88: 2947–2955, 2003.
144. Choi, J.S., and Park, W.H. "Effect of biodegradable plasticizers on thermal and mechanical properties of poly(3-hydroxybutyrate)." *Polymer Testing*. 23: 455–460, 2004.
145. Ke, T., and Sun, X. "Thermal and mechanical properties of poly(lactic acid) and starch blends with various plasticizers." *American Society of Agricultural Engineers*. 44(4): 945–953.
146. Jang, J., and Lee, D.K. "Plasticizer effect on the melting and crystallization behavior of polyvinyl alcohol." *Polymer*. 44: 8139-8346, 2003.
147. Mitomo, H., Enjôji, T., Watanabe, Y., Yoshii, F., Makuuchi, K., and Saito, T. "Radiation-Induced Graft Polymerization of Poly(3-Hydroxybutyrate) and Its Copolymer." *Journal of Macromolecular Science, Part A: Pure and Applied Chemistry*. 32(3), 1995.

148. Demirelli, K., Coskun, M., and Kaya, E. "A detailed study of thermal degradation of poly(2-hydroxyethyl methacrylate)." *Polymer Degradation and Stability*. 72(1), 75-80, 2001.
149. Yang, S.L., Wu, Z.H., Yang, W., and Yang, M.B. "Thermal and mechanical properties of chemical crosslinked polylactide (PLA)." *Polymer Testing*. 27: 957–963, 2008.
150. Shogrenz, R. "Water Vapor Permeability of Biodegradable Polymers." *Journal of Environmental Polymer Degradation*. 5(2): 91-95, 1997.
151. Kulkarni, U.D., Mahalingam, R., Li, X.L., Pather, I., and Jasti, B. "Effect of Experimental Temperature on the Permeation of Model Diffusants Across Porcine Buccal Mucosa." *American Association of Pharmaceutical Scientists*. 12(2): 579-586, 2011.
152. Sanchez-Garcia, M.D., Gimenez, E., and Lagaron, J.M. "Morphology and barrier properties of solvent cast composites of thermoplastic biopolymers and purified cellulose fibers." *Carbohydrate Polymers*. 71: 235–244, 2008.
153. Bell, L.N., and Labuza, T.P. *Moisture Sorption: Practical Aspects of Isotherm Measurement and Use, Second Edition*, The American Association of Cereal Chemists, Inc., 15-22 pp., 2000.
154. Rhim, J.W., Hong, S.I., and Ha, C.S. "Tensile, water vapor barrier and antimicrobial properties of PLA/nanoclay composite films." *LWT - Food Science and Technology*. 42: 612–617, 2009.
155. Suyatma, N.E., Copinet, A., Tighzert, L., and Coma, V. "Mechanical and Barrier Properties of Biodegradable Films Made from Chitosan and Poly (Lactic Acid) Blends." *Journal of Polymers and the Environment*. 12(1), 1-6, 2004.
156. Hernandez-Munoz, P., Kanavouras, A., Ng, P.K.W., Gavara, R. "Development and characterization of biodegradable films made from wheat gluten protein fractions." *Journal of Agricultural and Food Chemistry*. 51: 7647–7654, 2003.
157. Montheard, J.P., Chatzopoulos, M., and Chappard, D. "2-Hydroxyethyl Methacrylate (HEMA): Chemical Properties and Applications in Biomedical Fields." *Journal of Macromolecular Science, Part C: Polymer Reviews*. 32(1): 1-34, 1992.
158. Li, Y., Liu, L., Fang, Y. "Plasma-induced grafting of hydroxyethyl methacrylate (HEMA) onto chitosan membranes by a swelling method." *Polymer International*. 52: 285–290, 2003.
159. Shih, F.F. "Edible Films from Rice Protein Concentrate and Pullulan." *Cereal Chemistry*. 73(3): 406-409, 1996.

160. Hernandez-Munoz, P., Villalobos, R., and Chiralt, A. "Effect of cross-linking using aldehydes on properties of glutenin-rich films." *Food Hydrocolloids*. 18: 403-411, 2004.
161. Thellen, C., Coyne, M., Froio, D., Auerbach, M., Wirsén, C., and Ratto, J.A. "A Processing, Characterization and Marine Biodegradation Study of Melt-Extruded Polyhydroxyalkanoate (PHA) Films." *Journal of Polymers and the Environment*. 16(1): 1-11, 2008.
162. Costamagna, V., Strumia, M., Lopez-Gonzalez, M., and Riande, E. "Gas Transport in Surface-Modified Low-Density Polyethylene Films with Acrylic Acid as a Grafting Agent." *Journal of Polymer Science: Part B: Polymer Physics*. 44(19): 2828-2840, 2006.
163. Ray, S.S., Yamada, K., Okamoto, M., and Ueda, K. "Polylactide-Layered Silicate Nanocomposite: A Novel Biodegradable Material." *Nano Letters*. 2(10): 1093-1096, 2002.
164. Matteucci, S., Kusuma, V.A., Sanders, D., Swinnea, S., and Freeman, B.D. "Gas transport in TiO<sub>2</sub> nanoparticle-filled poly(1-trimethylsilyl-1-propyne)." *Journal of Membrane Science*. 307: 196-217, 2008.
165. Huang, I.Y.M., and Kanitz, P.J.F. "Permeation of Gases through Modified Polymer Films. I. PolyethyleneStyrene Graft Copolymers." *Journal of Applied Polymer Science*. 13(4): 669-683, 1969.
166. Haene, P.D., Remsen, E.E., and Asrar, J. "Preparation and Characterization of a Branched Bacterial Polyester." *Macromolecules*. 32: 5229-5235, 1999.
167. Bigi, A., Cojazzi, G., Panzavolta, S., Rubini, K., and Roveri, N. "Mechanical and thermal properties of gelatin films at different degrees of glutaraldehyde crosslinking." *Biomaterials*. 22: 763-768, 2001.
168. Sreedhar, B., Sairam, M., Chattopadhyay, D.K., Syamala Rathnam, P.A., and Mohan Rao, D.V. "Thermal, Mechanical, and Surface Characterization of Starch-Poly(vinyl alcohol) Blends and Borax-Crosslinked Films." *Journal of Applied Polymer Science*. 96: 1313-1322, 2005.
169. Khonakdar, H.A., Morshedien, J., Wagenknecht, U., and Jafari, S.H. "An investigation of chemical crosslinking effect on properties of high-density polyethylene." *Polymer*. 44: 4301-4309, 2003.
170. Han, C., Ran, X., Su, X., Zhang, K., Liu, N., and Dong, L. "Effect of peroxide crosslinking on thermal and mechanical properties of poly( $\epsilon$ -caprolactone)." *Polymer International*. 56: 593-600, 2007.

171. Krumova, M., Lopez, D., Benavente, R., Mijangos, C., and Perena, J.M. "Effect of crosslinking on the mechanical and thermal properties of poly(vinyl alcohol)." *Polymer*, 41: 9265–9272, 2000.
172. Khonakdar, H.A., Jafari, S.H., Haghighi-Asl, A., Wagenknecht, U., Haüssler, L., and Reuter, U. "Thermal and Mechanical Properties of Uncrosslinked and Chemically Crosslinked Polyethylene/Ethylene Vinyl Acetate Copolymer Blends." *Journal of Applied Polymer Science*. 103: 3261–3270, 2007.
173. Qu, J., Cheng, J., Wang, Z., Han, X., and Zhao, M. "Synthesis, thermal and optical properties of crosslinked poly(isobornyl methacrylate-co-butyl acrylate) copolymer films." *Optical Materials*. 36: 804–808, 2014.
174. Khonakdar, H.A., Morshedian, J., Eslami, H., and Shokrollahi, F. "Study of Heat Shrinkability of Crosslinked Low-Density Polyethylene/Poly(ethylene vinyl acetate) Blends." *Journal of Applied Polymer Science*. 91: 1389–1395, 2004.
175. Ke, Y., Wang, Y., Ren, L., Lu, L., Wu, G., Chen, X., and Chen, J. "Photografting Polymerization of Polyacrylamide on PHBV Films (I)." *Journal of Applied Polymer Science*. 104: 4088–4095, 2007.
176. Ouattara, B., Canh, L.T., Vachon, C., Mateescu, M.A., and Lacroix, M. "Use of  $\gamma$ -irradiation cross-linking to improve the water vapor permeability and the chemical stability of milk protein films." *Radiation Physics and Chemistry*. 63: 821–825, 2002.
177. Coma, V., Sebt, I., Pardon, P., Pichavant, F.H., and Deschamps, A. "Film properties from crosslinking of cellulosic derivatives with a polyfunctional carboxylic acid." *Carbohydrate Polymers*. 51: 265–271, 2003.
178. Tual, C., Espuche, E., Escoubes, M., and Domard, A. "Transport Properties of Chitosan Membranes: Influence of Crosslinking." *Journal of Polymer Science: Part B: Polymer Physics*. 38: 1521–1529, 2000.
179. Barillas, M.K., Enick, R.M., O'Brien, M., Perry, R., Luebke, D.R., and Morreale, B.D. "The CO<sub>2</sub> permeability and mixed gas CO<sub>2</sub>/H<sub>2</sub> selectivity of membranes composed of CO<sub>2</sub>-philic polymers." *Journal of Membrane Science*. 372(1-2): 29-39, 2011.